Eur. Phys. J. C (2009) 59: 557–588
DOI 10.1140/epjc/s10052-008-0830-0

THE EUROPEAN PHYSICAL JOURNAL C

Review

Dark-matter candidates

Axions, neutralinos, gravitinos, and axinos

Frank Daniel Steffen[a]

Max-Planck-Institut für Physik, Föhringer Ring 6, 80805 Munich, Germany

Received: 13 October 2008 / Published online: 9 January 2009

Abstract The existence of dark matter provides strong evidence for physics beyond the standard model. Extending the standard model with the Peccei–Quinn symmetry and/or supersymmetry, compelling dark-matter candidates appear. For the axion, the neutralino, the gravitino, and the axino, I review primordial production mechanisms, cosmological and astrophysical constraints, experimental searches, and prospects for experimental identification.

PACS 95.35.+d · 14.80.Mz · 14.80.Ly

Contents

[a] e-mail: steffen@mppmu.mpg.de

1 Introduction

Based on numerous cosmological and astrophysical studies, we believe today that our Universe is flat and thus that the total energy density is critical, $\rho_{\rm tot} \simeq \rho_c = 3H_0^2/8\pi G_{\rm N}$ or $\Omega_{\rm tot} \equiv \rho_{\rm tot}/\rho_c \simeq 100\%$, with contributions of [1, 2]

$$\Omega_\Lambda \simeq 72\%, \qquad \Omega_{\rm dm} \simeq 23\%, \qquad \Omega_{\rm b} \simeq 4.6\%,$$
$$\Omega_\gamma \simeq 0.005\%, \qquad 0.1\% \lesssim \Omega_\nu \lesssim 1.5\% \tag{1.1}$$

provided in the form of dark energy, non-baryonic dark matter, baryons, photons, and neutrinos, respectively. Here $\Omega_i \equiv \rho_i/\rho_c$, H_0 is the present Hubble expansion rate, and $G_{\rm N}$ is Newton's constant. The density parameter Ω_γ is given basically by the photons of the cosmic microwave background (CMB). The understanding of the remaining $\Omega_{\rm tot} - \Omega_\gamma \simeq 99.995\%$ requires physics beyond the standard model:

(i) The amount of dark energy Ω_Λ could be provided by a cosmological constant. However, the fact that the cosmological constant or vacuum energy inferred from a naive quantum field theoretical estimate exceeds Ω_Λ by 120 orders of magnitude is the most serious fine-tuning problem in physics. An alternative explanation of dark energy is a slowly evolving scalar field [3–5] that cannot be part of the standard model.

(ii) The amount of baryons $\Omega_{\rm b}$—inferred from the CMB anisotropies, the framework of primordial nucleosynthesis, and the observationally inferred abundances of light nuclei—indicates a matter-antimatter asymmetry that cannot be explained within the standard model.

(iii) The amount of neutrinos Ω_ν is understood to be provided in the form of the cosmic neutrino background (CνB) whose detection is a major challenge; cf. [6] and references therein. While $\Omega_\nu^{m_{\nu_i}=0} \simeq 0.003\%$ for

three massless neutrino species, we know from oscillation experiments that at least two neutrinos have small but non-zero masses, $\sum_i m_{\nu_i} \gtrsim 0.05$ eV, which are not part of the Standard Model, such that $\Omega_\nu \gtrsim 0.1\%$. Moreover, since light neutrinos are hot dark matter, which leaves an imprint on large-scale structure (LSS) [7], one can extract the cosmological limit $\sum_i m_{\nu_i} \lesssim \mathcal{O}(1\text{ eV})$ or equivalently $\Omega_\nu \lesssim 1.5\%$ [8].

(iv) The dominant amount of the non-baryonic dark-matter density $\Omega_{\rm dm}$ must reside in one or more species with a negligible (thermal) velocity to allow for structure formation. Moreover, relying on the astrophysical and cosmological considerations that point to the existence of dark matter (see [9, 10] and references therein), we think that a particle-physics candidate for dark matter has to be electrically neutral, color neutral, and stable or have a lifetime $\tau_{\rm dm}$ that is generally larger than the age of the Universe today, $t_0 \simeq 14$ Gyr, i.e.,[1]

$$\tau_{\rm dm} > t_0 \simeq 4.3 \times 10^{17}\text{ s}. \tag{1.2}$$

With the standard active neutrinos being too light, such a dark matter candidate cannot be found within the standard model. Thus, one can consider the existence of dark matter as evidence for new physics.

In this review we focus on dark-matter candidates that appear once the standard model is extended with the Peccei–Quinn (PQ) symmetry and/or supersymmetry (SUSY): the axion, the lightest neutralino, the gravitino, and the axino. These hypothetical particles are particularly well motivated.

- The PQ mechanism allows for an elegant solution of the strong CP problem [21, 22]. In fact, an additional global U(1) symmetry—referred to as PQ symmetry—that is broken spontaneously at the PQ scale [2, 23, 24] $f_a \gtrsim 6 \times 10^8$ GeV can explain the smallness (or vanishing) of the CP violating Θ-vacuum term in quantum chromodynamics (QCD). The associated pseudo-Nambu–Goldstone boson is the axion [25, 26] which becomes massive due to QCD instanton effects. Indeed, the axion is electrically neutral, color neutral, and sufficiently long-lived for being a compelling dark matter candidate [27–29].
- SUSY extensions of the standard model are an appealing concept because of their remarkable properties, for example, with respect to gauge coupling unification, the hierarchy problem, and the embedding of gravity [30–35]. As superpartners of the standard-model particles, new particles appear including fields that are electrically neutral and color neutral. Since they have not been detected at particle accelerators, these sparticles must be heavy or extremely weakly interacting. Moreover, because of the non-observation of reactions that violate lepton number L or baryon number B, it is often assumed—as also in this review—that SUSY theories respect the multiplicative quantum number

$$R = (-1)^{3B+L+2S}, \tag{1.3}$$

known as R-parity, with S denoting the spin. Since standard-model particles and superpartners carry respectively even $(+1)$ and odd (-1) R-parity, its conservation implies that superpartners can only be produced or annihilated in pairs and that the lightest supersymmetric particle (LSP) cannot decay even if it is heavier than most (or all) of the standard-model particles.[2] An electrically neutral and color neutral LSP candidate—such as the lightest neutralino, the gravitino, or the axino—may thus also be a compelling dark-matter candidate.

For each dark-matter candidate X, it is crucial to calculate its relic density Ω_X and to compare the result with the dark-matter density $\Omega_{\rm dm}$, for which a nominal 3σ range can be inferred from measurements of the CMB anisotropies by the Wilkinson Microwave Anisotropy Probe (WMAP) satellite [41]

$$\Omega_{\rm dm}^{3\sigma} h^2 = 0.105^{+0.021}_{-0.030} \tag{1.4}$$

with $h = 0.73^{+0.04}_{-0.03}$ denoting the Hubble constant in units of 100 km Mpc^{-1} s^{-1}. Note that the nominal 3σ range is derived assuming a restrictive six-parameter "vanilla" model. A larger range is possible—even with additional data from other cosmological probes—if the fit is performed in the context of a more general model that includes other physically motivated parameters such as non-zero neutrino masses [42]: $0.094 < \Omega_{\rm dm} h^2 < 0.136$. Moreover, there are limits on the present free-streaming velocity v_0^X of the dark-matter candidate X from observations and simulations of LSS. Indeed, as mentioned above, the dominant part of $\Omega_{\rm dm}$ has to have a negligible (thermal) velocity to allow for structure formation.

Primordial nucleosynthesis—or big-bang nucleosynthesis (BBN)—is another cosmological probe for the viability of dark-matter scenarios and, more generally, for the viability of models beyond the standard model. Relying on standard-model physics, general relativity, and the

[1] Studies of diffuse x-ray and γ-ray backgrounds, of the cosmic ionization history, and of the CMB point to radiative lifetimes of electromagnetically decaying dark matter that are orders of magnitude above t_0 [11–15]. Moreover, for dark matter with decays into weakly interacting relativistic particles such as neutrinos, $\tau_{\rm dm} \gg t_0$ is inferred from studies of LSS, of the CMB [16–18], of type Ia supernovae (SN) [19], and of constraints on the cosmic neutrino flux [20].

[2] While R-parity conservation is assumed in this review, its violation is a realistic option; see, e.g., [36–40].

baryon-to-photon ratio inferred from the CMB anisotropies, standard BBN (SBBN) predicts the primordial abundances of deuterium, helium, and lithium in good overall agreement with the observationally inferred values and provides thereby an important consistency check of standard cosmology [2, 43–48]. This agreement can be affected by new physics, e.g., in the three following ways. First, there can be changes in the timing of the nuclear reactions—caused, e.g., by a change in the Hubble expansion rate because of an increase of the energy density during BBN contributed by a new relativistic species [44, 49, 50]. Second, non-thermal processes—caused, e.g., by the injection of energetic standard-model particles in late decays of heavier particles into an extremely weakly interacting dark-matter candidate—can reprocess the produced light nuclei [51–63]. Third, long-lived electromagnetically or strongly interacting relics—which can occur, e.g., in scenarios with an extremely weakly interacting dark-matter candidate—can form bound states with light nuclei and thereby lead to a catalysis of nuclear reactions, i.e., to catalyzed BBN (CBBN) [63–79]. We will encounter the associated BBN constraints and other cosmological and astrophysical constraints explicitly in the discussions of the dark-matter scenarios given below.

The viability of a dark-matter scenario is tightly connected to the early history of the Universe. As suggested by the flatness, isotropy, and homogeneity of the Universe, we assume that its earliest moments were governed by inflation [80, 81]. The inflationary expansion is then followed by a phase in which the Universe is reheated. The reheating phase repopulates the Universe and provides the initial conditions for the subsequent radiation-dominated epoch. We refer to the reheating temperature $T_{\rm R}$ as the initial temperature of this early radiation-dominated epoch of our Universe. In fact, inflation models can point to $T_{\rm R}$ well above 10^{10} GeV [80–82]. Here one should stress that BBN requires a minimum temperature of [83–86]

$$T \gtrsim 0.7\text{–}4\ \text{MeV} \equiv T_{\rm min}, \tag{1.5}$$

and that any temperature above $T_{\rm min}$ is still speculative since BBN is currently the deepest reliable probe of the early Universe. Interestingly, futuristic space-based gravitational-wave detectors such as the Big Bang Observer (BBO) or the Deci-hertz Interferometer Gravitational Wave Observatory (DECIGO) [87] could allow for tests of the thermal history before BBN and could even probe the reheating temperature $T_{\rm R}$ after inflation [88, 89].

Let us now turn to the dark-matter candidates one by one: axions (Sect. 2), neutralinos (Sect. 3), gravitinos (Sect. 4), and axinos (Sect. 5). For each of those candidates, I review primordial production mechanisms, cosmological/astrophysical constraints, and prospects of experimental identification.

2 Axion dark matter

In this section we consider the axion which is a promising dark-matter candidate that is not tied to SUSY but that can coexist with any SUSY dark-matter candidate. Let us start this section with a brief review of the strong CP problem, the PQ mechanism, and a short description of basic properties of the axion. More detailed discussions can be found, e.g., in [2, 24, 81, 90–92].

The isoscalar η' meson being too heavy to qualify as a pseudo-Nambu–Goldstone boson of a spontaneously broken axial $\mathrm{U(1)_A}$ is the well-known $\mathrm{U(1)_A}$ problem of the strong interactions. This problem has an elegant solution in QCD based on non-trivial topological properties [93, 94]. The η' meson mass can be understood as a consequence of the Adler–Bell–Jackiw anomaly [95, 96] receiving contributions from gauge-field configurations with non-zero topological charge such as instantons [97]. The existence of such configurations implies the additional Θ-vacuum term in the QCD Lagrangian [93–96]

$$\mathcal{L}_\Theta = \Theta \frac{g_s^2}{32\pi^2} G^a_{\mu\nu} \widetilde{G}^{a\mu\nu} \tag{2.1}$$

with the strong coupling g_s and the gluon-field-strength tensor $G^a_{\mu\nu}$ whose dual is given by $\widetilde{G}^a_{\mu\nu} = \epsilon_{\mu\nu\rho\sigma} G^{a\,\rho\sigma}/2$. The Θ-vacuum term violates the discrete symmetries P, T, and CP for any value of $\Theta \neq n\pi$ with $n \in \mathbb{Z}$. Such violations have not been observed in strong interactions and experiments on the electric dipole moment of the neutron give an upper bound of $|\Theta| < 10^{-9}$. Within QCD, $\Theta = 0$ seems natural based on the observed conservation of those discrete symmetries. However, once QCD is embedded in the standard model of strong and electroweak interactions with CP violation being an experimental reality, Θ and the argument of the determinant of the quark mass matrix M—two *a priori* unrelated quantities—must cancel to an accuracy of 10^{-9} according to the upper bound:[3]

$$|\bar{\Theta}| \equiv |\Theta + \mathrm{Arg\,det}\, M| < 10^{-9}. \tag{2.2}$$

This fine-tuning problem is the strong CP problem (cf. also [90, 91] and references therein).

The elegant solution of the strong CP problem suggested by Peccei and Quinn [21, 22] requires a new global chiral U(1) symmetry—the PQ symmetry $\mathrm{U(1)_{PQ}}$—that is broken spontaneously at the PQ scale f_a. The corresponding pseudo-Nambu–Goldstone boson is the axion a [25, 26], which couples to gluons such that the chiral anomaly in the $\mathrm{U(1)_{PQ}}$ current is reproduced,

$$\mathcal{L}_{agg} = \frac{a}{f_a/N} \frac{g_s^2}{32\pi^2} G^a_{\mu\nu} \widetilde{G}^{a\mu\nu}, \tag{2.3}$$

[3] If one or more quarks are massless [98], $\bar{\Theta}$ can be rotated away by a chiral rotation; cf. [90, 91].

where the color anomaly N of the PQ symmetry depends on the axion model as discussed below. This interaction term (2.3) together with the vacuum term (2.1) for $\Theta \to \bar{\Theta} = \Theta + \arg\det M$ provide the axion field with an effective potential $V_{\rm eff}$ at low energies. This solves the strong CP problem since the coefficient of the CP violating $G\tilde{G}$ term becomes dynamical and vanishes for the value $\langle a\rangle = -\bar{\Theta} f_a/N$ at which $V_{\rm eff}$ has its minimum.

Because of the chiral $\mathrm{U}(1)_{\rm PQ}$ anomaly, the axion receives a mass from QCD instanton effects [99, 100] that govern the effective axion potential $V_{\rm eff}$ at low energies

$$m_a^2 = \frac{m_{\rm u} m_{\rm d}}{(m_{\rm u}+m_{\rm d})^2}\left(\frac{f_\pi m_\pi}{f_a/N}\right)^2, \tag{2.4}$$

where $m_{\rm u}$ ($m_{\rm d}$) is the mass of the up (down) quark and $f_\pi \approx 92$ MeV and $m_\pi = 135$ MeV are respectively the decay constant and mass of the pion. Using $z = m_{\rm u}/m_{\rm d}$,

$$m_a = \frac{\sqrt{z}}{1+z}\left(\frac{f_\pi m_\pi}{f_a/N}\right) \tag{2.5}$$

$$= 0.60\ \text{meV}\frac{2\sqrt{z/0.56}}{1+(z/0.56)}\left(\frac{10^{10}\,\text{GeV}}{f_a/N}\right). \tag{2.6}$$

This relation is shown for $z = 0.56$ [101] and $f_a/N \to f_a$ in Fig. 2.1 (from [24]); note that z could be within 0.3–0.6 [2].

While the original PQ proposal [21, 22] assumed f_a to be at the weak scale, axion searches, astrophysical observations, and cosmological arguments, which are discussed below, point to a significantly higher value of the PQ scale (cf. [2, 23, 24] and references therein)

$$f_a/N \gtrsim 6\times 10^8\ \text{GeV}. \tag{2.7}$$

Accordingly, the interactions of the axion are strongly suppressed and its mass must be very small, $m_a \lesssim 0.01$ eV, so that the axion can be classified as an extremely weakly interacting particle (EWIP).

Axion interactions are model dependent. The two most popular classes of phenomenologically viable "invisible axion" models are the hadronic or Kim–Shifman–Vainshtein–Zakharov (KSVZ) models [102, 103] and the Dine–Fischler–Srednicki–Zhitnitskii (DFSZ) models [104, 105]. In models of the KSVZ type, at least one additional heavy quark is introduced which couples directly to the axion while all other fields do not carry PQ charge. Thus, the axion interacts with ordinary matter through the anomaly term from loops of this new heavy quark. Integrating out the heavy-quark loops, one obtains the effective dimension-5 coupling of axions to gluons given in (2.3) with $N = 1$. In particular, couplings of the axion to standard-model matter fields are suppressed by additional loop factors. In the DFSZ schemes, no additional heavy quarks are introduced. Instead, the standard-model matter fields and at least two Higgs doublets carry appropriate PQ charges such that the axion also couples directly to the standard-model fields. Again, at low energies the axion–gluon interaction (2.3) arises, but now with $N = 6$. For more details on these axion models, we refer to the reviews [92,

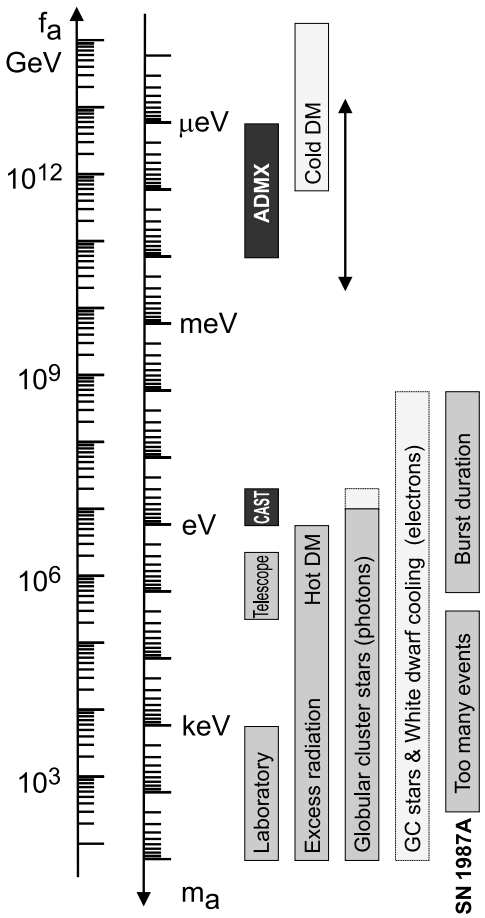

Fig. 2.1 The PQ scale f_a, its relation to the axion mass m_a (for $N = 1$) together with axion-search ranges (*dark-shaded*) and exclusion limits from axion searches, cosmological constraints, and astrophysical limits (*light-shaded* and *medium-shaded*, columns from left to right). The vertical line with the two arrowheads indicates the f_a range where Ω_a from the misalignment mechanism can provide naturally a sizable fraction of $\Omega_{\rm dm}$ for $f_a > T_{\rm R}$. For a scenario with $f_a < T_{\rm R}$, $\Omega_a > \Omega_{\rm dm}$ in the region shown by the "Cold DM" bar. The other bar in this column indicates the region that is excluded by constraints from LSS ("Hot DM") or by a thermal relic axion density $\Omega_a^{\rm therm} > \Omega_{\rm dm}$. The transition region between those constraints is excluded by telescope searches for $a \to \gamma\gamma$ decays as indicated by the "Telescope" bar in the leftmost column. The dark-shaded bars in that column indicate the search ranges of the axion-dark-matter-search experiment ADMX and of the axion helioscope CAST. The exclusion ranges in the rightmost column are inferred from the supernova SN 1987A, i.e., from the observed duration of the emitted neutrino burst ("Burst duration") and from the non-observation of axion-induced events ("Too many events"). The second column from the right applies to models with a direct axion–electron coupling and is inferred from globular-cluster (GC) stars and white-dwarf cooling. Also the middle column is inferred from GC stars but from the axion–photon coupling: While the medium-shaded bar applies to a DFSZ model, the exclusion range can be more extended in a KSVZ model as indicated by the *light-shaded* tip. Details are given in the main text. Reprinted (figure) with kind permission from [24]. Copyright (2008) by Springer Berlin/Heidelberg

106, 107]. In addition, axions with $f_a \sim 10^{16}$ GeV appear also in string theory; cf. [108–110].

For the axion lifetime τ_a and axion phenomenology, the axion–photon interaction plays a central role:

$$\mathcal{L}_{a\gamma\gamma} = \frac{g_{a\gamma\gamma}}{4} F_{\mu\nu}\widetilde{F}^{\mu\nu} \tag{2.8}$$

with the electromagnetic field-strength tensor $F_{\mu\nu}$, its dual $\widetilde{F}_{\mu\nu} = \epsilon_{\mu\nu\rho\sigma}F^{\rho\sigma}/2$, and the coupling constant

$$g_{a\gamma\gamma} = \frac{\alpha}{2\pi f_a/N}\left(\frac{E}{N} - \frac{2}{3}\frac{4+z}{1+z}\right) \tag{2.9}$$

$$= \frac{\alpha}{2\pi}\frac{1+z}{\sqrt{z}}\frac{m_a}{f_\pi m_\pi}\left(\frac{E}{N} - \frac{2}{3}\frac{4+z}{1+z}\right), \tag{2.10}$$

where both the electromagnetic anomaly E and the color anomaly N of the PQ symmetry depend on the axion model. For example, $E/N = 0$ in a KSVZ model with (an) electrically neutral new heavy quark(s) and $E/N = 8/3$ in DSFZ models. Note that $E/N = 2$ is a possibility for which the axion-photon coupling would be suppressed [111] due to cancellations in the bracket of (2.9) and (2.10).

The lifetime of the axion governed by the decay $a \to \gamma\gamma$ (and the associated rate $\Gamma_{a\to\gamma\gamma}$) is obtained from (2.8):

$$\tau_a = \Gamma^{-1}_{a\to\gamma\gamma} = \frac{64\pi}{g^2_{a\gamma\gamma}m_a^3} \tag{2.11}$$

$$\simeq 4.6\times 10^{40}\mathrm{s}\left(\frac{E}{N} - 1.95\right)^{-2}\left(\frac{f_a/N}{10^{10}\ \mathrm{GeV}}\right)^5, \tag{2.12}$$

where $z = 0.56$ was used. Comparing τ_a for $E/N = 0$ with the present age of the Universe t_0 given in (1.2), one finds $\tau_a \gtrsim t_0$ for $f_a/N \gtrsim 3\times 10^5$ GeV or equivalently $m_a \lesssim 20$ eV. Thus, the axion is stable on cosmological time scales for the f_a/N values (2.7) that are favored by cosmological and astrophysical constraints.

2.1 Primordial origin

Axion dark matter can have different origins and different properties depending on the cosmic history and on the value of f_a/N. A remarkable generic property of the axion is the fact that it is massless for $T \gtrsim 1$ GeV $\gtrsim \Lambda_{\mathrm{QCD}}$ and that it acquires mass only through instanton effects for $T \lesssim \Lambda_{\mathrm{QCD}}$ such that m_a is given by (2.5) for $T \to 0$.

The most straightforward situation is encountered when f_a/N is sufficiently small so that the axion couples sufficiently strong for being in thermal equilibrium with the early primordial plasma. The axion will then decouple (or freeze out) at a temperature $T_{\mathrm{f}} \gg m_a$ as a thermal relic

$$\Omega_a^{\mathrm{therm}}h^2 = 0.077\left(\frac{10}{g_{*S}(T_{\mathrm{f}})}\right)\left(\frac{m_a}{10\ \mathrm{eV}}\right), \tag{2.13}$$

where g_{*S} denotes the number of effectively massless degrees of freedom such that the entropy density reads $s = 2\pi^2 g_{*S}T^3/45$. For $f_a/N \lesssim 3\times 10^7$ GeV (corresponding to $m_a \gtrsim 0.2$ eV), the axion is a thermal relic that decouples after the quark–hadron transition, $T_{\mathrm{f}} \lesssim 150$ MeV, where $\pi\pi \leftrightarrow \pi a$ is a generic process that keeps the axions in thermal equilibrium before their decoupling [112, 113].[4] Accordingly, the dark-matter constraint $\Omega_a \le \Omega_{\mathrm{dm}}$ implies $m_a \lesssim 18$ eV, where also $\tau_a \gtrsim t_0$ is satisfied as discussed above. However, such axions are hot dark matter so that Ω_a can only be a minor fraction of Ω_{dm}. In fact, observations of LSS imply a restrictive limit of $m_a \lesssim 1.02$ eV (95% CL) [7, 113, 116], which is indicated as "Hot DM" in Fig. 2.1 (second column from the left).

For large values of f_a/N such that axions are never in thermal equilibrium with the primordial plasma, Ω_a becomes sensitive to the earliest cosmological history. In this limit, the simplest setting is encountered when the spontaneous breaking of the PQ symmetry occurs before inflation leading to a reheating temperature of $T_{\mathrm{R}} < f_a$ so that no PQ symmetry restoration takes place during inflation or in the course of reheating. In this setting, axionic strings can be neglected since they have been diluted by inflation and cannot be produced later on. Moreover, the initial misalignment angle Θ_i of the axion with respect to the CP-conserving position (i.e., its position in the mexican hat potential) is everywhere (basically) the same in our observable patch of the Universe. Since Θ_i is typically not at the minimum of the effective potential (i.e., not at the minimum of the tilted mexican hat) generated by instanton effects at $T \sim \Lambda_{\mathrm{QCD}}$, the field starts to oscillate coherently around its minimum for $m_a(T_{\mathrm{osc}}) \simeq 3H(T_{\mathrm{osc}})$. Once m_a takes on its T-independent value (2.4), (2.5), this axion condensate behaves as cold dark matter [27–29] with a relic density that is governed by the initial misalignment angle $-\pi < \Theta_i \le \pi$ [115, 117]:

$$\Omega_a h^2 \sim 0.15\xi f\left(\Theta_i^2\right)\Theta_i^2\left(\frac{f_a/N}{10^{12}\ \mathrm{GeV}}\right)^{7/6} \tag{2.14}$$

with $\xi = \mathcal{O}(1)$ parametrizing theoretical uncertainties related, e.g., to details of the quark–hadron transition and of the T-dependence of m_a [118] and $f(\Theta_i^2)$ accounting for anharmonicity at sizable Θ_i; $f(\Theta_i^2) \to 1$ for $\Theta_i^2 \to 0$. For 10^{10} GeV $\lesssim f_a/N \lesssim 10^{13}$ GeV, this "misalignment mechanism" can provide *naturally*, i.e., for $\Theta_i = \mathcal{O}(1)$, a sizable contribution Ω_a to Ω_{dm}, which is indicated by the vertical line with the two arrowheads in Fig. 2.1. However, with any value of $|\Theta_i| \in [0,\pi]$ being equally probable, there is always the possibility of $|\Theta_i| \approx 0$ in our patch of the Uni-

[4] Before the quark–hadron transition, axions can be kept in thermal equilibrium by QCD reactions that involve the axion-gluon interaction (2.3) with a sufficiently small f_a/N [114, 115].

verse.[5] In fact, for a finely tuned $|\Theta_i| < 10^{-2}$, this setting allows for the high values of $f_a \sim 10^{16}$ GeV suggested by concepts of grand unification and string theory [108–110]. With the original motivation for the axion residing in a solution of the fine-tuning problem (2.2), a finely tuned Θ_i is somewhat unpleasant but can be associated with anthropic considerations [119, 120]. Note that it would actually be more correct to replace Θ_i^2 in (2.14) by $\langle\Theta_i^2\rangle$ at $T \sim \Lambda_{\rm QCD}$, which cannot be arbitrarily small in the case of inflation with energy scale $E_{\rm I}$ or Hubble scale $H_{\rm I} = 8\pi G_{\rm N} E_{\rm I}^4/3$ defined when those modes exit the horizon that reenter the horizon today [108, 117, 121–124],

$$\langle\Theta_i^2\rangle \gtrsim 30\left(\frac{H_{\rm I}}{2\pi f_a/N}\right)^2, \tag{2.15}$$

due to fluctuations in the axion field from de Sitter quantum fluctuations during the inflationary epoch.

Let us now consider the case in which the spontaneous breaking of the PQ symmetry occurs after inflation, $T_{\rm R} > f_a$, again for large values of f_a/N such that axions are never in thermal equilibrium with the primordial plasma. After spontaneous breaking of the PQ symmetry at $T \sim f_a$, our observable patch of the Universe will consist of many smaller patches, each of which with an arbitrary value of $\Theta_i \in (-\pi, \pi]$, and of an associated network of axionic strings and domain walls. Indeed, since a uniform distribution of Θ_i is provided with $\langle\Theta_i^2\rangle = \pi^2/3$, the axion relic density from the misalignment mechanism becomes independent of Θ_i:

$$\Omega_a h^2 \sim 0.6\xi\left(\frac{f_a/N}{10^{12}\ {\rm GeV}}\right)^{7/6}, \tag{2.16}$$

which includes the anharmonic correction factor $f(\Theta_i^{\rm rms} = \pi/\sqrt{3}) = 1.2$. The dark-matter constraint $\Omega_a \leq \Omega_{\rm dm}$ thus implies, e.g., for a moderate $\xi \simeq 0.4$ the limit $f_a/N \lesssim 6 \times 10^{11}$ GeV ($m_a \gtrsim 10^{-5}$eV) as indicated in Fig. 2.1 (second column from the left). This limit is conservative since there can be additional sizable contributions to Ω_a from decays of axionic strings, domain walls, and non-zero momentum modes of the axion field. For a discussion of those contributions and potential domain-wall problems, see [115] and references therein.

2.2 Cosmological constraints

The thermal relic axions encountered for sufficiently small values of f_a/N will contribute to the radiation density at the time of BBN in a way analogous to the case of an extra light neutrino species. Thereby, these axions will give the following contribution to the effective number of neutrinos $N_\nu^{\rm eff}$ at $T \simeq 1$ MeV [112]:

$$\Delta N_\nu^{\rm eff} = \frac{4}{7}\left(\frac{10.75}{g_{*S}(T_{\rm f})}\right)^{4/3}. \tag{2.17}$$

For $T_{\rm f} > 1$ MeV, $\Delta N_\nu^{\rm eff} \leq 4/7 = 0.57$ which is compatible with the BBN limit [49]

$$N_\nu^{\rm eff} = 3.1^{+1.4}_{-1.2} \quad (95\%\ {\rm CL}); \tag{2.18}$$

see also Fig. 2 of Ref. [50]. However, in the literature also more restrictive limits on $\Delta N_\nu^{\rm eff}$ can be found, which can be associated with an m_a bound that is more restrictive than the limit $m_a \lesssim 1.02$ eV (95% CL) [7, 113, 116] from observations of cosmological LSS discussed in the previous section. For example, the limit $\Delta N_\nu^{\rm eff} < 0.25$ would imply $g_{*S}(T_{\rm f}) > 20$ and thereby $f_a \gtrsim 2 \times 10^7$ GeV (or $m_a \lesssim 0.3$ eV) as can be seen from Fig. 4 of Ref. [113].

For large f_a/N scenarios with PQ breaking before inflation and $T_{\rm R} < f_a$, in which axions are never in thermal equilibrium with the primordial plasma, axion density fluctuations produced during inflation lead to isocurvature [82, 117, 120, 122, 125–127] and non-Gaussian [123, 128, 129] effects in the temperature fluctuations of the CMB. Such effects are constrained by cosmological data.

With the axion field being essentially massless during inflation, de Sitter quantum fluctuations are imprinted on the axion as on any other light scalar field. Since the couplings of the axion are so weak, an isocurvature mode survives that is uncorrelated to the usual adiabatic mode seeded by the quantum fluctuations of the inflaton field. The resulting deviations from adiabaticity could manifest themselves in the temperature fluctuations of the CMB and could thereby support the existence of the axion (or, more generally, of at least two light scalar fields during inflation, one of which giving rise to dark matter that is never in thermal equilibrium with the primordial plasma).

So far, no evidence for dark-matter isocurvature perturbations has been found. Using α_0 to parameterize the ratio of the power spectrum of entropy perturbation, $P_S(k)$, to the one of curvature perturbation, $P_R(k)$, at the pivot wave number $k_0 = 0.002\ {\rm Mpc}^{-1}$,

$$\frac{\alpha(k_0)}{1-\alpha(k_0)} \equiv \frac{P_S(k_0)}{P_R(k_0)}, \tag{2.19}$$

current limits on axionic entropy perturbations are $\alpha_0 < 0.16$ (95% CL) and $\alpha_0 < 0.067$ (95% CL) obtained respectively from a WMAP-only and a WMAP + BAO + SN[6] analysis [1]. Confronting the α_0 limit with the expression

[5] In fact, as a matter of principle, it is impossible to calculate the precise value of Ω_a from first principles in this setting.

[6] Here BAO refers to baryon acoustic oscillations and SN to supernovae of type Ia. See [1] for references and details.

derived for an axion that receives quantum fluctuations with a nearly scale-invariant spectrum during inflation and $N = 1$ [117],[7]

$$\alpha(k) \simeq 2.4 \times 10^{10} \frac{G_N E_I^4 R_a^2}{\pi f_a^2 \langle \Theta_i^2 \rangle}, \tag{2.20}$$

one obtains cosmological constraints on f_a that depend on E_I (or H_I) and on the fraction $R_a = \Omega_a/\Omega_{dm}$ [117, 120].

Figure 2.2 (from [120]) shows isocurvature limits inferred from $\alpha_0 < 0.067$ for $R_a = 1$ (cyan) and $R_a \geq 0.25$ (purple) and $\Omega_a \leq \Omega_{dm}$ limits (green). The R_a independent limits (pink) are associated with the lower limit (2.15). For each of the constraints that depend on (2.14), a more and a less conservative limit obtained respectively for $\xi = 0.05$ and $\xi = 1$ is indicated by the darker and lighter shadings. The kink of these limits for $f_a > 10^{16}$ GeV results from $T_{osc} \lesssim \Lambda_{QCD}$ and an associated Ω_a expression with a different parametric dependence on f_a/N than in (2.14) derived for $T_{osc} \gtrsim \Lambda_{QCD}$; for details, see e.g. [108, 120]. The upper (lower) panel shows the case of very inefficient (efficient) thermalization at the end of inflation. The thick solid (red) lines indicate $f_a = H_I/2\pi$ and $f_a = T_{max} = \epsilon_{eff} E_I$ for $\epsilon_{eff} = 1,\ 10^{-1.5},\ 10^{-3}$. Below (above) the corresponding line, PQ symmetry restoration does (not) occur during/after inflation. Obtained from a WMAP + BAO + SN analysis [1], the current limit on the amplitude of primordial gravitational waves expressed in terms of the tensor to scalar ratio $r < 0.2$ (95% CL) excludes $E_I > 3.8 \times 10^{16}$ GeV as indicated by the orange region. In the region indicated by the horizontal (brown) bar, axion models with an unsuppressed axion-photon coupling $g_{a\gamma\gamma}$ are excluded by the axion dark-matter search experiment ADMX; cf. Fig. 2.3 and discussions in the next section. The (yellow) region with $f_a < 10^9$ GeV is disfavored by conservative astrophysical constraints; cf. Fig. 2.1. The dashed lines indicate targets of future experiments/observations.

While the quantum fluctuations in Θ_i during inflation are Gaussian distributed, the axion-induced temperature fluctuations in the CMB are governed by fluctuations in the axion number density after formation of the axion condensate with $n_a \propto \Theta_i^2$ modulo anharmonic corrections. Thereby a non-linearity enters that leads to a non-Gaussian contribution to the CMB temperature fluctuation [123, 128, 129]. This may allow one to probe axions cosmologically even for the case $\Omega_a \ll \Omega_{dm}$ [129].

If the PQ symmetry is not broken before inflation, there will be no light axion field present to acquire de Sitter quantum fluctuations and thus no axionic source of isocurvature perturbations. Also if the PQ symmetry is restored during inflation, $H_I/2\pi > f_a$ (i.e., the typical amplitude of quan-

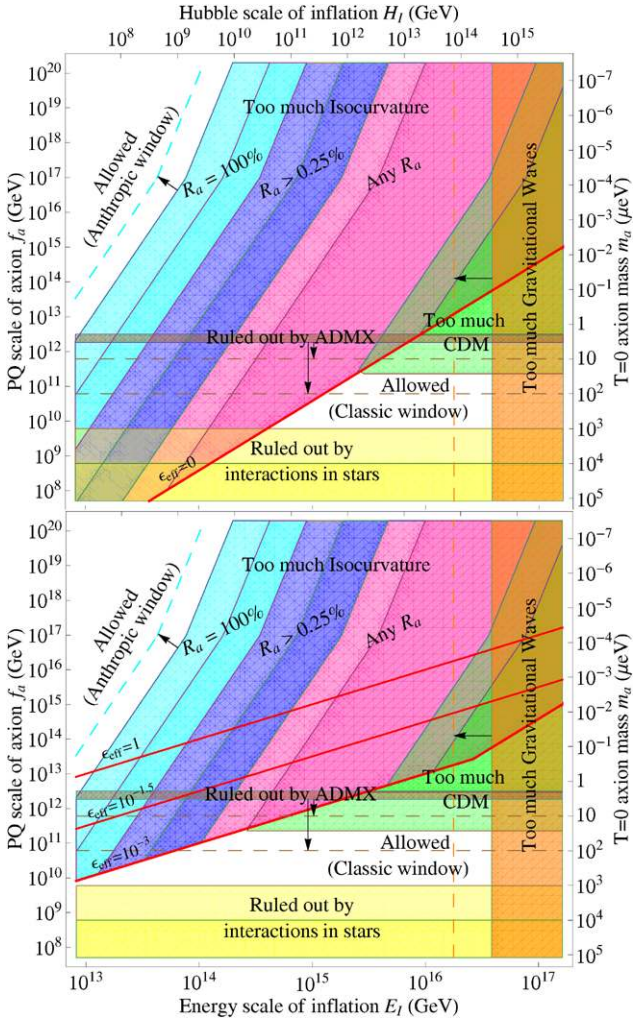

Fig. 2.2 Constraints on the PQ scale f_a (for $N = 1$) as a function of the energy scale of inflation E_I or Hubble scale $H_I = 8\pi G_N E_I^4/3$ defined when those modes exit the horizon that reenter the horizon today. The *thick solid* (*red*) lines show $f_a = H_I/2\pi$ (*upper panel*) and $f_a = T_{max} = \epsilon_{eff} E_I$ for $\epsilon_{eff} = 1,\ 10^{-1.5},\ 10^{-3}$ (*lower panel*). Below (above) the corresponding line, PQ symmetry restoration does (not) occur during/after inflation. The hatched regions above those lines show the cosmological constraints from the WMAP + BAO + SN limit $\alpha_0 < 0.067$ (95% CL) on axionic isocurvature perturbations (2.20). Those constraints depend on $R_a = \Omega_a/\Omega_{dm}$ as labeled and as indicated by the different shadings. The constraints labeled as "Any R_a" result from the lower limit on axion fluctuations due to quantum fluctuations during inflation (2.15). For $E_I > 10^{15}$ GeV, this can lead to $\Omega_a > \Omega_{dm}$ as indicated by the (*green*) region labeled as "Too much CDM". The WMAP + BAO + SN limit on the tensor to scalar ratio $r < 0.2$ (95% CL) excludes the region with $E_I > 3.8 \times 10^{16}$ GeV. The exclusion ranges from axion searches and astrophysical considerations are indicated respectively by the *dark* (*brown*) *horizontal bar* and by the *light-shaded* (*yellow*) *region* with $f_a < 10^9$ GeV. For $f_a > M_P$, the PQ scale is super-Planckian. More details are given in the main text. Reprinted (figure) with kind permission from [120]. Copyright (2008) by the American Physical Society

[7] Note that there are typos in (44) and (27) of Ref. [117]. The corrected prefactor in (44) is 2.4×10^{10} and the associated limit in (27) should read 1.2×10^{16} GeV. I thank J. Lesgourgues for the clarification.

tum fluctuations exceeds the PQ scale), or during reheating, $T_{\max} > f_a$ (i.e., thermal PQ symmetry restoration), primordial axionic perturbations will be washed out which implies negligible axion-induced deviations from adiabaticity. Moreover, as described in the previous section, the subsequent PQ breaking will lead to a sample of Θ_i values with a flat probability distribution after PQ breaking. Since these Θ_i values are distributed at random throughout our observable Universe, spatial axion density variations are expected once the axion acquires its mass. These variations can then lead to "axion mini-clusters" containing a sizable contribution to $\Omega_{\rm dm}$ [115].

2.3 Astrophysical constraints

Axions could be produced not only in the early Universe but also in hot and dense astrophysical environments such as those encountered in ordinary stars, white dwarfs, and supernovae. The axion luminosity L_a of such sources depends on f_a, the relevant axion-production processes (and thereby on the axion couplings and model), and on the astrophysical understanding/model of the source under consideration. A sizable axion luminosity is associated with an additional energy transport out of the corresponding astrophysical source. This can affect the behavior/characteristics of the source strongly. Astrophysical studies of stars, white dwarfs, and supernovae can thus be used to derive constraints on f_a/N or m_a [24, 81, 130–134].

To allow for axion production, the relevant energy/temperature in the source must be sufficiently large with respect to m_a already for kinematical reasons. In addition, the interaction strength of the axion enters in the following two ways. On the one hand, a stronger axion interaction (smaller f_a/N or larger m_a) allows for a more efficient production in the source. On the other hand, stronger interactions are also associated with smaller mean free paths in medium and possibly with rescatterings within the source which can delay energy emission via the axion channel.

The current status of astrophysical axion bounds is reviewed, e.g., in Refs. [2, 24] and shown in Fig. 2.1 (three rightmost columns). Here only a brief summary is given.

In stars including our sun, axions can be produced via their coupling to photons $g_{a\gamma\gamma}$ through the Primakoff process $\gamma + Ze \to Ze + a$ [130, 135–137]. The axionic energy drain (described by $L_a \propto g_{a\gamma\gamma}^2$) can then lead to an enhanced consumption of nuclear fuel within the star and can thereby, e.g., shorten the lifetime of a star. In this respect globular clusters (GCs), which are bound systems of a homogeneous population of low-mass stars, are particularly valuable since they allow for tests of stellar-evolution theory. In fact, studies of GC stars point to $g_{a\gamma\gamma} \lesssim 10^{-10}$ GeV^{-1} [24, 134, 138] which implies $f_a > 2.3 \times 10^7$ GeV in a KSVZ axion model with $E/N = 0$ and $f_a > 0.8 \times 10^7$ GeV in a DFSZ axion model with $E/N = 8/3$ for $z = 0.56$. These limits are indicated by the middle column in Fig. 2.1. Not shown are the limits inferred from studies of our sun since they are less restrictive. For example, helioseismological studies of the sound-speed profile give the limit $g_{a\gamma\gamma} \lesssim 10^{-9}$ GeV^{-1} [139]. Moreover, $g_{a\gamma\gamma} \lesssim 5 \times 10^{-10}$ GeV^{-1} [24] is inferred from measurements of the solar ^{8}B neutrino flux which is sensitive to enhanced nuclear burning [139].

Axion production via $\gamma + e^- \to e^- + a$ and $e^- + Ze \to Ze + e^- + a$ is more efficient than the Primakoff processes in models with a direct axion-electron coupling g_{aee}. Studies of GC stars [140] and of white-dwarf cooling [141–144] thereby lead to restrictive limits on g_{aee}. For the DSFZ model with two Higgs doublets carrying PQ charge and the ratio of the associated Higgs vacuum expectation values (VEVs) given by $\tan\beta$, these limits imply $f_a < 1.3 \times 10^9 \text{GeV} \cos^2\beta$ [24] which is indicated for $\cos^2\beta = 0.5$ by the second column from the right in Fig. 2.1.

In core-collapse supernovae (SN of type II) that lead to the formation of a hot—$T = \mathcal{O}(10$ MeV)—proto-neutron star, axions can be produced via their coupling to nucleons g_{aNN} through axion bremsstrahlung emission $N + N \to N + N + a$ [145, 146] in the dense nuclear medium [145, 147–151]. In fact, in these dense environments even the mean free path of neutrinos is such that they rescatter and diffuse out before carrying away energy. This picture was confirmed by the observed duration of about 10 s of the neutrino burst from the supernova SN 1987A. Since axion emission would be an additional energy drain, it would reduce the cooling time and this burst duration. The observed burst duration thereby implies $f_a \gtrsim 4 \times 10^8$ GeV [24] as indicated by the upper bar in the rightmost column of Fig. 2.1. For $f_a \lesssim 6 \times 10^5$ GeV, axions cannot affect the neutrino burst duration significantly since their coupling becomes so strong that they rescatter within the dense medium [152, 153]. For $f_a \lesssim 3 \times 10^5$ GeV, the axion coupling would have been strong enough for axion-induced events that have not been observed for the supernova SN 1987A [154]. This is indicated by the lower bar in the rightmost column of Fig. 2.1. The gap between the two bars is known as the "hadronic axion window" which was thought to be an allowed region for KSVZ models with strongly suppressed $g_{a\gamma\gamma}$ [155]. However, this window is closed by the hot dark-matter constraint from LSS observations [7, 113, 116] discussed in Sect. 2.1 and indicated by the second column from the left in Fig. 2.1.

2.4 Experimental searches and prospects

Axion searches started already more than 30 years ago and excluded soon f_a values close to the weak scale, e.g., from studies of the branching ratio BR($K^+ \to \pi^+ +$ nothing), as indicated by the bar at the bottom ("Laboratory") of the

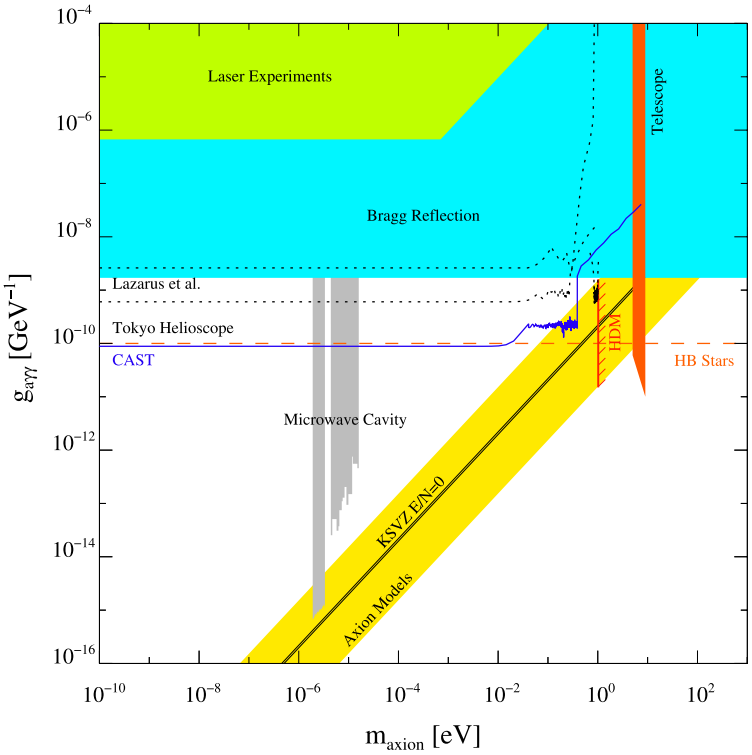

Fig. 2.3 Axion exclusion limits in the plane spanned by m_a and $g_{a\gamma\gamma}$. The *diagonal* (*yellow*) *bar* ("Axion Models") and the *solid diagonal line* ("KSVZ E/N = 0") show respectively the region of typical invisible axion models and $g_{a\gamma\gamma}$ in the KSVZ model with $E/N = 0$. The cosmological hot dark-matter constraint [7, 113, 116] is shown by the *short vertical* (*orange*) *line* ("HDM") within this region and the astrophysical limit from studies of stars on the horizontal branch (HB) in GBs by the *vertical dashed* (*orange*) *line* ("HB stars") [24, 134, 138]. The telescope search for $a \to \gamma\gamma$ decays reported in Ref. [159] excludes the *pencil-like* (*orange*) *region* ("Telescope") and direct axion searches with microwave cavities the *pencil-like gray region* ("Microwave Cavity") [156, 160, 161]. Solar axion searches with axion helioscopes exclude the regions above the upper ("Lazarus et al.") and lower ("Tokyo Helioscope") dotted lines and the one above the solid (blue) line ("CAST") [162–165]. The *medium-shaded* (*cyan*) *region* ("Bragg Reflection") is excluded by searches for axion conversion in the Coulomb field of nuclei in a crystal lattice [166–168] and the *light-shaded* (*green*) *region* ("Laser Experiments") by searches for a "light-shining through a wall" event [169]. I thank M. Kuster for providing this update of Fig. 10.26 of Ref. [156]

leftmost column in Fig. 2.1. Present day axion searches are probing much larger values of f_a/N including those of invisible axion models and those in which axions can provide the dominant component of dark matter [2, 23, 156]. Depending on the expected origin of the axions, these searches can be classified into those for cosmic axions, solar axions (or more generally axions from astrophysical sources), and axions produced in the laboratory.

Most axion searches rely on the axion–photon coupling $g_{a\gamma\gamma}$.[8] Since the axion has not been discovered so far, negative searches can be translated into m_a-dependent (or f_a-dependent) limits on $g_{a\gamma\gamma}$. A summary of those exclusion limits is given in Fig. 2.3 which is an update of Fig. 10.26 of Ref. [156] by courtesy of M. Kuster. Here the diagonal (yellow) bar and the solid diagonal line indicate the region of typical invisible axion models and $g_{a\gamma\gamma}$ in the KSVZ model with $E/N = 0$, respectively. The cosmological hot dark matter constraint $m_a \lesssim 1$ eV [7, 113, 116] is shown by the short vertical (orange) line ("HDM") within this region and the astrophysical limit from studies of stars on the horizontal branch (HB) in GBs $g_{a\gamma\gamma} \lesssim 10^{-10}$ GeV^{-1} by the vertical dashed (orange) line ("HB stars") [24, 134, 138]. Let us recall that axions can provide a significant contribution to $\Omega_{\rm dm}$ for $m_a \lesssim 3 \times 10^{-4}$ eV.

Sizable cosmic axion densities are expected in galaxy clusters and galaxies and thereby also on Earth. There are indirect and direct searches for those cosmic axions. In the indirect ones, telescopes are used to look for photons from $a \to \gamma\gamma$ decays, for example, in the Abell clusters [159, 170, 171] and in nearby dwarf galaxies [172]. After correcting for the Doppler shift due to the motion of the host, one expects a basically mono-chromatic spectrum of the resulting γ's at $E_\gamma = m_a/2$. In addition to possible insights into m_a, also τ_a is probed in these telescope searches. No such γ's have been identified unambiguously so far which implies that τ_a can respect (1.2). The associated exclusion lim-

[8] Fifth-force experiments allow for $g_{a\gamma\gamma}$-independent axion searches [157]; see [158] and references therein.

its (labeled as "Telescope") are shown by the corresponding bar in the leftmost column in Fig. 2.1 and by the vertical pencil-like (orange) region in Fig. 2.3.

In direct searches for cosmic axions, microwave cavities are used to look for resonant conversion of those axions—pervading Earth—into photons [160, 161, 173–177] along the haloscope technique proposed in [178]. Through the cavity frequency at which the resonance would appear and through the width of the resonance, these experiments are sensitive to m_a and to the virial distribution of thermalized axions and thereby to the axion distribution in the galactic halo. In fact, microwave resonant-cavity experiments probe exactly the m_a range in which axions can provide a sizable contribution to $\Omega_{\rm dm}$; cf. bar labeled as "ADMX" in the leftmost column in Fig. 2.1. Moreover, the ADMX experiment has achieved a sensitivity such that realistic axion models have already been probed and excluded at 90% CL in a narrow m_a range [160, 161]. Indeed, no axion signal has been observed so far. The associated exclusion limits are shown by the horizontal (brown) bar in Fig. 2.2 and by the vertical pencil-like gray regions labeled as "Microwave Cavity" in Fig. 2.3. An upgrade of ADMX is underway that should allow one to probe realistic axion models over a much larger m_a range [176, 177]. Relying on Rydberg-atom detectors, an upgrade of the cavity experiment CARRACK is aiming at a similar sensitivity and search range [176, 179].

As already addressed in the previous section, axions could be produced in astrophysical sources such as our sun. Searching for solar axions means to look for the conversion of such axions into γ's in an electromagnetic field via the inverse Primakoff process. In axion helioscopes [162, 163, 178, 180–182], this field is provided by a strong magnet that is pointed at the sun. Using Bragg diffraction at crystal detectors [166–168], it is the Coulomb field of the nuclei in the crystal lattice that provides the field. Also the geomagnetic field of the Earth can allow in principle for the conversion of solar axions into photons which could be detected by a satellite on the dark side of the Earth [183]. Existing solar axion searches provide so far only m_a-dependent exclusion limits on $g_{a\gamma\gamma}$. The ones from axion helioscopes are indicated by the upper ("Lazarus et al.") and lower ("Tokyo Helioscope") dotted lines and by the solid (blue) line ("CAST") line in Fig. 2.3. Among those limits, the most restrictive one is provided by the CERN Axion Solar Telescope (CAST): $g_{a\gamma\gamma} < 8.8 \times 10^{-11}$ GeV^{-1} for $m_a < 0.02$ eV [162, 163]. Currently, the Tokyo Helioscope and CAST are probing already the parameter region with realistic axion models [164, 165] but for $m_a > 10^{-2}$ eV which is associated with warm/hot axion dark-matter scenarios. Indeed, an axion discovery in that region would imply that axions cannot be the dominant component of $\Omega_{\rm dm}$ for a standard cosmological history[9] so that there is room, for example, for the LSP to take over that part. The m_a-independent exclusion limit from Bragg reflection $g_{a\gamma\gamma} \lesssim 1.7 \times 10^{-9}$ GeV^{-1} obtained by the DAMA collaboration [167] is indicated by the medium-shaded (cyan) region (labeled accordingly) in Fig. 2.3; similar limits were obtained by COSME [166] and SOLAX [168]. Not shown is the limit $g_{a\gamma\gamma} \lesssim 10^{-11}$ GeV for $m_a \lesssim 10^{-9}$ eV that has been inferred from the absence of γ-ray bursts in coincidence with the SN 1987A neutrino burst [185, 186]. Such bursts could have originated from axions produced in the SN 1987A that had been converted subsequently into photons in the galactic magnetic field.

Axion searches are also performed purely in the laboratory. Using the Primakoff process, one should in principle be able to convert a small fraction of the photons of a laser beam in a strong transverse magnetic field into axions. In contrast to the photons, those axions should be able to traverse a wall. In a second strong magnetic field behind the wall, there should also be a non-zero probability for the inverse Primakoff effect in which the axion is reconverted into a detectable photon. The overall probability of such a "light-shining through a wall" event is proportional to $g_{a\gamma\gamma}^4$. No event of this sort has been observed so far and the Brookhaven-Fermilab-Rutherford-Trieste (BFRT) collaboration has inferred $g_{a\gamma\gamma} < 6.7 \times 10^{-7}$ GeV (95% CL) for $m_a < 10^{-3}$ eV [169] as indicated by the light-shaded (green) region labeled as "Laser Experiments" in Fig. 2.3.

Another way to search for axions in the laboratory relies on the prediction that axions can affect the polarization of light that propagates in vacuum through a transverse magnetic field. In fact, because of their coupling to photons $g_{a\gamma\gamma}$, axions can induce dispersive and absorptive processes and thereby the following two phenomena [187]: (i) linear dichroism, which refers to a rotation of the polarization vector by a finite angle, and (ii) birefringence, which refers to the introduction of an ellipticity and an rotation of an initially linearly polarized beam. Searching for these phenomena, the BFRT experiment has extracted the exclusion limit $g_{a\gamma\gamma} < 3.6 \times 10^{-7}$ GeV (95% CL) for $m_a < 5 \times 10^{-4}$ eV. Note that the evidence for vacuum dichroism claimed by the PVLAS collaboration in the year 2006 [188] has been retracted recently [189]. Originally, they had interpreted their findings in terms of the presence of an axion-like particle (ALP) with a mass of (1–1.5) $\times 10^{-3}$ eV and a coupling to photons in the range (1.7–5) $\times 10^{-6}$ GeV^{-1} [188]. The retraction reassures the validity of the astrophysical constraints that had already excluded the region in which this signal was reported.

With new experiments and updates underway, the next years will become very exciting for axion searches. Both helioscope and haloscope experiments are about to probe significant parts of complementary parameter regions of realistic axion models. For example, an axion signal at ADMX

[9] For axion cosmology with a non-standard cosmological history, see e.g. [184].

would support the hypothesis of $\Omega_{\rm dm}$ provided by axions from the misalignment mechanism. In contrast, an axion observation at CAST would point to axion hot/warm dark matter which can only provide a minor fraction of $\Omega_{\rm dm}$ so that the dominant contribution can still be provided, e.g., by the LSP if SUSY is realized in nature. In fact, if the axino—the fermionic superpartner of the axion—is the LSP, collider signatures predicted for the axino LSP [190] could become an additional hint towards the existence of the axion and the solution of the strong CP problem proposed by Peccei and Quinn.

3 Neutralino dark matter

In this section we consider SUSY scenarios in which the lightest neutralino $\widetilde{\chi}_1^0$ is the LSP. This hypothetical particle is probably the most studied and most popular SUSY dark-matter candidate and a concrete example for a weakly interacting massive particle (WIMP). Before discussing $\widetilde{\chi}_1^0$ dark-matter scenarios, let us review some generic properties of SUSY extensions of the standard model. For details, we refer to dedicated reviews on SUSY [30–35].

Extending the standard model with SUSY, there is a superpartner of each standard-model particle and an extended Higgs sector with a least two Higgs doublets. The couplings of these superpartners arise by supersymmetrizing the standard-model couplings and are thus fixed by symmetry. This allows for model independent SUSY predictions that can be tested in collider experiments [191–193]. The masses of the standard-model superpartners are governed by the Higgs-higgsino mass parameter μ and by soft SUSY breaking parameters which depend on the SUSY breaking mechanism and thereby on physics at high-energy scales such as the one of grand unification $M_{\rm GUT} \simeq 2 \times 10^{16}$ GeV. The experimental determination of the SUSY mass spectrum and of the Higgs masses at colliders can thus provide insights into high-scale physics and into the SUSY breaking mechanism [194–197].

Assuming that SUSY is realized not only as global but as a local symmetry [30], the gravitino $\widetilde{G}$ appears as the spin-3/2 superpartner of the graviton in addition to the standard-model superpartners. The gravitino is the gauge field associated with local SUSY transformations and a singlet with respect to the gauge groups of the standard model. Its interactions—given by the supergravity Lagrangian [30, 198]—are suppressed by the (reduced) Planck scale [2]

$$\mathrm{M_P} = 2.4 \times 10^{18}\ \mathrm{GeV}. \tag{3.1}$$

Once SUSY is broken, the extremely weak gravitino interactions are enhanced through the super-Higgs mechanism, in particular, at energy/mass scales that are large with respect to the gravitino mass $m_{\widetilde{G}}$. Nevertheless, the gravitino can be classified as an extremely weakly interacting particle (EWIP). Since the gravitino $\widetilde{G}$ is the gauge field of local SUSY, its mass $m_{\widetilde{G}}$ is governed by the scale of SUSY breaking and can range from the eV scale to scales beyond the TeV region [31, 33, 199–204]. For example, in gauge-mediated SUSY breaking schemes [199–201], the mass of the gravitino is typically less than 1 GeV, while in gravity-mediated schemes [31, 33] it is expected to be in the GeV to TeV range. In fact, SUSY scenarios in which the gravitino is the stable LSP are well motivated and will be discussed in the next section. In this section, $m_{\widetilde{G}}$ is assumed to be above the neutralino mass $m_{\widetilde{\chi}_1^0}$. This implies an unstable $\widetilde{G}$ which can be associated with an additional source of $\widetilde{\chi}_1^0$ dark matter (cf. Sect. 3.1) and with restrictive BBN constraints on the reheating temperature $T_{\rm R}$ (cf. Sect. 3.2).

The lightest neutralino $\widetilde{\chi}_1^0$ appears in the minimal supersymmetric standard model (MSSM) as the lightest mass eigenstate among the four neutralinos being mixtures of the bino $\widetilde{B}$, the wino $\widetilde{W}$, and the neutral higgsinos $\widetilde{H}_{\rm u}^0$ and $\widetilde{H}_{\rm d}^0$. Accordingly, $\widetilde{\chi}_1^0$ is a spin 1/2 fermion with weak interactions only. Its mass $m_{\widetilde{\chi}_1^0}$ depends on the gaugino mass parameters M_1 and M_2, on the ratio of the two MSSM Higgs doublet vacuum expectation values $\tan\beta$, and on the Higgs-higgsino mass parameter μ. Expecting $m_{\widetilde{\chi}_1^0} = \mathcal{O}(100\ \mathrm{GeV})$, $\widetilde{\chi}_1^0$ is classified as a WIMP.

Motivated by theories of grand unification and supergravity [205] and by experimental constraints on flavor mixing and CP violation [2], one often assumes universal soft SUSY breaking parameters at the scale of grand unification $M_{\rm GUT}$; cf. [33–35, 206] and references therein. For example, in the framework of the constrained MSSM (CMSSM), the gaugino masses, the scalar masses, and the trilinear scalar interactions are assumed to take on the respective universal values $m_{1/2}$, m_0, and A_0 at $M_{\rm GUT}$. Specifying $m_{1/2}$, m_0, A_0, $\tan\beta$, and the sign of μ, the low-energy mass spectrum is given by the renormalization group running from $M_{\rm GUT}$ downwards.

For $A_0 = 0$, for example, the lightest standard-model superpartner—or lightest ordinary superpartner (LOSP)—is either the lightest neutralino $\widetilde{\chi}_1^0$ or the lighter stau $\widetilde{\tau}_1$, whose mass is denoted by $m_{\widetilde{\tau}_1}$. If the LSP is assumed to be the LOSP, the parameter region in which $m_{\widetilde{\tau}_1} < m_{\widetilde{\chi}_1^0}$ is usually not considered because of severe upper limits on the abundance of stable charged particles [2]. However, in gravitino/axino LSP scenarios, in which the LOSP is the next-to-lightest supersymmetric particle (NLSP), the $\widetilde{\tau}_1$ LOSP case is viable and particularly promising for collider phenomenology as will be discussed in Sects. 4 and 5.

In Fig. 3.1 (from [207]) the dotted (blue) lines show contours of $m_{\rm LOSP}$ in the $(m_{1/2}, m_0)$ plane for $A_0 = 0$, $\mu > 0$, $\tan\beta = 10$. Above (below) the dashed line, $m_{\widetilde{\chi}_1^0} < m_{\widetilde{\tau}_1}$ ($m_{\widetilde{\tau}_1} < m_{\widetilde{\chi}_1^0}$). The medium gray and the light gray regions at small $m_{1/2}$ are excluded respectively by the mass

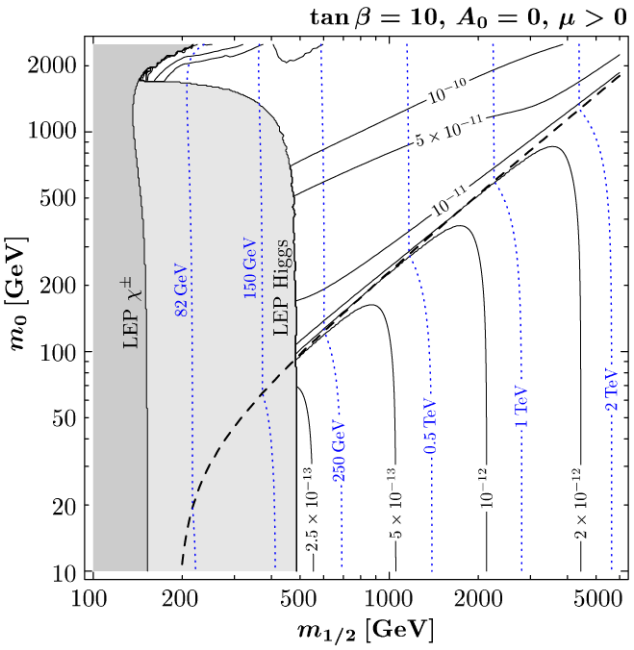

Fig. 3.1 Contours of m_{LOSP} (*dotted blue lines*) and $Y^{\mathrm{dec}}_{\mathrm{LOSP}}$ (*solid black lines*) in the $(m_{1/2}, m_0)$ plane for $A_0 = 0$, $\mu > 0$, $\tan\beta = 10$. Above (below) the dashed line, $m_{\widetilde{\chi}^0_1} < m_{\widetilde{\tau}_1}$ ($m_{\widetilde{\tau}_1} < m_{\widetilde{\chi}^0_1}$). The *medium gray* and the *light gray regions* show the LEP bounds $m_{\widetilde{\chi}^\pm_1} > 94$ GeV and $m_{\mathrm{H}} > 114.4$ GeV, respectively [2]. The contours are obtained with the spectrum generator `SuSpect 2.34` [208] using $m_t = 172.5$ GeV and $m_{\mathrm{b}}(m_{\mathrm{b}})^{\overline{\mathrm{MS}}} = 4.23$ GeV, and with `micrOMEGAs 1.3.7` [209, 210]. Reprinted (figure) with kind permission from [207]. Copyright (2007) by Elsevier

bounds $m_{\widetilde{\chi}^\pm_1} > 94$ GeV and $m_{\mathrm{H}} > 114.4$ GeV from chargino and Higgs searches at LEP [2]. It can be seen that $m_{\widetilde{\chi}^0_1} = \mathcal{O}$ (100 GeV) appears naturally within the CMSSM.

Before proceeding, let us comment on other potential LOSP/LSP/NLSP candidates. For $A_0 \neq 0$ and in less constrained frameworks such as models with non-universal Higgs masses (NUHM), there are parameter regions in which the LOSP is the lighter stop $\widetilde{t}_1$ [211–213] or the lightest sneutrino $\widetilde{\nu}_1$ [214–219]. In fact, since the lightest sneutrino $\widetilde{\nu}_1$ is electrically neutral and color neutral, the $\widetilde{\nu}_1$ LSP looks at first sight like another promising WIMP dark-matter candidate within the MSSM. It turns out however that its couplings (and in particular the one to the Z-boson) are "too strong." From the invisible Z-boson width, we know that the sneutrino must have a mass $m_{\widetilde{\nu}_1} > M_{\mathrm{Z}}/2$, where the its relic density is typically well below Ω_{dm} and/or its interactions with nuclei are such that it should have already been observed in direct dark-matter searches (assuming a standard dark matter halo profile); cf. Figs. 1 and 2 in Ref. [220]. Thus, the MSSM sneutrino LSP is not considered a viable dark-matter candidate [221] but it may well be the NLSP, e.g., in a gravitino/axino LSP scenario [217–219, 222–224].[10] The lighter stop $\widetilde{t}_1$ is not viable as a stable LSP due to severe constraints on exotic stable colored particles [2] but another NLSP candidate.[11] While the NLSP governs cosmological constraints and experimental prospects in gravitino/axino dark-matter scenarios in a crucial way (cf. Sects. 4 and 5), it can also be important in a neutralino dark-matter scenario (e.g., through coannihilation processes) as will become clear below.

3.1 Primordial origin

The $\widetilde{\chi}^0_1$'s were in thermal equilibrium for primordial temperatures of $T > T_{\mathrm{f}} \simeq m_{\widetilde{\chi}^0_1}/20$. At T_{f}, the annihilation rate of the (by then) non-relativistic $\widetilde{\chi}^0_1$'s becomes smaller than the Hubble rate so that they decouple from the thermal plasma. Thus, for $T \lesssim T_{\mathrm{f}}$, their yield $Y_{\widetilde{\chi}^0_1} \equiv n_{\widetilde{\chi}^0_1}/s$ is given by $Y^{\mathrm{dec}}_{\widetilde{\chi}^0_1} \approx Y^{\mathrm{eq}}_{\widetilde{\chi}^0_1}(T_{\mathrm{f}})$, where $n^{(\mathrm{eq})}_{\widetilde{\chi}^0_1}$ is the (equilibrium) number density of $\widetilde{\chi}^0_1$'s. Depending on details of the $\widetilde{\chi}^0_1$ decoupling, $Y^{\mathrm{dec}}_{\widetilde{\chi}^0_1}$ is very sensitive to the mass spectrum and the couplings of the superparticles. Indeed, convenient computer programs such as `DarkSUSY` [225] or `micrOMEGAs` [209, 210, 226, 227] are available which allow for a numerical calculation of LOSP decoupling and of the resulting thermal relic abundance in a given SUSY model.

The $Y^{\mathrm{dec}}_{\mathrm{LOSP}}$ contours shown by the solid black lines in Fig. 3.1 illustrate that the $\widetilde{\chi}^0_1$ LSP yield can easily vary by more than an order of magnitude. Because of this sensitivity, the associated thermal relic density

$$\Omega^{\mathrm{therm}}_{\widetilde{\chi}^0_1} h^2 = m_{\widetilde{\chi}^0_1} Y^{\mathrm{dec}}_{\widetilde{\chi}^0_1} s(T_0) h^2/\rho_c \tag{3.2}$$

agrees with $\Omega^{3\sigma}_{\mathrm{dm}} h^2$ only in narrow regions in the parameter space; $\rho_c/[s(T_0)h^2] = 3.6 \times 10^{-9}$ GeV [2]. This can be seen in Fig. 3.2 (from [228]) where the black strips indicate the region with $0.087 \leq \Omega^{\mathrm{therm}}_{\widetilde{\chi}^0_1} h^2 \leq 0.138$.

Remarkably, it is exactly the small width of the regions with $\Omega^{\mathrm{therm}}_{\widetilde{\chi}^0_1} = \Omega_{\mathrm{dm}}$, which could help us to identify $\widetilde{\chi}^0_1$ dark matter. If sparticles exist and if they are produced at colliders, the data analysis will aim at determining the SUSY model realized in nature [196, 197]. For the reconstructed model, a precise calculation of $\Omega^{\mathrm{therm}}_{\widetilde{\chi}^0_1}$ is possible assuming a standard thermal history of the Universe. Because of the sensitivity of $\Omega^{\mathrm{therm}}_{\widetilde{\chi}^0_1}$ with respect to the SUSY model,

[10] Variants of the MSSM sneutrinos are actively pursued as dark matter candidates; see [220, 255] and references therein. With an admixture of less strongly interacting "right-handed" sneutrinos, sneutrino dark-matter interactions can become compatible with $\Omega_{\widetilde{\nu}_1} \simeq \Omega_{\mathrm{dm}}$ and with constraints from direct searches.

[11] Note that the mass of a long-lived $\widetilde{t}_1$ NLSP has to respect the collider bound, $m_{\widetilde{t}_1} > 250$ GeV, inferred from SUSY searches at the Fermilab Tevatron [213].

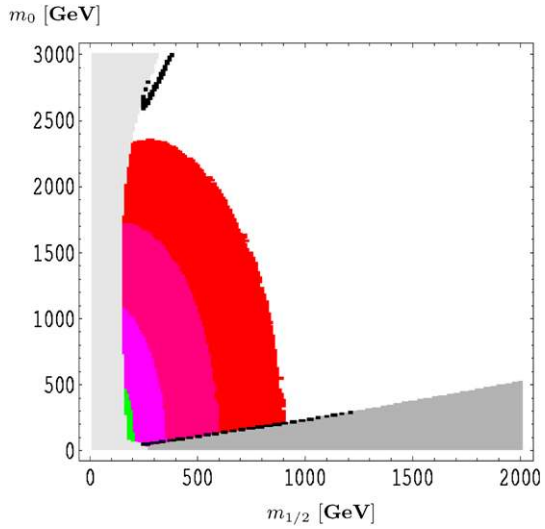

Fig. 3.2 Regions (*black*) with $0.087 \leq \Omega^{\rm therm}_{\widetilde{\chi}^0_1} h^2 \leq 0.138$ in the $(m_{1/2}, m_0)$ plane for $A_0 = 0$, $\mu > 0$, $\tan\beta = 10$, and $m_t = 172.7$ GeV. In the *dark gray triangular region*, $m_{\widetilde{\chi}^0_1} > m_{\widetilde{\tau}_1}$. The *light gray region* at small $m_{1/2}$ is excluded by the requirement of correct electroweak symmetry breaking or by sparticle search limits [228], the two *medium-shaded* (*light pink*) *bands* by the LEP bound $m_{\rm H} > 114$ GeV, and the small *light-shaded* (*green*) *spot* by the $b \to s\gamma$ constraint: $2.65 \leq {\rm BR}(b \to s\gamma)/10^{-4} \leq 4.45$. The *dark-shaded* (*red*) *band* is compatible with having a standard-model-like Higgs boson near 115 GeV. Reprinted (figure) with kind permission from [228]. Copyright (2006) by SISSA

an agreement of the obtained $\Omega^{\rm therm}_{\widetilde{\chi}^0_1}$ with $\Omega_{\rm dm}$ will then be a strong hint for the $\widetilde{\chi}^0_1$ LSP providing $\Omega_{\rm dm}$ and for a standard thermal history up to the $\widetilde{\chi}^0_1$-decoupling temperature $T_{\rm f}$. Since $\widetilde{\chi}^0_1$'s decouple already as a non-relati vistic species, it is also guaranteed that they are sufficiently cold to allow for cosmic structure formation.

In fact, $\Omega^{\rm therm}_{\widetilde{\chi}^0_1}$ exceeds $\Omega_{\rm dm}$ in most of the parameter space. Thus, regions with $\Omega^{\rm therm}_{\widetilde{\chi}^0_1} \simeq \Omega_{\rm dm}$ are somewhat special and associated with particularly efficient neutralino annihilation in the early Universe. Depending on the origin for the efficient annihilation, these regions can be classified as follows; cf. [34, 35, 206, 228, 254] and references therein.

- Bulk region: this region is associated with light sleptons $\tilde{l}_1$, $m_{\tilde{l}_1} \lesssim 200$ GeV, so that neutralinos can annihilate efficiently via slepton exchange into a lepton pair: $\widetilde{\chi}^0_1\widetilde{\chi}^0_1 \to l^+l^-$. This region is often in tension with the LEP Higgs bound. For example, in the CMSSM scenarios considered in Figs. 3.1 and 3.2, the bulk region appears around $(m_0, m_{1/2}) \simeq (60\ {\rm GeV}, 200\ {\rm GeV})$.
- Focus point region/hyperbolic branch: this region is associated with a $\widetilde{\chi}^0_1$ with a significant higgsino admixture so that $\widetilde{\chi}^0_1\widetilde{\chi}^0_1 \to W^+W^-, Z^0Z^0$ become efficient. (In fact, for a purely bino-like neutralino, $\widetilde{\chi}^0_1 = \widetilde{B}$, annihilation into these final states cannot occur.) In Fig. 3.2, the black region with $\Omega^{\rm therm}_{\widetilde{\chi}^0_1} \simeq \Omega_{\rm dm}$ at large m_0 is associated with these neutralino annihilation channels being efficient.
- Coannihilation region: in this region, the NLSP has a mass very close to the one of the neutralino LSP. Thereby, the number density of the NLSP during the freeze out of the $\widetilde{\chi}^0_1$ LSP is sizable and $\widetilde{\chi}^0_1$–NLSP coannihilation processes can enhance the efficiency of neutralino annihilation. In Fig. 3.2, the black region with $\Omega^{\rm therm}_{\widetilde{\chi}^0_1} \simeq \Omega_{\rm dm}$ just above the dark gray stau LOSP region is associated with efficient $\widetilde{\chi}^0_1$–$\widetilde{\tau}_1$ coannihilation processes. Moreover, in regions in which $m_{\widetilde{t}_1}$ is close to $m_{\widetilde{\chi}^0_1}$, also $\widetilde{\chi}^0_1$–$\widetilde{t}_1$ coannihilation can allow for $\Omega^{\rm therm}_{\widetilde{\chi}^0_1} \simeq \Omega_{\rm dm}$.
- Higgs funnel: in this region, $2m_{\widetilde{\chi}^0_1}$ is close to the mass of the CP odd Higgs boson A^0, $m_{A^0} \sim 2m_{\widetilde{\chi}^0_1}$, so that neutralino annihilation proceeds very efficiently via the A^0 resonance. For large $\tan\beta$, the following annihilation channel becomes particularly efficient due to an $\tan\beta$-enhanced A^0 coupling of the b quark: $\widetilde{\chi}^0_1\widetilde{\chi}^0_1 \to A^0 \to {\rm b\bar{b}}$.

In addition to $\Omega^{\rm therm}_{\widetilde{\chi}^0_1}$ from thermal freeze out, $\widetilde{\chi}^0_1$'s can also be produced non-thermally in late decays of gravitinos. Because of their extremely weak interactions, unstable gravitinos with $m_{\widetilde{\chi}^0_1} < m_{\widetilde{G}} \lesssim 5$ TeV have long lifetimes, $\tau_{\widetilde{G}} \gtrsim 100$ s (cf. Fig. 1 of Ref. [63]), and decay typically during or after BBN into the LSP and into standard-model particles. While the decay into the LSP can proceed either directly or via a cascade, each gravitino decays into one LSP. Thus, the resulting non-thermally produced (NTP) neutralino density is given by

$$\Omega^{\rm NTP}_{\widetilde{\chi}^0_1} h^2 = m_{\widetilde{\chi}^0_1} Y_{\widetilde{G}}\, s(T_0) h^2/\rho_c, \tag{3.3}$$

where $Y_{\widetilde{G}} = n_{\widetilde{G}}/s$ denotes the gravitino yield prior to decay. Although gravitinos with $m_{\widetilde{G}} > m_{\widetilde{\chi}^0_1} = \mathcal{O}(100\ {\rm GeV})$ are extremely weakly interacting and not in thermal equilibrium with the primordial plasma, they can be produced efficiently in thermal scattering of particles in the hot plasma.[12] Derived in a gauge-invariant treatment, the resulting thermally produced (TP) gravitino yield at a temperature $T_{\rm low} \ll T_{\rm R}$ reads [207, 231–233]

$$Y^{\rm TP}_{\widetilde{G}}(T_{\rm low}) \equiv \sum_{i=1}^{3} y_i g_i^2(T_{\rm R}) \left(1 + \frac{M_i^2(T_{\rm R})}{3m^2_{\widetilde{G}}}\right) \times \ln\left(\frac{k_i}{g_i(T_{\rm R})}\right)\left(\frac{T_{\rm R}}{10^{10}\ {\rm GeV}}\right), \tag{3.4}$$

with y_i, the gauge couplings g_i, the gaugino mass parameters M_i, and k_i as given in Table 3.1. Here M_i and g_i are

[12] In this review I do not discuss gravitino production from inflaton decays which can be substantial depending on the inflation model; see, e.g., [229, 230].

understood to be evaluated at the reheating temperature after inflation T_R [232].[13] Using $Y_{\widetilde{G}} = Y_{\widetilde{G}}^{TP}(T_{low})$ as given by (3.4), one finds that $\Omega_{\widetilde{\chi}_1^0}^{NTP}$ is sensitive to the gravitino mass $m_{\widetilde{G}}$ and to the reheating temperature T_R. Thus, the dark matter constraint $\Omega_{\widetilde{\chi}_1^0}^{therm} + \Omega_{\widetilde{\chi}_1^0}^{NTP} \leq \Omega_{dm}$ does imply an upper limit on T_R. This limit is particularly restrictive in scenarios with $\Omega_{\widetilde{\chi}_1^0}^{therm} \simeq \Omega_{dm}$ [235] and/or $m_{\widetilde{G}}^2 \ll M_i^2(T_R)$. Since non-thermally produced $\widetilde{\chi}_1^0$'s can be hot/warm dark matter, additional constraints from LSS and potential solutions to small scale structure problems can occur, in particular, for $\Omega_{\widetilde{\chi}_1^0}^{NTP} \simeq \Omega_{dm}$ [236, 237].

Let us comment at this point on the T_R definition as discussed in Ref. [207]. The analytic expression (3.4) is derived by assuming a radiation-dominated epoch with an initial temperature of T_R [231, 232]. In a numerical treatment, the epoch in which the coherent oscillations of the inflaton field dominate the energy density of the Universe can also be taken into account, where one usually defines T_R in terms of the decay width Γ_ϕ of the inflaton field [61, 207]. In fact, the numerical result for $Y_{\widetilde{G}}^{TP}(T_{low})$ agrees with the analytic expression (3.4) for [207]

$$T_R \simeq \left[\frac{90}{g_*(T_R)\pi^2}\right]^{1/4} \sqrt{\frac{\Gamma_\phi M_P}{1.8}}, \tag{3.5}$$

which satisfies $\Gamma_\phi \simeq 1.8 H_{rad}(T_R)$ with the Hubble parameter $H_{rad}(T) = \sqrt{g_*(T)\pi^2/90}T^2/M_P$ and an effective number of relativistic degrees of freedom of $g_*(T_R) = 228.75$. Thus, (3.5) provides the T_R definition to which the yield (3.4) applies. For an alternative definition $T_R^{[\xi]} \equiv [90/(g_*(T_R^{[\xi]})\pi^2)]^{1/4}\sqrt{\Gamma_\phi M_P/\xi}$ given by $\Gamma_\phi = \xi H_{rad}(T_R^{[\xi]})$, the associated numerically obtained $Y_{\widetilde{G}}^{TP}(T_{low})$ is reproduced by the analytical expression (3.4) after substituting T_R with $\sqrt{\xi/1.8}T_R^{[\xi]}$ [207].

Figure 3.3 (from [63]) shows the T_R limit imposed by $\Omega_{\widetilde{\chi}_1^0}^{NTP}h^2 \leq 0.118$ (dotted line labeled as "Ω_{LSP}") as a function of $m_{\widetilde{G}}$ for the CMSSM scenario with $m_{1/2} = 300$ GeV, $m_0 = 141$ GeV, $A_0 = 0$, and $\tan\beta = 30$. Here the T_R limits apply to the T_R definition associated with $\xi = 3$, i.e., $\Gamma_\phi \simeq 3H_{rad}(T_R)$. In the shaded (light-orange) region, $m_{\widetilde{G}} \leq m_{\widetilde{\chi}_1^0} = 117$ GeV. The T_R limit becomes more restrictive for $m_{\widetilde{G}} \to m_{\widetilde{\chi}_1^0}$ due to the $m_{\widetilde{G}}$-dependent goldstino component in (3.4). For large $m_{\widetilde{G}}$, this spin-1/2 component becomes negligible and the T_R limit is governed by the $m_{\widetilde{G}}$-independent spin-3/2 contribution in (3.4). Note that the shown limit is conservative since the thermal relic density associated with this SUSY scenario, $\Omega_{\widetilde{\chi}_1^0}^{therm}h^2 = 0.111$, is not taken into account.

[13] Note that the field-theoretical methods applied in the derivation of (3.4) [207, 231–233] require weak couplings $g_i \ll 1$ and thus $T \gg 10^6$ GeV. For an alternative approach, see [234].

Table 3.1 Assignments of the index i, the gauge coupling g_i, and the gaugino mass parameter M_i, to the gauge groups $U(1)_Y$, $SU(2)_L$, and $SU(3)_c$, and the constants k_i, y_i, and ω_i

Gauge group	i	g_i	M_i	k_i	$(y_i/10^{-12})$	ω_i
$U(1)_Y$	1	g'	M_1	1.266	0.653	0.018
$SU(2)_L$	2	g	M_2	1.312	1.604	0.044
$SU(3)_c$	3	g_s	M_3	1.271	4.276	0.117

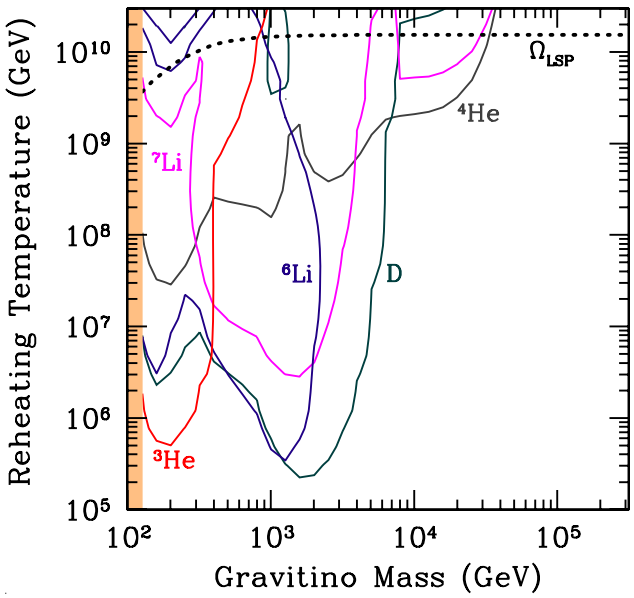

Fig. 3.3 Upper limits on the reheating temperature T_R after inflation as a function of the gravitino mass $m_{\widetilde{G}}$ in the CMSSM with $\widetilde{\chi}_1^0$ dark matter for $m_{1/2} = 300$ GeV, $m_0 = 141$ GeV, $A_0 = 0$, $\tan\beta = 30$ and for the T_R definition associated with $\Gamma_\phi \simeq 3H_{rad}(T_R)$. The associated $\widetilde{\chi}_1^0$ LSP mass is $m_{\widetilde{\chi}_1^0} = 117$ GeV—as indicated by the *shaded* (*light orange*) *region* in which $m_{\widetilde{G}} \leq m_{\widetilde{\chi}_1^0}$—and the thermal relic density $\Omega_{\widetilde{\chi}_1^0}^{therm}h^2 = 0.111$. Above the dotted line labeled as "Ω_{LSP}", the $\widetilde{\chi}_1^0$ density from decays of thermally produced gravitinos exceeds $\Omega_{\widetilde{\chi}_1^0}^{NTP}h^2 = 0.118$. The lines labeled as D, ^{3}He, ^{4}He, ^{6}Li, and ^{7}Li are upper limits on T_R (95% CL) inferred from observationally inferred primordial abundances of the corresponding light elements. Above those limits, BBN is reprocessed in an intolerable way by the standard-model particles emitted in late decays of thermally produced gravitinos. Reprinted (figure) with kind permission from [63]. Copyright (2008) by the American Physical Society

3.2 Cosmological constraints

Late decaying gravitinos are not only associated with the contribution (3.3) to $\Omega_{\widetilde{\chi}_1^0}h^2$ but also with the injection of energetic standard-model particles. Because of the long $\widetilde{G}$ lifetime of $\tau_{\widetilde{G}} > 1$ s for $m_{\widetilde{G}} \lesssim 20$ TeV [63], those decay products are emitted during/after BBN and can thus affect the abundances of the primordial light elements [52, 59–63, 235]. In fact, this is a concrete (and probably the most

prominent) example for the non-thermal BBN-affecting processes mentioned in the Introduction.

The dominant mechanism affecting BBN depends on $\tau_{\widetilde{G}}$, or, more generally, on the time t at which the electromagnetic or hadronic energy is injected into the Universe. For 1 s $\lesssim t \lesssim$ 100 s, energetic hadrons are stopped efficiently through electromagnetic interactions so that the direct destruction of light elements is subdominant. The presence of additional slow hadrons still can change the ratio of protons to neutrons through interconversion processes and thus affect the abundance of the light elements. For 100 s $\lesssim t \lesssim 10^7$ s, energetic hadrons and, in particular, neutrons cannot be slowed down significantly. Accordingly, they can reprocess efficiently the produced light elements through hadrodissociation processes. The effect of electromagnetic energy release is negligible for $t \lesssim 10^4$ s as the interaction with the background particles thermalizes quickly any high-energy photons or leptons emitted in the gravitino decay. Towards later times, electromagnetic energy release becomes important. For 10^7 s $\lesssim t \lesssim 10^{12}$ s, the reprocessing of light elements through energetic electromagnetic showers, i.e., photodissociation, can become more significant than hadrodissociation. (For more details, see, e.g., [54, 61] and references therein.)

Including these mechanisms in calculations of BBN, observationally inferred abundances of primordial D, ^{3}He, ^{4}He, ^{6}Li, and ^{7}Li have been used to provide limits on quantities such as [59, 61, 62]

$$\xi_{\mathrm{em,had}} \equiv \epsilon_{\mathrm{em,had}} Y_{\widetilde{G}}, \tag{3.6}$$

where $\epsilon_{\mathrm{em,had}}$ is the (average) electromagnetic/hadronic energy emitted in a single $\widetilde{G}$ decay. While the yield prior to decay $Y_{\widetilde{G}}$ is given for thermally produced gravitinos by (3.4), $\epsilon_{\mathrm{em,had}}$ depends strongly on the sparticle spectrum. Once $\epsilon_{\mathrm{em,had}}$ is calculated for a given SUSY model, $\xi_{\mathrm{em,had}}$ limits can basically be translated into $m_{\widetilde{G}}$-dependent upper limits on the reheating temperature [63, 235].

For the exemplary CMSSM point $m_{1/2} = 300$ GeV, $m_0 = 141$ GeV, $A_0 = 0$, and $\tan\beta = 30$, the $m_{\widetilde{G}}$-dependent BBN constraints on T_{R} (95% CL) are shown in Fig. 3.3 (from [63]) for the T_{R} definition given by $\Gamma_\phi \simeq 3H_{\mathrm{rad}}(T_{\mathrm{R}})$. The curves are inferred from observationally inferred abundances of D, ^{3}He, ^{4}He, ^{6}Li, and ^{7}Li (as labeled). The ^{4}He limit governs the BBN constraints for $m_{\widetilde{G}} \gtrsim 7$ TeV ($\tau_{\widetilde{G}} \lesssim 10^2$ s) where proton–neutron interconversion can affect BBN. The D (^{3}He) limit is the most restrictive one in the region in which the constraints from hadrodissociation (photodissociation) are most relevant, 0.3 TeV $\lesssim m_{\widetilde{G}} \lesssim 7$ TeV ($m_{\widetilde{G}} \lesssim 0.3$ TeV) or 10^2 s $\lesssim \tau_{\widetilde{G}} \lesssim 10^7$ s ($\tau_{\widetilde{G}} \gtrsim 10^7$ s). For $m_{\widetilde{G}} \gtrsim 40$ TeV, the BBN bounds disappear since the $\widetilde{G}$'s decay well before the onset of BBN, i.e., $\tau_{\widetilde{G}} \ll 1$ s.

The range of allowed values of the reheating temperature is crucial for our understanding of inflation and for the viability of potential explanations of the matter-antimatter asymmetry in our Universe. For example, thermal leptogenesis with hierarchical heavy right-handed Majorana neutrinos—which provides an attractive explanation of this asymmetry—requires very high reheating temperatures of $T_{\mathrm{R}} \gtrsim 10^9$ GeV [238–242] and thus $m_{\widetilde{G}} \gtrsim 7$ TeV for the SUSY model considered in Fig. 3.3. For smaller $m_{\widetilde{G}}$, the T_{R} limit can be as restrictive as $T_{\mathrm{R}} < 10^6$ GeV which is known as the gravitino problem. Note that flavor effects [241–244] do not change the lower bound $T_{\mathrm{R}} > 10^9$ GeV required by successful thermal leptogenesis with hierarchical right-handed neutrinos [241, 242]. However, there are special settings [245–247] that allow for a CP asymmetry above the Davidson–Ibarra bound [239] and for a relaxed lower T_{R} bound. Moreover, for (nearly) mass-degenerate heavy right-handed Majorana neutrinos, resonant leptogenesis can explain the matter-antimatter asymmetry at smaller values of T_{R} [248–251]. Another example for a framework in which the limit $T_{\mathrm{R}} > 10^9$ GeV is relaxed is non-thermal leptogenesis; see, e.g., [252] and references therein.

Before proceeding one should stress that the T_{R} limits inferred from $\Omega^{\mathrm{NTP}}_{\widetilde{\chi}^0_1} \leq \Omega_{\mathrm{dm}}$ and from BBN rely crucially on assumptions on the cosmological history and the evolution of physical parameters. For example, for a non-standard thermal history with late-time entropy production, the thermally produced gravitino yield can be diluted $Y_{\widetilde{G}} \to Y_{\widetilde{G}}/\delta$ by a factor $\delta > 1$ [207] so that $T_{\mathrm{R}}^{\max} \to \delta T_{\mathrm{R}}^{\max}$. Moreover, $T_{\mathrm{R}}^{\max}$ can be relaxed if, e.g., the strong coupling g_s levels off in a non-standard way at high temperatures [253]. This emphasizes that the T_{R} limits discussed above rely on the assumptions of a standard cosmological history and of gauge couplings that behave at high temperatures as described by the renormalization group equation in the MSSM. While tests of these assumptions seem inaccessible to terrestrial accelerator experiments, the futuristic space-based gravitational-wave detectors BBO or DECIGO [87]—mentioned already in the Introduction—could allow for tests of the thermal history after inflation and could even probe T_{R} [88, 89] in a complementary way.

3.3 Experimental searches and prospects

For experimental tests of the $\widetilde{\chi}^0_1$ dark-matter hypothesis, three complementary techniques exist: indirect, direct, and collider searches. While there is an enormous activity in each of those fields, I will summarize only the main ideas. For more detailed discussions, see [254, 256–259] and references therein.

Let us first turn to indirect searches. Since dark matter clumps, one expects regions with an increased $\widetilde{\chi}^0_1$ density such as galaxy halos, the center of galaxies, and the center of stars. While $\widetilde{\chi}^0_1$ pair annihilation well after $\widetilde{\chi}^0_1$ decoupling is basically negligible for calculations of $\Omega_{\widetilde{\chi}^0_1}$, it should occur

at a significant rate in these regions. The resulting standard-model particles should then lead to energetic cosmic rays and thereby to an excess of photons, neutrinos, positrons, and antiprotons over backgrounds expected from standard cosmic ray models without dark matter annihilation. In fact, for example, data from the Energetic Gamma Ray Experiment Telescope (EGRET) has already been interpreted as evidence for $\widetilde{\chi}_1^0$ annihilation [260] within SUSY models that will be testable in direct and collider searches. For a discussion of these and other potential hints, see [256, 258, 259] and references therein.

In direct searches, one looks for signals of $\widetilde{\chi}_1^0$'s—or more generally WIMPs—passing through Earth that scatter elastically off nuclei. Being located in environments deep underground that are well shielded against unwanted background, an enormous sensitivity has been reached by a number of experiments [261–269]. Since no unambiguous signal of a $\widetilde{\chi}_1^0$-nucleus scattering event has been observed so far, $m_{\widetilde{\chi}_1^0}$-dependent upper limits on the respective $\widetilde{\chi}_1^0$ cross section are obtained.

Figure 3.4 shows current limits on the spin-independent neutralino–nucleon cross section provided by CDMS [267] (red), XENON10 [266] (dark blue), CRESST II [268, 269] (light blue), ZEPLIN II [265] (dark green), WARP [264] (medium green), and EDELWEISS I [262] (light green) (from bottom to top at a WIMP mass of 80 GeV, as labeled). The light (yellow) patch indicates the region in which the DAMA experiment is reporting the observation of a signal with the expected annual modulation [270, 271]. As can be seen, this DAMA signal region is in a region in which null events were observed by ZEPLIN II, CRESST II, CDMS, and XENON10. The DAMA signals might thus be interpreted as signals of a "non-standard" dark-matter candidate (see e.g. [272]), where cosmological and astrophysical constraints can allow for crucial viability tests (see e.g. [273]); see also [274–276] and references therein. The various patches, crosses, and contours within the light gray region labeled as "supersymmetric models" indicate the (favored) parameter space of SUSY models with a $\widetilde{\chi}_1^0$ LSP [277–281]. As can be seen, the current best limits given by the CDMS [263, 267] and the XENON10 [266] experiments disfavor already a sizable part of the SUSY parameter space; see, for example, [206, 256, 257] and references therein. These limits, however, depend on the assumed $\widetilde{\chi}_1^0$ flux at the detector location. Standard galactic halo parameter are assumed, i.e., a local halo density of dark matter of $\rho_0 = 0.3$ GeV/cm^3 and a characteristic halo velocity of $v_0 = 220$–240 km/s. Indeed, those assumptions are subject to significant uncertainties due to possible inhomogeneities in the dark-matter distribution in galaxies. Such inhomogeneities should manifest themselves also in indirect searches which can help to reduce those uncertainties. Once $\widetilde{\chi}_1^0$ events are observed in direct searches, one can succeed

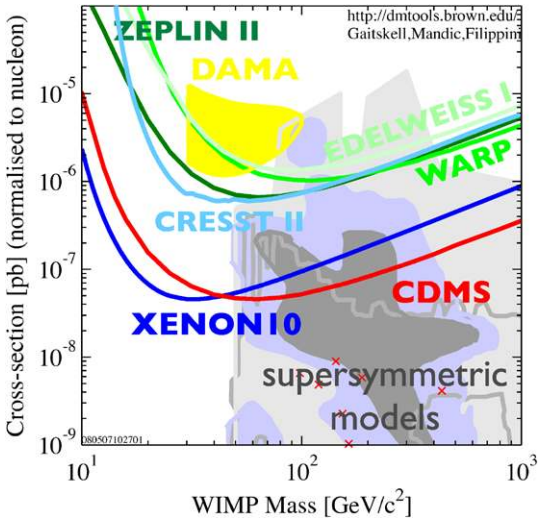

Fig. 3.4 Limits on the spin-independent neutralino–nucleon cross section from direct searches as a function of the neutralino mass (or WIMP mass). The shown limits are provided by CDMS [267] (*red*), XENON10 [266] (*dark blue*), CRESST II [268, 269] (*light blue*), ZEPLIN II [265] (*dark green*), WARP [264] (*medium green*), and EDELWEISS I [262] (*light green*) (from bottom to top at a WIMP mass of 80 GeV, as labeled). The DAMA signal region [270, 271] is indicated by the *light-shaded patch* (*yellow*, as labeled) and the (favored) parameter space of SUSY models with a $\widetilde{\chi}_1^0$ LSP [277–281] by the *shadings/contours/crosses* at WIMP masses $m_{\widetilde{\chi}_1^0} > 40$ GeV (*gray/purple/red*, as labeled). Standard galactic halo parameters are assumed, i.e., a local halo density of dark matter of $\rho_0 = 0.3$ GeV/cm^3 and a characteristic halo velocity of $v_0 = 220$–240 km/s. The figure was built by using the dark-matter plotter available at http://dmtools.berkeley.edu/limitplots/ and maintained by Gaitskell and Filippini

in reconstructing the $\widetilde{\chi}_1^0$ velocity distribution [282]. By analyzing the recoil spectra, $m_{\widetilde{\chi}_1^0}$ can even be estimated in a way that is independent of the dark matter density on Earth [283].

In most searches for SUSY at colliders, it is assumed that R-parity is conserved. Accordingly, one expects that superpartners are produced in pairs before decaying via cascades into the LSP and energetic fermions. As a weakly interacting particle, every $\widetilde{\chi}_1^0$ LSP produced will escape the detector without leaving a track. Thus, the existence of SUSY and the $\widetilde{\chi}_1^0$ LSP has to be inferred from studies of missing transverse energy E_T^{miss} and of energetic jets and leptons emitted along the cascades. Along these lines, ongoing investigations are pursued based on data from $p\bar{p}$ collisions with a center-of-mass energy of $\sqrt{s} = 2$ TeV at the Fermilab Tevatron Collider. While lower limits on the masses of squarks and gluinos have been extracted, no evidence for SUSY or the $\widetilde{\chi}_1^0$ LSP has been reported so far [284, 285]. With the first pp collisions with $\sqrt{s} = 14$ TeV at the CERN Large Hadron Collider (LHC) expected in the year 2009, there are high hopes that the new energy range will allow for copious production of superpartners. Here large E_T^{miss} will be the key quantity for early SUSY searches [286, 287].

Despite an enormous potential for mass and spin measurements of SUSY particles at the LHC [288], additional precision studies at the planned International Linear Collider (ILC) [289, 290] appear to be crucial for the identification of the $\widetilde{\chi}_1^0$ LSP [254, 291].

4 Gravitino dark matter

The gravitino $\widetilde{G}$ has already been introduced in the previous section and its appearance is an unavoidable implication of SUSY theories including gravity. In this section we consider the possibility of the gravitino LSP which is well motivated, for example, in gauge-mediated and gravity-mediated SUSY breaking schemes [199–201]. Indeed, without consensus on the SUSY breaking mechanism and the SUSY breaking scale, one may well consider the gravitino mass $m_{\widetilde{G}}$ as a free parameter to be constrained by cosmological considerations (cf. Sects. 4.1 and 4.2) and by collider experiments (cf. Sect. 4.3).[14]

Being a singlet with respect to the gauge groups of the Standard Model, the gravitino LSP is a promising dark-matter candidate that can be classified as an EWIP as mentioned above. In fact, it must not be massive since even a light gravitino (e.g., $m_{\widetilde{G}} = 1$ keV) can evade its production at colliders because of its tiny interaction strength.

Let us recall important characteristics of gravitino interactions: (i) Gravitino interactions are suppressed by inverse powers of M_P. Indeed, for example, gravitino-gaugino-gauge boson couplings are described by dimension five operators and an energy scale appears in the numerator of the respective vertex. Gravitino interactions can thereby be enhanced at very high energies. (ii) Through the super-Higgs mechanism, the interactions of the spin-1/2 components of the gravitino (i.e., the interactions of the goldstino components) are enhanced at energy/mass scales that are large with respect to the gravitino mass $m_{\widetilde{G}}$, i.e., a light gravitino interacts more strongly than a heavy gravitino.[15]

Considering the case of the $\widetilde{G}$ LSP, in which the LOSP is the unstable NLSP that decays eventually into the $\widetilde{G}$ LSP, both cases $m_{\widetilde{\chi}_1^0} < m_{\widetilde{\tau}_1}$ and $m_{\widetilde{\tau}_1} < m_{\widetilde{\chi}_1^0}$ (cf. Fig. 3.1) are viable as already mentioned. In less constrained frameworks such as models with non-universal Higgs masses (NUHM), also other LOSP/NLSP candidates are still possible such as the lighter stop $\widetilde{t}_1$ [212, 213][16] or the lightest sneutrino $\widetilde{\nu}_1$ [217–219, 223, 224]. However, the $\widetilde{\tau}_1$ NLSP case is probably the most promising one from the phenomenological point view and is discussed more extensively than the other NLSP cases in this review.

4.1 Primordial origin

The potential primordial origin of gravitino dark matter depends on the mass $m_{\widetilde{G}}$ that governs its interaction strength, on the SUSY model, on the cosmological history, on the inflation model, and on the reheating temperature after inflation. The gravitino LSP can be a thermal relic [293] or be produced in thermal scattering of particles in the primordial plasma [207, 231, 232, 234, 294, 295]. Additional more model-dependent gravitino sources are NLSP decays [223, 296–298] and decays of scalar fields such as the inflaton [229, 230]. The latter production mechanism is not discussed in this review but can be substantial depending on the inflation model.

Light gravitinos can have sufficiently strong interactions for being in thermal equilibrium with the primordial plasma. For example, for $m_{\widetilde{G}} \lesssim 2$ keV, the gravitino decoupling temperature is $T_f \lesssim 1$ TeV; cf. [34]. Before gravitinos decouple as a relativistic species at T_f, i.e., for $T_R > T > T_f$, the spin-1/2 components of the gravitino were in thermal equilibrium. Thus, their "hot" thermal relic density is the one of a spin-1/2 Majorana fermion

$$\Omega_{\widetilde{G}}^{\mathrm{therm}} h^2 = 0.115 \left(\frac{100}{g_{*S}(T_f)} \right) \left(\frac{m_{\widetilde{G}}}{100\ \mathrm{eV}} \right) \tag{4.1}$$

and the right amount of dark matter, $\Omega_{\widetilde{G}}^{\mathrm{therm}} \simeq \Omega_{\mathrm{dm}}$, is provided for $m_{\widetilde{G}} \simeq 100$ eV and $g_{*S}(T_f) \simeq 100$. However, the present root mean square velocity of such gravitinos

$$\left(v_{\mathrm{FS}}^{\mathrm{rms},0}\right)_{\widetilde{G}} = 0.77 \frac{\mathrm{km}}{\mathrm{s}} \left(\frac{\Omega_{\widetilde{G}}^{\mathrm{therm}} h^2}{0.113} \right)^{1/3} \left(\frac{100\ \mathrm{eV}}{m_{\widetilde{G}}} \right)^{4/3} \tag{4.2}$$

exceeds significantly the constraints from observations and simulations of cosmic structures listed, e.g., in Table 1 of Ref. [299]. In fact, for $\Omega_{\widetilde{G}}^{\mathrm{therm}} \simeq \Omega_{\mathrm{dm}}$, these constraints imply $m_{\widetilde{G}} > 500$ eV and $g_{*S}(T_f) > 500$ which is well above the 228.75 degrees of freedom of the MSSM. Indeed, for $g_{*S}(T_f) = 228.75$, this scenario is excluded by the dark-matter constraint $\Omega_{\widetilde{G}} \leq \Omega_{\mathrm{dm}}$ once a standard cosmological history is assumed. With a non-standard thermal history, light gravitinos can still be viable thermal relics if their abundance is diluted by entropy production, which can result, for example, from decays of messenger fields in gauge-mediated SUSY breaking scenarios [300–305].

Gravitinos with $m_{\widetilde{G}} \gtrsim 0.1$ GeV (1 GeV) have a high decoupling temperature of $T_f > 10^{11}$ GeV (10^{13} GeV) [207] because of their extremely weak interactions. Thus, those gravitinos have never been in thermal equilibrium with the

[14] In scenarios with R-parity violation, the gravitino LSP can decay into standard-model particles. Then, one may be able to infer its mass $m_{\widetilde{G}}$ from the decay spectra possibly observed in indirect dark-matter searches [292].

[15] Note that this interaction-strength dependence on the mass is different than in the axion case, i.e., a light axion is less strongly interacting than a heavy axion; cf. Sect. 2.

[16] A long-lived stop $\widetilde{t}_1$ NLSP is not feasible in the CMSSM [212, 213].

primordial plasma even for a reheating temperature as high as $T_R = 10^{10}$ GeV. At high temperatures, however, those gravitinos can be produced efficiently in thermal scattering of particles in the primordial plasma, as already discussed for the case of an unstable $\widetilde{G}$ in Sect. 3.1. In the case of the stable $\widetilde{G}$ LSP, the thermally produced gravitino yield $Y_{\widetilde{G}}^{\rm TP}(T_0) = Y_{\widetilde{G}}^{\rm TP}(T_{\rm low})$ given in (3.4) leads to the following thermally produced (TP) gravitino density [207, 231, 232]

$$\begin{aligned}\Omega_{\widetilde{G}}^{\rm TP}h^2 &= m_{\widetilde{G}}Y_{\widetilde{G}}^{\rm TP}(T_0)s(T_0)h^2/\rho_c \\ &= \sum_{i=1}^{3}\omega_i g_i^2(T_R)\left(1+\frac{M_i^2(T_R)}{3m_{\widetilde{G}}^2}\right)\ln\left(\frac{k_i}{g_i(T_R)}\right) \\ &\quad\times\left(\frac{m_{\widetilde{G}}}{100\ \text{GeV}}\right)\left(\frac{T_R}{10^{10}\ \text{GeV}}\right) \qquad (4.3)\end{aligned}$$

with ω_i as given in Table 3.1. For the case of universal gaugino masses $M_{1,2,3} = m_{1/2}$ at $M_{\rm GUT}$ and $m_{\widetilde{G}} \ll M_i$, i.e., $(1 + M_i^2/3m_{\widetilde{G}}^2) \simeq M_i^2/3m_{\widetilde{G}}^2$, $\Omega_{\widetilde{G}}^{\rm TP}h^2$ can be approximated by the convenient expression [74][17]

$$\Omega_{\widetilde{G}}^{\rm TP}h^2 \simeq 0.32\left(\frac{10\ \text{GeV}}{m_{\widetilde{G}}}\right)\left(\frac{m_{1/2}}{1\ \text{TeV}}\right)^2\left(\frac{T_R}{10^8\ \text{GeV}}\right). \qquad (4.4)$$

The thermally produced gravitinos do not affect the thermal evolution of the LOSP (or NLSP) prior to its decay which occurs typically after decoupling from the thermal plasma. Moreover, since each NLSP decays into one $\widetilde{G}$ LSP, the NLSP decay leads to a non-thermally produced (NTP) gravitino density [223, 296, 297, 307]

$$\Omega_{\widetilde{G}}^{\rm NTP}h^2 = m_{\widetilde{G}}Y_{\rm NLSP}^{\rm dec}s(T_0)h^2/\rho_c \qquad (4.5)$$

so that the guaranteed gravitino density is given by

$$\Omega_{\widetilde{G}}h^2 = \Omega_{\widetilde{G}}^{\rm TP}h^2 + \Omega_{\widetilde{G}}^{\rm NTP}h^2. \qquad (4.6)$$

While $\Omega_{\widetilde{G}}^{\rm TP}$ is sensitive to M_i and T_R for a given $m_{\widetilde{G}}$, $\Omega_{\widetilde{G}}^{\rm NTP}$ depends on $Y_{\rm NLSP}^{\rm dec} = Y_{\rm LOSP}^{\rm dec}$ and thereby on details of the SUSY model realized in nature; cf. Sect. 3.1. For the case of a charged slepton $\tilde{l}_1$—such as the lighter stau $\widetilde{\tau}_1$—being the NLSP,[18] simple approximations have been used such as [74, 79, 222, 297, 299, 310]

$$Y_{\tilde{l}_1}^{\rm dec} \simeq 0.7\times10^{-12}\left(\frac{m_{\tilde{l}_1}}{1\ \text{TeV}}\right), \qquad (4.7)$$

where $Y_{\tilde{l}_1} \equiv n_{\tilde{l}_1}/s$ and $n_{\tilde{l}_1}$ denotes the total $\tilde{l}_1$ number density assuming an equal number density of positively and negatively charged $\tilde{l}_1$'s. Note that the yield (4.7) is in good agreement with the curve in Fig. 1 of Ref. [297] that has been derived for the case of a purely 'right-handed' $\widetilde{\tau}_1 \simeq \widetilde{\tau}_R$ NLSP with a mass that is significantly below the masses of the lighter selectron and the lighter smuon, $m_{\widetilde{\tau}_1} \ll m_{\widetilde{e}_1,\widetilde{\mu}_1}$, and with a bino-like lightest neutralino, $\widetilde{\chi}_1^0 \simeq \widetilde{B}$, which has a mass of $m_{\widetilde{B}} = 1.1m_{\widetilde{\tau}_1}$. In the case of an approximate slepton mass degeneracy, $m_{\widetilde{\tau}_1} \lesssim m_{\widetilde{e}_1,\widetilde{\mu}_1} \lesssim 1.1m_{\widetilde{\tau}_1}$, the $\widetilde{\tau}_1$ NLSP yield (4.7) can become twice as large due to slepton coannihilation processes [207, 297]. Approaching the $\widetilde{\chi}_1^0$–$\widetilde{\tau}_1$ coannihilation region, $m_{\widetilde{\chi}_1^0} \approx m_{\widetilde{\tau}_1}$, even larger enhancement factors occur; cf. Fig. 3.1. On the other hand, while existing studies of $Y_{\tilde{l}_1}^{\rm dec}$ focus mainly on the $\tilde{l}_1 \simeq \tilde{l}_R$ case [207, 222, 297, 309], it has recently been found that a sizable left–right mixing of the stau NLSP can be associated with an increase of its MSSM couplings and thus with a significant reduction of $Y_{\widetilde{\tau}_1}^{\rm dec}$ [311, 312]. The study [312] shows also explicitly that stau annihilation at the resonance of the heavy CP even Higgs H^0 can be particularly efficient via $\widetilde{\tau}_1\widetilde{\tau}_1 \to H^0 \to b\bar{b}$ and thus be associated with exceptionally small values of $Y_{\widetilde{\tau}_1}^{\rm dec}$.

Figure 4.1 (from [312]) shows that $Y_{\widetilde{\tau}_1}^{\rm dec} < 4\times10^{-15}$ occurs in special regions even within the CMSSM. The points B and C mark the regions in which $Y_{\widetilde{\tau}_1}^{\rm dec}$ is exceptionally small due to stau annihilation at the H^0 resonance and due to enhanced stau–Higgs couplings leading to efficient annihilation into Higgs bosons, respectively. Within these regions, $\Omega_{\widetilde{G}}^{\rm NTP}$ is negligible and otherwise restrictive cosmological constraints can be evaded as will be explained in more detail in the next section.

An exceptional reduction of $Y_{\tilde{l}_1}^{\rm dec}$ can occur also in a non-standard thermal history with late-time entropy production after the decoupling of the $\tilde{l}_1$ NLSP and before BBN [68, 207, 314] or in low T_R scenarios [71]. Focusing on a standard cosmological history, we disregard such possibilities and consider in the following mainly the more generic $Y_{\tilde{l}_1}^{\rm dec}$ values described approximately by (4.7).

Let us proceed with the discussion of the relic gravitino density. Indeed, scenarios with $\Omega_{\widetilde{G}} = \Omega_{\rm dm}$ are found for natural mass spectra and for a wide range of $m_{\widetilde{G}}$–T_R combinations. This is illustrated in Figs. 4.2, 4.3, and 4.4.

[17] Here the one-loop evolution described by the renormalization group equation in the MSSM is used to evaluate $g_i(T_R)$ at a representative scale of $T_R = 10^8$ GeV and to express $M_i(T_R)$ at that scale in terms of $M_{1,2,3}(M_{\rm GUT}) = m_{1/2}$. Note that the use of the two-loop evolution will lead to a somewhat smaller prefactor. Going in the other direction, i.e., using the two-loop evolution to express $M_3(T_R)$ in terms of the physical gluino mass, a prefactor has been found that is about twice as large [306] as the one obtained when the one-loop evolution is used to express $M_3(T_R)$ in terms of $M_3(1\ \text{TeV})$ [231].

[18] For $Y_{\rm NLSP}^{\rm dec}$ in the sneutrino and stop NLSP cases, see Refs. [219, 220, 222, 223] and [212, 222, 308, 309], respectively. Reference [309] covers also the stau NLSP case for $\widetilde{\tau}_1 \simeq \widetilde{\tau}_R$ and the effects of Sommerfeld enhancement on $Y_{\rm NLSP}^{\rm dec}$.

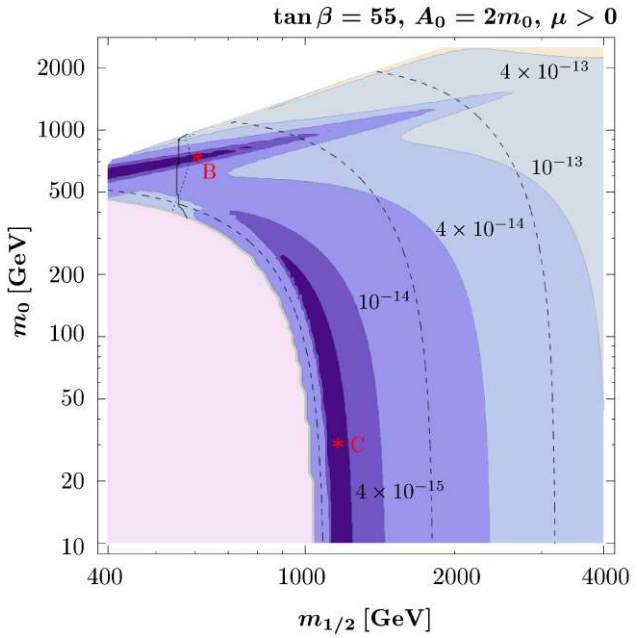

Fig. 4.1 Contours of $Y^{\rm dec}_{\tilde\tau_1}$ (as labeled) in the $(m_{1/2}, m_0)$ plane for $\tan\beta = 55$, $A_0 = 2m_0$, and $\mu > 0$. *Darker shadings* imply smaller $Y^{\rm dec}_{\tilde\tau_1}$ values. The *dashed lines* are contours of $m_{\tilde\tau_1} = 100, 300$, and 600 GeV (*from left to right*). The *large light-shaded region in the lower left corner* is excluded by bounds from direct Higgs and SUSY searches (or by the appearance of a tachyonic spectrum). In the region to the left of the vertical solid and dotted lines, $m_{h^0} \leq 114.4$ GeV [2] and $B(b \to s\gamma) \geq 4.84 \times 10^{-4}$ [313], respectively. In the *white area*, $m_{\widetilde\chi^0_1} < m_{\tilde\tau_1}$. Reprinted (figure) with kind permission from [312]. Copyright (2009) by Elsevier

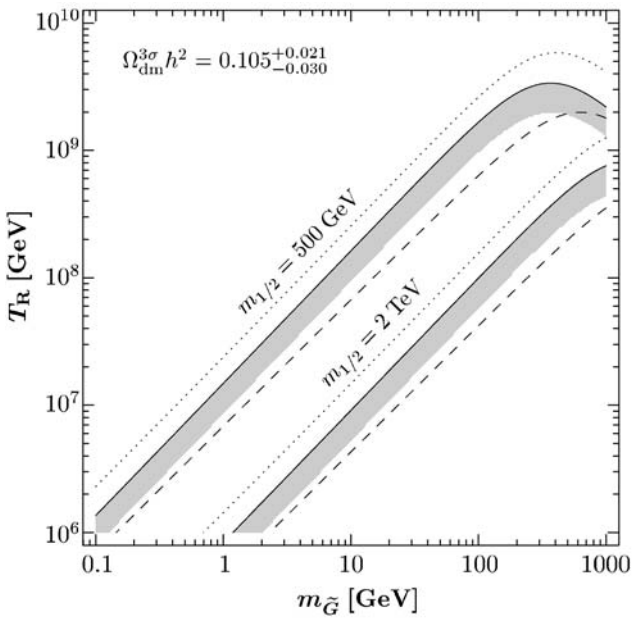

Fig. 4.2 Upper limits on the reheating temperature $T_{\rm R}$ in the $\widetilde G$ LSP case, which are associated with the $T_{\rm R}$ definition (3.5). On the *upper* (*lower*) *gray band*, $\Omega^{\rm TP}_{\widetilde G} \in \Omega^{3\sigma}_{\rm dm}$ for $M_{1,2,3} = m_{1/2} = 500$ GeV (2 TeV) at $M_{\rm GUT}$. The corresponding limits from $\Omega^{\rm TP}_{\widetilde G} h^2 \leq 0.126$ shown by the *dashed* and *dotted lines* are obtained respectively with (4.3) for $M_1/10 = M_2/2 = M_3 = m_{1/2}$ at $M_{\rm GUT}$ and with the result of Ref. [231] for $M_3 = m_{1/2}$ at $M_{\rm GUT}$. Reprinted (figure) with kind permission from [207]. Copyright (2007) by Elsevier

In $\widetilde G$ LSP scenarios, upper limits on $T_{\rm R}$ can be derived since $\Omega^{\rm TP}_{\widetilde G} \leq \Omega_{\rm dm}$ [207, 294, 297, 299, 315–317]. These $m_{\widetilde G}$-dependent limits are shown in Fig. 4.2 (from [207]) for the $T_{\rm R}$ definition (3.5). They can be confronted with inflation models and with potential explanations of the cosmic matter-antimatter asymmetry in the same way as in the case of the $\widetilde\chi^0_1$ LSP (cf. Fig. 3.3) in Sect. 3.2. For a given $\Omega^{\rm TP}_{\widetilde G}$ and a $\tilde l_1$ NLSP with (4.7), the bound $\Omega^{\rm NTP}_{\widetilde G} \leq \Omega_{\rm dm} - \Omega^{\rm TP}_{\widetilde G}$ gives upper limits on $m_{\widetilde G}$ and $m_{\tilde l_1}$. Those limits are shown by the thin solid lines in Fig. 4.3 (from [79]). In Fig. 4.4 (from [318]) regions with $\Omega_{\widetilde G} \in \Omega^{3\sigma}_{\rm dm}$ are shown for $T_{\rm R} = 10^7, 10^8$, and 10^9 GeV, where $T_{\rm R}$ is defined as in (3.5). Here both $\Omega^{\rm TP}_{\widetilde G}$ and $\Omega^{\rm NTP}_{\widetilde G}$ are taken into account for $m_{\widetilde G} = m_0$ within the CMSSM.

While thermally produced gravitinos have a negligible free–streaming velocity today, gravitinos from NLSP decays can be warm/hot dark matter. In the $\widetilde\tau_1$ NLSP case, for example, upper limits on the free–streaming velocity from simulations and observations of cosmic structures exclude $m_{\tilde\tau_1} \lesssim 0.7$ TeV for $\Omega^{\rm NTP}_{\widetilde G} \simeq \Omega_{\rm dm}$ [299]. Such scenarios (gray band in Fig. 4.3), however, require[19] $m_{\tilde\tau_1} \gtrsim 0.7$ TeV anyhow and could even resolve the small scale structure problems inherent to cold dark matter [319–321].

4.2 Cosmological constraints

In the $\widetilde G$ LSP case with conserved R-parity, the NLSP can have a long lifetime $\tau_{\rm NLSP}$.[20] This is illustrated by the dotted $\tau_{\rm NLSP}$ contours in Figs. 4.3 and 4.4. In particular, for a $\tilde l_1$ NLSP, one finds in the limit $m_l \to 0$,

$$\tau_{\tilde l_1} \simeq \Gamma^{-1}(\tilde l_1 \to \widetilde G l) = \frac{48\pi m^2_{\widetilde G} \mathrm{M}^2_{\rm P}}{m^5_{\tilde l_1}} \left(1 - \frac{m^2_{\widetilde G}}{m^2_{\tilde l_1}}\right)^{-4}, \qquad (4.8)$$

which holds not only for a charged slepton NLSP but also for the sneutrino NLSP $\widetilde\nu_1$. Expressions for the lifetimes of the $\widetilde\chi^0_1$ NLSP and the $\widetilde t_1$ NLSP are given, e.g., in Sect. IIC of Ref. [223] and in Sect. 2.2 of Ref. [212], respectively.

[19] Note that the BBN constraints discussed below can point to a $\widetilde\tau_1$ NLSP mass of $m_{\tilde\tau_1} \gtrsim 2$ TeV for $\Omega^{\rm NTP}_{\widetilde G} \simeq \Omega_{\rm dm}$ as shown in Fig. 4.3. In the part of the gray band in which $m_{\tilde\tau_1} \lesssim 3$ TeV and in which the BBN constraints are respected, the present velocity of gravitinos emitted in $\widetilde\tau_1$ decays is between 0.004 and 0.01 km/s which is comparable to that of a thermal relic warm dark-matter species with a mass between 1 and 5 keV; cf. Fig. 14 of Ref. [299].

[20] For the case of broken R-parity, see, e.g., [38–40].

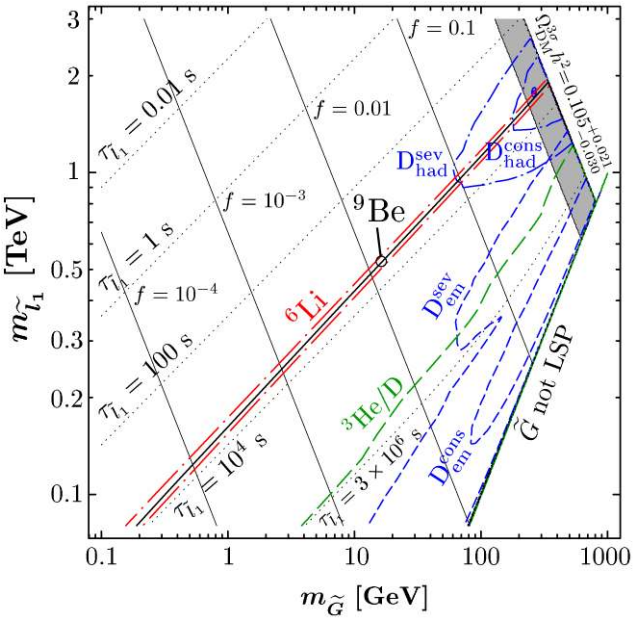

Fig. 4.3 Cosmological constraints on the masses of the gravitino LSP and a purely 'right-handed' $\tilde{l}_1$ NLSP with (4.7). The *gray band* indicates $\Omega^{\rm NTP}_{\widetilde{G}} \in \Omega^{3\sigma}_{\rm dm}$. Above this band, $\Omega_{\widetilde{G}} h^2 > 0.126$. On the *thin solid lines* labeled with f values only $f\Omega_{\rm dm}$ is provided by $\Omega^{\rm NTP}_{\widetilde{G}}$. The *dotted lines* show contours of $\tau_{\tilde{l}_1}$. Due to CBBN, the region below the solid and the long-dash-dotted (red) lines is disfavored by observationally inferred abundances of ^{9}Be and ^{6}Li, respectively [79]. The effect of electromagnetic and hadronic energy injection on primordial D disfavors the regions inside the short-dash-dotted (blue) curves and to the right or inside of the short-dashed (blue) curves, respectively. Those curves are obtained from the severe and conservative upper limits defined in Sect. 4.1 of [299] based on results of [59, 61]. The region below the dashed (green) line is disfavored by the effect of electromagnetic energy injection on ^{3}He/D [61]. While the constraints from hadronic energy injection are obtained for a purely 'right-handed' $\tilde{l}_1 \simeq \tilde{l}_{\rm R}$ NLSP, the ones from electromagnetic energy injection are valid for the $\widetilde{\tau}_1$ NLSP case with a visible electromagnetic energy of $E_{\rm vis} = \epsilon_{\rm em} = 0.3 E_\tau$ released in $\widetilde{\tau}_1 \to \widetilde{G}\tau$. Reprinted (figure) with kind permission from [79]. Copyright (2008) by IOP Publishing

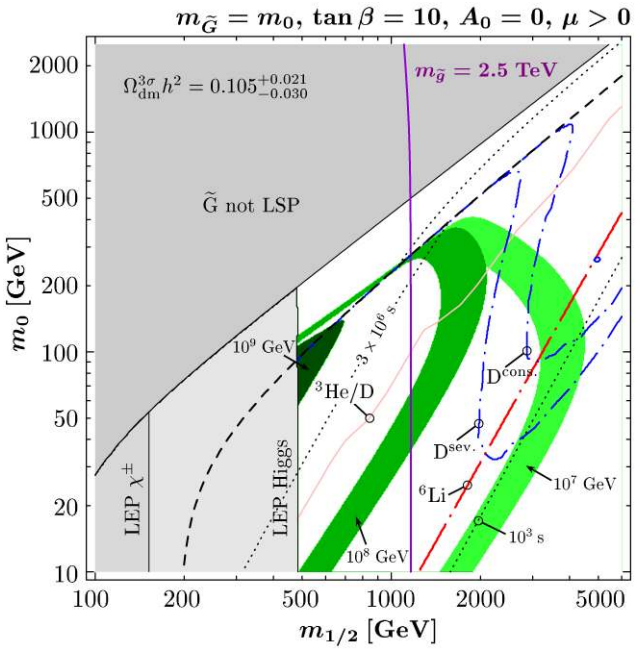

Fig. 4.4 CMSSM regions with $\Omega_{\widetilde{G}} h^2 \in \Omega^{3\sigma}_{\rm dm}$ for $T_{\rm R} = 10^7$, 10^8, and 10^9 GeV indicated respectively by the *light*, *medium*, and *dark-shaded* (*green*) *bands* in the $(m_{1/2}, m_0)$ planes for $\tan\beta = 10$, $A_0 = 0$, $\mu > 0$, and $m_{\widetilde{G}} = m_0$. The $T_{\rm R}$ values are associated with the $T_{\rm R}$ definition given in (3.5). The regions excluded by the chargino and Higgs mass bounds and the line indicating $m_{\widetilde{\chi}^0_1} = m_{\widetilde{\tau}_1}$ are identical to the ones shown in Fig. 3.1. In the *dark gray region*, the gravitino is not the LSP. The *dotted lines* show contours of the NLSP lifetime. The region to the left of the long-dash-dotted (red) line and to the left of the thin gray (pink) line is disfavored by the observationally inferred abundances of primordial ^{6}Li [74] and ^{3}He/D [61]. The effect of hadronic energy injection on primordial D [299] disfavors the $\widetilde{\tau}_1$ NLSP region above the short-dash-dotted (blue) lines. The $\widetilde{\chi}^0_1$ NLSP region is disfavored by BBN constraints from energy injection [67, 223, 298, 315]. On the *solid vertical line* (*violet*) $m_{\widetilde{g}} = 2.5$ TeV. Reprinted (figure) with kind permission from [318]. Copyright (2008) by The European Physical Journal (EPJ)

If the NLSP decays into the $\widetilde{G}$ LSP occur during or after BBN, the standard-model particles emitted in addition to the gravitino can affect the abundances of the primordial light elements as explained in Sect. 3.2 for scenarios with late-decaying $\widetilde{G}$'s. Indeed, these BBN constraints disfavor the $\widetilde{\chi}^0_1$ NLSP for $m_{\widetilde{G}} \gtrsim 100$ MeV [67, 223, 315]. For the charged slepton NLSP case, the BBN constraints associated with electromagnetic/hadronic energy injection have also been considered and found to be much weaker but still significant in much of the parameter space [67, 207, 223, 299, 315]. This can be seen for a $\tilde{l}_1 \simeq \tilde{l}_{\rm R}$ NLSP with (4.7) in Fig. 4.3, where the constraints from electromagnetic and hadronic energy release are shown respectively by the short-dashed (blue, labeled as $D^{\rm sev,cons}_{\rm em}$) and long-dashed (green, labeled as ^{3}He/D) lines and by the short-dash-dotted (blue, labeled as $D^{\rm sev,cons}_{\rm had}$) lines. For the $\tilde{l}_1$ NLSP within the CMSSM with $Y^{\rm dec}_{\tilde{l}_1}$ calculated by `micrOMEGAs 1.3.7` [209, 210], the electromagnetic ^{3}He/D and the hadronic $D^{\rm sev,cons}_{\rm had}$ constraints are also shown respectively by the thin gray (pink) and the short-dash-dotted (blue) lines in Fig. 4.4.[21] In the $\widetilde{\nu}_1$ NLSP case, there are basically no electromagnetic constraints while the hadronic ones are similar to those in the charged slepton NLSP case; see Refs. [63, 219, 223, 224] for details. In the $\widetilde{t}_1$ NLSP case, there can be electromagnetic and hadronic energy injection. Indeed, the (average) hadronic energy emitted in a single $\widetilde{t}_1$ decay $\epsilon_{\rm had}$ can be relatively large. However, since BBN constraints apply often to combinations such as $\epsilon_{\rm had} Y^{\rm dec}_{\widetilde{t}_1}$, this can be compensated to some extend by a relatively small $Y^{\rm dec}_{\widetilde{t}_1}$, which results from

[21] The electromagnetic constraints shown in Figs. 4.3 and 4.4 apply to the $\widetilde{\tau}_1$ NLSP and are obtained from Fig. 42 of Ref. [61] for a 'visible' electromagnetic energy of $E_{\rm vis} = \epsilon_{\rm em} = 0.3 E_\tau$ of the τ energy $E_\tau = (m^2_{\widetilde{\tau}_1} - m^2_{\widetilde{G}} + m^2_\tau)/2m_{\widetilde{\tau}_1}$ released in $\widetilde{\tau}_1 \to \widetilde{G}\tau$.

efficient annihilation due to the strong coupling of the colored $\widetilde{t}_1$ [212, 222, 309]. In fact, a $\widetilde{t}_1$ NLSP can experience color confinement due to its color charge and thus allows for intriguing non-trivial scenarios [212, 213, 308].

An additional constraint on electromagnetic energy injection can be inferred from the observed Planck spectrum of the CMB [322, 323]. This CMB constraint is not shown. According to the results of [323] for the case of a $\widetilde{\tau}_R$ NLSP, this limit is everywhere less severe than the severe electromagnetic limit $D_{\rm em}^{\rm sev}$ given by the short-dashed (blue) line in Fig. 4.3.

As already mentioned in the Introduction, also the mere presence of a long-lived negatively charged particle X^-—such as a long-lived $\tilde{l}_1^-$—can lead to bound states that catalyze BBN reactions and can thereby be associated with BBN constraints. In fact, the possibility that BBN can be affected by bound-state formation of an X^- with primordial nuclei had already been realized almost twenty years ago [324–326]. It was however only less than three years ago [64] when it was realized that bound-state formation of X^- with ^{4}He can lead to a substantial production of primordial ^{6}Li via the CBBN reaction

$$\left(^4\mathrm{He}X^-\right) + \mathrm{D} \rightarrow {}^6\mathrm{Li} + X^-. \tag{4.9}$$

Since then, there has been a considerable effort to refine various aspects of CBBN and to understand its implications in the framework of specific models [63, 65–79, 207, 310, 317, 318, 327, 328]. In particular, it has been pointed out in [78] that there is also the possibility of efficient ^{9}Be production via a radiative fusion of ^{4}He and $(^4\mathrm{He}X^-)$ leading to $(^8\mathrm{Be}X^-)$, which can capture a neutron resonantly,[22]

$$^4\mathrm{He} + \left(^4\mathrm{He}X^-\right) \rightarrow \left(^8\mathrm{Be}X^-\right) + \gamma, \tag{4.10}$$

$$\left(^8\mathrm{Be}X^-\right) + n \rightarrow {}^9\mathrm{Be} + X^-. \tag{4.11}$$

The efficiency of CBBN of both ^{6}Li and ^{9}Be depends strongly on the abundance of X^- at the relevant times, which is given by $Y_{\tilde{l}_1^-}^{\rm dec}$ and $\tau_{\tilde{l}_1}$ for $X^- = \tilde{l}_1^-$, i.e., in the slepton NLSP case. Observationally inferred limits on the primordial abundances of both ^{6}Li and ^{9}Be can thus be used to extract $\tau_{\tilde{l}_1}$-dependent upper limits on $Y_{\tilde{l}_1^-}^{\rm dec}$. Indeed, from the limits $^6\mathrm{Li/H}|_{\rm obs} \leq 10^{-11}$–$10^{-10}$ (cf. [59, 75, 329]) and $^9\mathrm{Be/H}|_{\rm obs} \leq 2.1 \times 10^{-13}$ [79], the $\tau_{\tilde{l}_1}$-dependent bounds on $Y_{\tilde{l}_1^-}^{\rm dec}$ shown in Fig. 5 of Ref. [79] have been obtained. Confronting (4.7) with those bounds, one finds the ^{9}Be and ^{6}Li constraints shown respectively by the solid and by the long-dash-dotted (red) lines in Fig. 4.3. The long-dash-dotted (red) line in Fig. 4.4 shows the constraint associated with $^6\mathrm{Li/H}|_{\rm obs} \lesssim 2 \times 10^{-11}$ [59] as obtained from the CBBN treatment of [74] with $Y_{\tilde{l}_1}^{\rm dec}$ from `micrOMEGAs`.

For a typical yield (4.7), the CBBN constraints associated with ^{6}Li and ^{9}Be imply [64, 68, 69, 71, 74, 79]

$$\tau_{\tilde{l}_1} \lesssim 5 \times 10^3 \text{ s}. \tag{4.12}$$

While numerous other CBBN reactions can also affect the abundances of ^{6}Li, ^{9}Be, and other primordial elements [67, 69, 73, 75, 78, 79, 328], the approximate $\tau_{\tilde{l}_1}$ bound is relatively robust. In particular, the possibility of allowed islands in the parameter region with large $Y_{\tilde{l}_1}^{\rm dec}$/large $\tau_{\tilde{l}_1}$—which was advocated to remain viable in Ref. [73]—does not exist [79]. The finding of relaxed $Y_{\tilde{l}_1^-}^{\rm dec}$ limits at long lifetimes $\tau_{\tilde{l}_1}$ in Ref. [73] did rely on the presence of $(p\tilde{l}_1^-)$ bound states and on a claimed significant reprocessing of ^{6}Li by nuclear reactions such as $(p\tilde{l}_1^-) + {}^6\mathrm{Li} \rightarrow \tilde{l}_1^- + {}^4\mathrm{He} + {}^3\mathrm{He}$. However, it is clarified in Ref. [79] that the presence of $(p\tilde{l}_1^-)$ bound states cannot relax the $Y_{\tilde{l}_1^-}^{\rm dec}$ limits at long lifetimes $\tau_{\tilde{l}_1}$ in any substantial way because of charge exchange reactions such as $(p\tilde{l}_1^-) + {}^4\mathrm{He} \rightarrow ({}^4\mathrm{He}\tilde{l}_1^-) + p$ and $(p\tilde{l}_1^-) + {}^6\mathrm{Li} \rightarrow ({}^6\mathrm{Li}\tilde{l}_1^-) + p$ that can be very efficient [79]. This finding has recently been confirmed in quantum three-body calculations [328].

As can be seen in Fig. 4.3, the cosmological constraints provide an upper bound on $m_{\widetilde{G}}$ once $m_{\tilde{\tau}_1}$ is measured. This bound implies upper bounds on the SUSY breaking scale, on $\Omega_{\widetilde{G}}^{\rm NTP}$, and—as can be seen in Fig. 4.2—on T_R. Figure 4.4 shows that the cosmological constraints imply not only an upper limit on T_R [207] but also a lower limit on $m_{1/2}$ [67, 207]. Indeed, $m_{\widetilde{G}}$-dependent limits on the reheating temperature,

$$T_R \leq 4.9 \times 10^7 \text{ GeV} \left(\frac{m_{\widetilde{G}}}{10 \text{ GeV}}\right)^{1/5}, \tag{4.13}$$

and on the gaugino mass parameter,

$$m_{1/2} \geq 0.9 \text{ TeV} \left(\frac{m_{\widetilde{G}}}{10 \text{ GeV}}\right)^{2/5}, \tag{4.14}$$

have been derived within the CMSSM [74] from the limit (4.12), i.e., under the assumption that $Y_{\tilde{l}_1}^{\rm dec}$ is described approximately by (4.7).[23] While the T_R bound can be restrictive for models of inflation and of baryogenesis, the $m_{1/2}$ bound can have implications for SUSY searches at the LHC. Depending on $m_{\widetilde{G}}$, (4.14) implies sparticle masses

[22] The large ^{9}Be-production cross section reported and used in Refs. [78, 79] has very recently been questioned by Ref. [328], in which a study based on a four-body model is announced as work in progress to clarify the efficiency of ^{9}Be production.

[23] Similar limits have also been discussed in models where the ratio $m_{\widetilde{G}}/m_{1/2}$ is bounded from below [327].

which can be associated with a mass range that will be difficult to probe at the LHC. This is illustrated by the vertical (violet) line in Fig. 4.4 which indicates the gluino mass $m_{\widetilde{g}} = 2.5$ TeV [318].[24]

Here one should emphasize that the $T_{\rm R}$ limit (4.13) relies on the CMSSM-specific minimal splitting [74] $m^2_{\widetilde{\tau}_1} \leq 0.21 m^2_{1/2}$. In a less restrictive model, higher $T_{\rm R}$ values can be viable for a smaller splitting between the masses of the gluino and the $\tilde{l}_1$ NLSP [317]. This is shown in Fig. 4.5 (from [317]), where the maximum reheating temperature $T_{\rm R}^{\rm max}$ imposed by $\Omega^{\rm TP}_{\widetilde{G}} \leq \Omega_{\rm dm}$ and $\tau_{\tilde{l}_1} \leq 5 \times 10^3$ GeV (10^4 GeV) is shown by the solid (dashed) lines in the plane spanned by $m_{\tilde{l}_1}$ and the ratio $c = m_{\widetilde{g}}/m_{\tilde{l}_1}$ at the weak scale. Note that the shown $T_{\rm R}^{\rm max}$ values are given by [317]

$$T_{\rm R} \leq \frac{2.37 \times 10^9 \text{ GeV}}{c^2} \left(\frac{\Omega_{\rm dm} h^2}{0.1}\right) \times \left(\frac{\tau_{\tilde{l}_1}}{10^4 \text{ s}}\right)^{\frac{1}{2}} \left(\frac{m_{\tilde{l}_1}}{100 \text{ GeV}}\right)^{\frac{1}{2}} \equiv T_{\rm R}^{\rm max} \tag{4.15}$$

which has been derived in a very conservative way taking into account only the SUSY QCD contribution to $\Omega^{\rm TP}_{\widetilde{G}}$.

The BBN constraints shown in Figs. 4.3, 4.4, and 4.5 and (4.12), (4.13), and (4.14) rely on typical $Y^{\rm dec}_{\tilde{l}_1}$ values such as the ones given by (4.7). However, $Y^{\rm dec}_{\widetilde{\tau}_1} < 4 \times 10^{-15}$ can be found even within the CMSSM as is shown in Fig. 4.1. Indeed, for a $\widetilde{\tau}_1$ NLSP with a sizable left-right mixing, exceptional values of $Y^{\rm dec}_{\widetilde{\tau}_1} \lesssim 10^{-15}$ can occur [311, 312] for which even the restrictive CBBN bounds associated with $^6{\rm Li/H}|_{\rm obs} \leq 10^{-10}$ and $^9{\rm Be/H}|_{\rm obs} \leq 2.1 \times 10^{-13}$ (cf. Fig. 5 of [79]) can be evaded. In these exceptional cases, the $\tau_{\tilde{l}_1}$ limit (4.12) does not exist and the $T_{\rm R}$ limit is governed by $\Omega^{\rm TP}_{\widetilde{G}} \leq \Omega_{\rm dm}$ only (cf. Fig. 4.2) since $\Omega^{\rm NTP}_{\widetilde{G}}$ is negligible.

4.3 Experimental prospects

Because of its extremely weak couplings, gravitino dark matter is inaccessible to direct and indirect searches if R-parity is conserved.[25] Also the direct production of gravitinos with $m_{\widetilde{G}} \gtrsim 0.1$ keV at colliders is extremely suppressed. Instead, one expects a large sample of (quasi-) stable NLSPs if the NLSP belongs to the MSSM spectrum and if its mass is within the kinematical reach.

The $\widetilde{\chi}^0_1$ and the $\widetilde{\nu}_1$ NLSP cases will be associated with an excess of missing transverse energy and it might become a major challenge to distinguish such cases from the $\widetilde{\chi}^0_1$ LSP case; cf. [218, 219]. Indeed, the phenomenological prospects

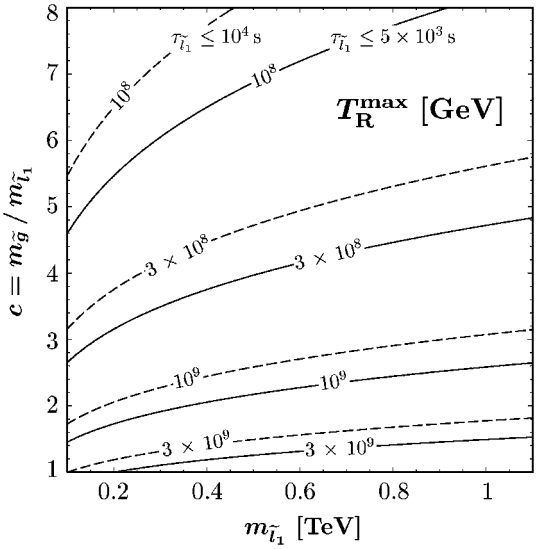

Fig. 4.5 Upper limits on the mass ratio $c = m_{\widetilde{g}}/m_{\tilde{l}_1}$ imposed by $\Omega^{\rm TP}_{\widetilde{G}} h^2 \leq \Omega_{\rm dm} h^2 \leq 0.126$ and $\tau_{\tilde{l}_1} \leq 5 \times 10^3$s ($10^4$s) are shown as a function of $m_{\tilde{l}_1}$ by the *solid* (*dashed*) *lines* for values of $T_{\rm R}^{\rm max}$ ranging from 10^8 GeV up to 3×10^9 GeV. These values refer to the $T_{\rm R}$ definition given in (3.5). Reprinted (figure) with kind permission from [317]. Copyright (2008) by Elsevier

will be much more promising in scenarios with the $\tilde{l}_1$ NLSP or the $\widetilde{t}_1$ NLSP. These particles can appear respectively as (quasi-) stable electrically charged elementary particles or as stop hadrons in the collider detectors. Because of possibly non-trivial hadronization properties of the $\widetilde{t}_1$ NLSP, we focus on the simpler $\widetilde{\tau}_1$ NLSP case in the remainder of this section.

In the $\widetilde{\tau}_1$ NLSP case, each heavier superpartner produced will cascade down to the $\widetilde{\tau}_1$ which will appear as a (quasi-) stable particle in the detector. Such a heavy charged particle would penetrate the collider detector in a way similar to muons [336–338]. If the produced staus are slow, the associated highly ionizing tracks and time–of–flight measurements will allow one to distinguish the $\widetilde{\tau}_1$ from a muon [336–339]. With measurements of the $\widetilde{\tau}_1$ velocity $\beta_{\widetilde{\tau}_1} \equiv v_{\widetilde{\tau}_1}/c$ and the slepton momentum $p_{\widetilde{\tau}_1} \equiv |\vec{p}_{\widetilde{\tau}_1}|$, $m_{\widetilde{\tau}_1}$ can be determined: $m_{\widetilde{\tau}_1} = p_{\widetilde{\tau}_1}(1-\beta^2_{\widetilde{\tau}_1})^{1/2}/\beta_{\widetilde{\tau}_1}$ [339]. For the upcoming LHC experiments, studies of hypothetical scenarios with long-lived charged particles are actively pursued; see, e.g., [340–343]. For example, it has been found that one should be able to measure the mass $m_{\widetilde{\tau}_1}$ of a (quasi-) stable $\widetilde{\tau}_1$ quite accurately [340, 341].[26]

If some of the staus decay already in the collider detectors, the statistical method proposed in [339] could allow one to measure the $\widetilde{\tau}_1$ lifetime. With (4.8) and the measured

[24] Note that the mass of the lighter stop is $m_{\widetilde{t}_1} \simeq 0.7 m_{\widetilde{g}}$ in the considered $\widetilde{\tau}_1$ NLSP region with $m_{\rm h} > 114.4$ GeV.

[25] For broken R-parity, the $\widetilde{G}$ LSP is unstable and its decay products can lead to signals in indirect searches [39, 330–335].

[26] (Quasi-) stable $\widetilde{\tau}_1$'s could also be pair-produced in interactions of cosmic neutrinos in the Earth matter and be detected in a neutrino telescope such as IceCube [344].

value of $m_{\widetilde{\tau}_1}$, one will then be able to determine also the gravitino mass $m_{\widetilde{G}}$ and thereby the scale of SUSY breaking. As a test of our understanding of the early Universe, it will also be interesting to confront the experimentally determined $(m_{\widetilde{G}}, m_{\widetilde{\tau}_1})$ point with the cosmological constraints in Fig. 4.3.

Ways to stop and collect charged long-lived particles for an analysis of their decays have also been proposed [345–350]. It was found that up to $\mathcal{O}(10^3$–$10^4)$ and $\mathcal{O}(10^3$–$10^5)$ $\widetilde{\tau}_1$'s could be trapped per year at the LHC and the ILC, respectively, by placing 1–10 kt of massive additional material around existing or planned collider detectors [346, 347]. A measurement of $\tau_{\widetilde{\tau}_1}$ can then be used to determine $m_{\widetilde{G}}$ as already described above. If $m_{\widetilde{G}}$ can be determined independently from the kinematics of the two-body decay $\widetilde{\tau}_1 \to \widetilde{G}\tau$,

$$m_{\widetilde{G}} = \sqrt{m_{\widetilde{\tau}_1}^2 + m_\tau^2 - 2m_{\widetilde{\tau}_1} E_\tau}, \tag{4.16}$$

the lifetime $\tau_{\widetilde{\tau}_1}$ can allow for a measurement of the Planck scale [349, 351–353],

$$\mathrm{M_P^2} = \frac{\tau_{\widetilde{\tau}_1}}{48\pi} \frac{m_{\widetilde{\tau}_1}^5}{m_{\widetilde{G}}^2} \left(1 - \frac{m_{\widetilde{G}}^2}{m_{\widetilde{\tau}_1}^2}\right)^4. \tag{4.17}$$

Agreement with (3.1), which is inferred from Newton's constant [2] $G_\mathrm{N} = 6.709 \times 10^{-39}\ \mathrm{GeV}^{-2}$, would then provide a strong experimental hint for the existence of supergravity in nature [351]. In fact, this agreement would be a striking signature of the gravitino LSP. Unfortunately, the required kinematical determination of $m_{\widetilde{G}}$ appears to be feasible only for [349, 352, 353] $m_{\widetilde{G}}/m_{\widetilde{\tau}_1} \gtrsim 0.1$ which seems to be disfavored in most of the SUSY parameter space according to our present understanding of the cosmological constraints (see Fig. 4.3).[27] Accordingly, alternative methods such as the ones proposed in [190, 354] could become essential to identify the gravitino as the LSP. In the special regions with exceptionally small $Y_{\widetilde{\tau}_1}^{\mathrm{dec}} \lesssim 10^{-15}$ [311, 312], however, the cosmological constraints could be evaded even within a standard cosmological history and $m_{\widetilde{G}}$ can still be sufficiently close to $m_{\widetilde{\tau}_1}$ so that the kinematical $m_{\widetilde{G}}$ determination can still be viable. Here, also the spin-3/2 character of the gravitino can become relevant so that it could be probed in principle by analyzing the decays $\widetilde{\tau}_1 \to \widetilde{G}\tau\gamma$ [351].

With additional experimental insights into the masses of the gluino and of the neutralinos (and thereby into $M_{1,2,3}$ and their possibly universal value $m_{1/2}$ at M_{GUT}), the determination of $m_{\widetilde{G}}$ (or $\tau_{\widetilde{\tau}_1}$) can allow one to probe also the upper limit on the reheating temperature $T_\mathrm{R}^{\mathrm{max}}$ at colliders [71, 222, 231, 232, 294, 295, 299, 316, 317]; cf. Figs. 4.2, 4.4, and 4.5. This possibility results from the extremely weak gravitino couplings, the associated T_R dependence of $\Omega_{\widetilde{G}}^{\mathrm{TP}}$, and the limit $\Omega_{\widetilde{G}}^{\mathrm{TP}} \leq \Omega_{\mathrm{dm}}$. Any $T_\mathrm{R}^{\mathrm{max}}$ value inferred from collider experiments will however depend crucially on assumptions on the cosmological history and on the evolution of physical parameters as discussed already for T_R bounds in $\widetilde{\chi}_1^0$ LSP scenarios in Sect. 3.2. It would still be very insightful to compare, e.g., the minimum temperature required by thermal leptogenesis in its simplest setting, $T \gtrsim 10^9$ GeV, with the $T_\mathrm{R}^{\mathrm{max}}$ value obtained under the assumptions of a standard cosmological history and of couplings that behave at high temperatures as described by the renormalization group equations in the MSSM.

5 Axino dark matter

The axino $\widetilde{a}$ [355–358] appears as the spin-1/2 superpartner of the axion once the MSSM is extended with the PQ mechanism [21, 22] in order to solve the strong CP problem. Depending on the model and on the SUSY breaking scheme, the axino mass $m_{\widetilde{a}}$ can range between the eV and the GeV scale [357, 359–363]. The axino is a singlet with respect to the gauge groups of the standard model. It interacts extremely weakly since its couplings are suppressed by the PQ scale $f_a \gtrsim 6 \times 10^8$ GeV [2, 24, 115, 364] and thus can be classified as an EWIP. The detailed form of the axino interactions depends on the axion model under consideration; cf. Sect. 2. We focus on hadronic (or KSVZ) axion models [102, 103] in a SUSY setting, in which the axino couples to the MSSM particles only indirectly through loops of additional heavy KSVZ (s)quarks. Considering $\widetilde{a}$ LSP scenarios in which the LOSP is the NLSP, $m_{\widetilde{\tau}_1} < m_{\widetilde{\chi}_1^0}$ is again viable as also the alternative $\widetilde{\chi}_1^0$, $\widetilde{\nu}_1$, and $\widetilde{t}_1$ NLSP cases.

Before proceeding, it should be stressed that the bosonic partners of the axino, the axion and the saxion, can have important implications for cosmology: (i) Those associated with the axion have already been discussed in Sect. 2 and most important for this section is the possibly significant axion contribution to Ω_{dm} which can tighten the constraints from $\Omega_{\widetilde{a}}^{\mathrm{TP}} < \Omega_{\mathrm{dm}}$ discussed below. (ii) Late decays of the saxion can lead to significant entropy production [365–368] and can thereby affect the cosmological constraints [369]. In this review, however, a standard thermal history is assumed which implies that saxion effects are negligible.

5.1 Primordial origin

Because of their extremely weak interactions, the temperature T_f at which axinos decouple from the thermal plasma in the early Universe is very high. For example, an axino decoupling temperature of $T_\mathrm{f} \approx 10^9$ GeV is obtained for

[27] Note that the cosmological constraints described in Sect. 4.2 assume a standard thermal history. In fact, entropy production after NLSP decoupling and before BBN can weaken the BBN constraints significantly [207, 314].

$f_a = 10^{11}$ GeV [360, 370]. For $T_R > T_f$, axinos were in thermal equilibrium before decoupling as a relativistic species so that [360, 370–372]

$$\Omega_{\widetilde{a}}^{\rm therm} h^2 \approx 0.1 \left(\frac{m_{\widetilde{a}}}{0.2\ {\rm keV}} \right), \tag{5.1}$$

where $g_{*S}(T_f) = 228.75$ is assumed.

For $T_R < T_f$, axinos have never been in thermal equilibrium with the primordial plasma but can be generated efficiently in scattering processes of particles that are in thermal equilibrium within the hot MSSM plasma [370–373]. Within SUSY QCD, the associated thermally produced (TP) axino density can be calculated in a consistent gauge-invariant treatment that requires weak couplings ($g_s \ll 1$) [370]:

$$\Omega_{\widetilde{a}}^{\rm TP} h^2 \simeq 5.5 g_s^6(T_R) \ln\left(\frac{1.108}{g_s(T_R)} \right) \left(\frac{10^{11}\ {\rm GeV}}{f_a/N} \right)^2 \times \left(\frac{m_{\widetilde{a}}}{0.1\ {\rm GeV}} \right) \left(\frac{T_R}{10^4\ {\rm GeV}} \right), \tag{5.2}$$

with the axion-model-dependent color anomaly N of the PQ symmetry. The thermally produced axinos do not affect the thermal evolution of the LOSP (or NLSP) which decays after its decoupling into the $\widetilde{a}$ LSP. Taking into account the non-thermally produced (NTP) density from NLSP decays [372, 374]

$$\Omega_{\widetilde{a}}^{\rm NTP} h^2 = m_{\widetilde{a}} Y_{\rm NLSP}^{\rm dec} s(T_0) h^2/\rho_c, \tag{5.3}$$

the guaranteed axino density is[28]

$$\Omega_{\widetilde{a}} = \Omega_{\widetilde{a}}^{\rm therm/TP} + \Omega_{\widetilde{a}}^{\rm NTP}. \tag{5.4}$$

In Fig. 5.1 (from [370]) the $(m_{\widetilde{a}}, T_R)$ region with $0.097 \leq \Omega_{\widetilde{a}}^{\rm TP} \leq 0.129$ for $f_a/N = 10^{11}$GeV is shown by the gray band. Note that (5.2) shows a different dependence on the LSP mass than the corresponding expression in the $\widetilde{G}$ LSP case (4.3). Accordingly, one finds the different $m_{\rm LSP}$ dependence of the T_R limits inferred from $\Omega_{\widetilde{a}/\widetilde{G}}^{\rm TP} < \Omega_{\rm dm}$. Since thermally produced axinos are generated in kinetic equilibrium with the primordial plasma, they have a thermal spectrum which allows for the $m_{\widetilde{a}}$-dependent classification into cold, warm, and hot dark matter [372] shown in Fig. 5.1. As can be seen, the T_R limit does not exist for $m_{\widetilde{a}} \lesssim 0.2$ keV because of the equality of $\widetilde{a}$ production and $\widetilde{a}$ disappearance rates for $T > T_f \approx 10^9$ GeV. With a thermal relic density (5.1) in this regime, there will be a limit on $m_{\widetilde{a}}$ depending on the constraints inferred from studies of warm/hot dark matter [7].

[28] Axino production in inflaton decays is not considered.

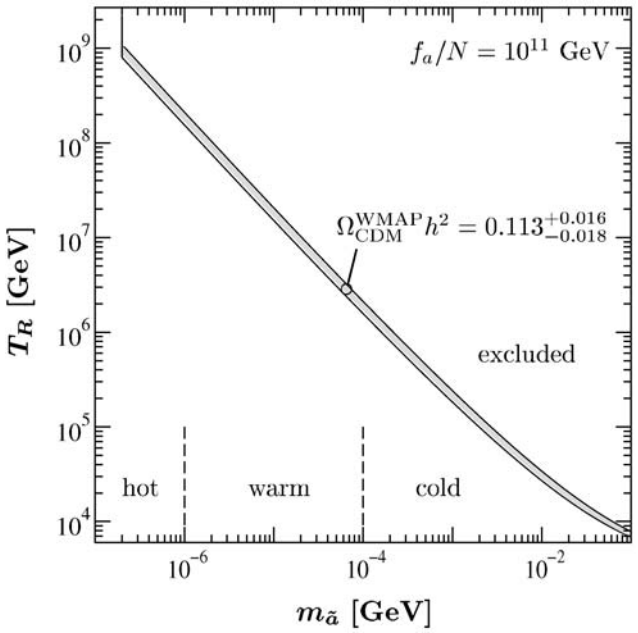

Fig. 5.1 Upper limits on the reheating temperature T_R in the $\widetilde{a}$ LSP case for $f_a/N = 10^{11}$ GeV. On (above) the gray band, $\Omega_{\widetilde{a}}^{\rm TP} h^2 \in 0.113^{+0.016}_{-0.018}$ ($\Omega_{\widetilde{a}}^{\rm TP} h^2 > 0.129$). Thermally produced axinos can be classified as hot, warm, and cold dark matter [372] as indicated. Reprinted (figure) with kind permission from [370]. Copyright (2004) by IOP Publishing

The non-thermally produced axino density $\Omega_{\widetilde{a}}^{\rm NTP}$ differs from the corresponding expression in the $\widetilde{G}$ LSP case (4.5) only by the obvious difference in $m_{\widetilde{a}/\widetilde{G}}$. In particular, for given $\Omega_{\widetilde{a}}^{\rm TP}$, the bound $\Omega_{\widetilde{a}}^{\rm NTP} \leq \Omega_{\rm dm} - \Omega_{\widetilde{a}}^{\rm eq/TP}$ as obtained with (4.7) implies limits on $m_{\widetilde{a}}$ and $m_{\widetilde{\tau}_1}$ which can be read off directly from Fig. 4.3 after the replacement $m_{\widetilde{G}} \to m_{\widetilde{a}}$. Note, however, that the $\tau_{\widetilde{\tau}_1}$ contours and the cosmological constraints are different in the axino LSP case. For the $\widetilde{\tau}_1$ NLSP, the following lifetime was estimated [190]

$$\tau_{\widetilde{\tau}_1} \simeq \Gamma^{-1}(\widetilde{\tau}_1 \to \tau \widetilde{a}) \simeq 25\ {\rm s}\, \xi^{-2} \left(1 - \frac{m_{\widetilde{a}}^2}{m_{\widetilde{\tau}_1}^2} \right)^{-1} \times \left(\frac{100\ {\rm GeV}}{m_{\widetilde{\tau}_1}} \right) \left(\frac{f_a/C_{\rm aYY}}{10^{11}\ {\rm GeV}} \right)^2 \left(\frac{100\ {\rm GeV}}{m_{\widetilde{B}}} \right)^2 \tag{5.5}$$

with the KSVZ-model dependence expressed by $C_{\rm aYY} \simeq \mathcal{O}(1)$ and the uncertainty of the estimate absorbed into $\xi \simeq \mathcal{O}(1)$. One thus finds a $\widetilde{\tau}_1$ lifetime in the $\widetilde{a}$ LSP case that cannot be as large as the one in the $\widetilde{G}$ LSP case (4.8). Accordingly, the BBN constraints are much weaker for the $\widetilde{a}$ LSP. For discussions of $\widetilde{a}$ LSP scenarios with the $\widetilde{\chi}_1^0$ NLSP, see [372, 374, 375]. For both the $\widetilde{\tau}_1$ NLSP and the $\widetilde{\chi}_1^0$ NLSP, it has been shown that non-thermally produced axinos with $m_{\widetilde{a}} \lesssim 10$ GeV would be warm/hot dark matter [321].

5.2 Experimental prospects

Being an EWIP, the axino LSP is inaccessible in direct and indirect dark-matter searches if R-parity is conserved. Also direct $\widetilde{a}$ production at colliders is strongly suppressed. Nevertheless, (quasi-) stable $\widetilde{\tau}_1$'s could appear in collider detectors (and neutrino telescopes [344]) as a possible signature of the $\widetilde{a}$ LSP. However, since the M_P measurement at colliders [351], which would have been a decisive test of the $\widetilde{G}$ LSP, seems cosmologically disfavored in most of the parameter space of R-parity conserving SUSY models, it may very well be a challenge to distinguish between the $\widetilde{a}$ LSP and the $\widetilde{G}$ LSP.

For $m_{\widetilde{\tau}_1} = 100$ GeV and $m_{\widetilde{B}} = 110$ GeV, for example, the $\widetilde{\tau}_1$ lifetime in the $\widetilde{a}$ LSP scenario (5.5) can range from $\mathcal{O}(10^{-4}$ s) for $f_a = 5 \times 10^8$ GeV to $\mathcal{O}(10$ h) for $f_a = 5 \times 10^{12}$ GeV. In the $\widetilde{G}$ LSP case, the corresponding lifetime (4.8) can vary over an even wider range, e.g., from 6×10^{-8} s for $m_{\widetilde{G}} = 1$ keV to 15 years for $m_{\widetilde{G}} = 50$ GeV. Thus, both a very short lifetime, $\tau_{\widetilde{\tau}_1} \lesssim$ ms, and a very long one, $\tau_{\widetilde{\tau}_1} \gtrsim$ days, will point to the $\widetilde{G}$ LSP. On the other hand, if the LSP mass cannot be measured kinematically and if $\tau_{\widetilde{\tau}_1} = \mathcal{O}(0.01$ s)–$\mathcal{O}(10$ h), the stau lifetime alone will not allow us to distinguish between the $\widetilde{a}$ LSP and the $\widetilde{G}$ LSP.

The situation is considerably improved when one considers the three-body decays $\widetilde{\tau}_1 \to \tau\gamma\widetilde{a}/\widetilde{G}$. From the corresponding differential rates [190], one obtains the differential distributions of the visible decay products. These are illustrated in Fig. 5.2 (from [190]) in terms of

$$\frac{1}{\Gamma(\widetilde{\tau}_1 \to \tau\gamma i; x_\gamma^{\rm cut}, x_\theta^{\rm cut})} \frac{\mathrm{d}^2\Gamma(\widetilde{\tau}_1 \to \tau\gamma i)}{\mathrm{d}x_\gamma\, \mathrm{d}\cos\theta}, \tag{5.6}$$

where $x_\gamma \equiv 2E_\gamma/m_{\widetilde{\tau}_1}$ is the scaled photon energy, θ the opening angle between the directions of γ and τ,

$$\Gamma\big(\widetilde{\tau}_1 \to \tau\gamma i; x_\gamma^{\rm cut}, x_\theta^{\rm cut}\big) \equiv \int_{x_\gamma^{\rm cut}}^{1-A_i} \mathrm{d}x_\gamma \int_{-1}^{1-x_\theta^{\rm cut}} \mathrm{d}\cos\theta \times \frac{\mathrm{d}^2\Gamma(\widetilde{\tau}_1 \to \tau\gamma i)}{\mathrm{d}x_\gamma\, \mathrm{d}\cos\theta} \tag{5.7}$$

the respective integrated three-body decay rate with the cuts $x_\gamma > x_\gamma^{\rm cut}$ and $\cos\theta < 1 - x_\theta^{\rm cut}$, and $A_i \equiv m_i^2/m_{\widetilde{\tau}_1}^2$. Note that (5.6) is independent of the two-body decay, of the total NLSP decay rate, and of the PQ/Planck scale. The figure shows (5.6) for the axino LSP ($i = \widetilde{a}$) with $m_{\widetilde{a}}^2/m_{\widetilde{\tau}_1}^2 \ll 1$ (upper panel) and the gravitino LSP ($i = \widetilde{G}$) with $m_{\widetilde{G}} = 10$ MeV (lower panel), where $m_{\widetilde{\tau}_1} = 100$ GeV, $m_{\widetilde{B}} = 110$ GeV, and $x_\gamma^{\rm cut} = x_\theta^{\rm cut} = 0.1$. In the $\widetilde{G}$ LSP case, the events are peaked only in the region where photons are soft and emitted with a small opening angle with respect to the tau ($\theta \simeq 0$). In contrast, in the $\widetilde{a}$ LSP case, the events are also peaked in the region where the photon energy is large and the photon and the tau are emitted back-to-back ($\theta \simeq \pi$). Thus, if the observed number of events peaks in both regions, this can be evidence against the gravitino LSP and a hint towards the axino LSP [190].[29]

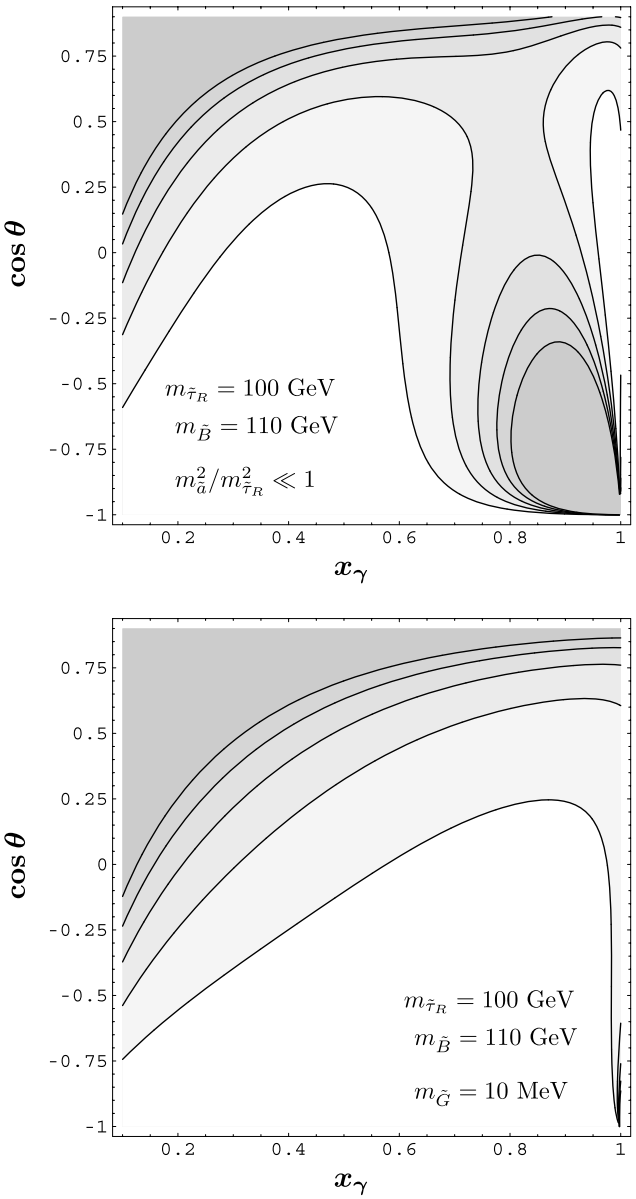

Fig. 5.2 The normalized differential distributions (5.6) of the visible decay products in the decays $\widetilde{\tau}_1 \to \tau + \gamma + \widetilde{a}/\widetilde{G}$ for the cases of the $\widetilde{a}$ LSP (*upper panel*) and the $\widetilde{G}$ LSP (*lower panel*) for $m_{\widetilde{\tau}_1} = 100$ GeV, $\widetilde{\chi}_1^0 \simeq \widetilde{B}$, $m_{\widetilde{B}} = 110$ GeV, $m_{\widetilde{a}}^2/m_{\widetilde{\tau}_1}^2 \ll 1$, and $m_{\widetilde{G}} = 10$ MeV. The cut parameters are set to $x_\gamma^{\rm cut} = x_\theta^{\rm cut} = 0.1$. The *contour lines* represent the values 0.2, 0.4, 0.6, 0.8, and 1.0, where the *darker shading* implies a higher number of events. Reprinted (figure) with kind permission from [190]. Copyright (2005) by Elsevier

[29] There is a caveat: if $m_{\widetilde{G}} < m_{\widetilde{a}} < m_{\widetilde{\tau}_1}$ and $\Gamma(\widetilde{\tau}_1 \to \widetilde{a}X) \gg \Gamma(\widetilde{\tau}_1 \to \widetilde{G}X)$, one would still find the distribution shown in the upper panel of

To be specific, with 10^4 analyzed stau NLSP decays, one expects about 165±13 (stat.) events for the $\widetilde{a}$ LSP and about 100±10 (stat.) events for the $\widetilde{G}$ LSP [190], which will be distributed over the respective $(x_\gamma, \cos\theta)$ planes shown in Fig. 5.2. In particular, in the region of $x_\gamma \gtrsim 0.8$ and $\cos\theta \lesssim -0.3$, we expect about 28% of the 165±13 (stat.) events in the $\widetilde{a}$ LSP case and about 1% of the 100±10 (stat.) events in the $\widetilde{G}$ LSP case. These numbers illustrate that $\mathcal{O}(10^4)$ of analyzed stau NLSP decays could be sufficient for the distinction based on the differential distributions. To establish the feasibility of this distinction, dedicated studies including details of the detectors and the additional massive material will be crucial [349].

5.3 Probing the Peccei–Quinn scale f_a and $m_{\widetilde{a}}$

If $\widetilde{a}$ is the LSP and $\widetilde{\tau}_1$ the NLSP, the analysis of the two-body decay $\widetilde{\tau}_1 \to \tau\widetilde{a}$ will allow us to probe the PQ scale f_a and the axino mass $m_{\widetilde{a}}$. In fact, the measurement of $\tau_{\widetilde{\tau}_1}$ (5.5) with methods described in Sect. 4.3 leads to the following estimate of the Peccei–Quinn scale f_a [190]:

$$f_a^2 \simeq \xi^2 C_{\mathrm{aYY}}^2 \bigl(10^{11}\ \mathrm{GeV}\bigr)^2 \biggl(1 - \frac{m_{\widetilde{a}}^2}{m_{\widetilde{\tau}_1}^2}\biggr)\biggl(\frac{\tau_{\widetilde{\tau}_1}}{25\ \mathrm{s}}\biggr) \times \biggl(\frac{m_{\widetilde{\tau}_1}}{100\ \mathrm{GeV}}\biggr)\biggl(\frac{m_{\widetilde{B}}}{100\ \mathrm{GeV}}\biggr)^2, \tag{5.8}$$

which can be confronted with f_a limits from axion studies; cf. Sect. 2. Indeed, we expect that $m_{\widetilde{\tau}_1}$ and $m_{\widetilde{B}}$ will already be known from other processes when the $\widetilde{\tau}_1$ NLSP decays are analyzed; cf. Sect. 4.3. The dependence on $m_{\widetilde{a}}$ is negligible for $m_{\widetilde{a}}/m_{\widetilde{\tau}_1} \lesssim 0.1$. For larger values of $m_{\widetilde{a}}$, the $\widetilde{\tau}_1$ NLSP decays can be used to determine $m_{\widetilde{a}}$ from the kinematics of the two-body decay, i.e., from a measurement of the energy of the emitted tau E_τ,

$$m_{\widetilde{a}} = \sqrt{m_{\widetilde{\tau}_1}^2 + m_\tau^2 - 2m_{\widetilde{\tau}_1} E_\tau}, \tag{5.9}$$

with an error governed by the experimental uncertainties on $m_{\widetilde{\tau}_1}$ and E_τ. As is evident from (5.2) and (5.3), the determination of both the PQ scale f_a and the axino mass $m_{\widetilde{a}}$ is crucial for insights into the cosmological relevance of the axino LSP.

In principle, the determination of both f_a and $m_{\widetilde{a}}$ at colliders would allow one to probe an upper limit on the reheating temperature $T_{\mathrm{R}}^{\max}$ at colliders for $m_{\widetilde{a}} \gtrsim 0.2$ keV as can be seen in Fig. 5.1; see also [316]. Indeed, Ref. [316] has outlined theoretical ways to probe T_{R} values as low as 100 GeV with $\Omega_{\widetilde{a}}^{\mathrm{NTP}}$ taken into account but without addressing the difficulties to determine an axino mass $m_{\widetilde{a}} \lesssim 10$ GeV experimentally. In analogy to the $\widetilde{G}$ LSP case, the theoretical possibility results from the extremely weak axino couplings, the associated T_{R} dependence of $\Omega_{\widetilde{a}}^{\mathrm{TP}}$, and the limit $\Omega_{\widetilde{a}}^{\mathrm{TP}} \leq \Omega_{\mathrm{dm}}$. However, the high T_{R} values at which the gauge-invariant result for $\Omega_{\widetilde{a}}^{\mathrm{TP}}$ is reliable, $T_{\mathrm{R}} \gtrsim 10^6$ GeV, are associated with $m_{\widetilde{a}} \ll 1$ GeV, while the kinematical determination (5.9) appears to be feasible only for $m_{\widetilde{a}} \gtrsim 0.1 m_{\widetilde{\tau}_1} \gtrsim 10$ GeV, as in the $\widetilde{G}$ LSP case [349, 352, 353]. Since also $\tau_{\widetilde{\tau}_1}$ is practically $m_{\widetilde{a}}$-independent for $m_{\widetilde{a}} \lesssim 10\ \mathrm{GeV} \lesssim 0.1 m_{\widetilde{\tau}_1}$, it seems unfortunately to be impossible to probe those T_{R} values in the axino LSP case at colliders.

Fig. 5.2. The axino would then eventually decay into the gravitino LSP and the axion.

6 Conclusion

The existence of dark matter provides strong evidence for physics beyond the standard model. Extending the standard model with PQ symmetry and/or SUSY, the axion and/or an electrically neutral and color neutral LSP appear as promising dark-matter candidates. The axion is well motivated by the PQ solution to the strong CP problem. With and without SUSY being realized in nature, the axion can exist and can contribute significantly to Ω_{dm}. In SUSY extensions of the standard model, the lightest neutralino $\widetilde{\chi}_1^0$, the gravitino $\widetilde{G}$, or the axino $\widetilde{a}$ can be the LSP and as such explain the non-baryonic dark matter in our Universe. The neutralino $\widetilde{\chi}_1^0$ is already part of the MSSM which provides a solution of the hierarchy problem and allows for gauge coupling unification. Being the superpartner of the graviton and the gauge field associated with supergravity, the gravitino $\widetilde{G}$ is equally well motivated with a mass $m_{\widetilde{G}}$ that reflects the SUSY breaking scale. As the superpartner of the axion, also the axino $\widetilde{a}$ appears naturally once the strong CP problem is solved with the PQ mechanism in a SUSY setting.

While mass values and interactions can be very different for the a, the $\widetilde{\chi}_1^0$ LSP, the $\widetilde{G}$ LSP, and the $\widetilde{a}$ LSP, I have illustrated for each of these dark-matter candidates that there are natural regions in the associated parameter space in which $\Omega_{a/\mathrm{LSP}} = \Omega_{\mathrm{dm}}$. In the axion case, the $\Omega_a = \Omega_{\mathrm{dm}}$ region can be subject to constraints from limits on axionic isocurvature and non-Gaussian perturbations inferred from the CMB anisotropies. In the SUSY case, regions with $\Omega_{\mathrm{LSP}} = \Omega_{\mathrm{dm}}$ are limited most importantly by bounds from electroweak precision observables, B-physics observables, Higgs and sparticle searches at LEP, and by BBN constraints. The constraints from Ω_{dm} and BBN also imply restrictive upper limits on the reheating temperature after inflation T_{R} which can be relevant for models of inflation and of baryogenesis.

Most promising are the experimental prospects in the case of the $\widetilde{\chi}_1^0$ LSP. Being a WIMP, the $\widetilde{\chi}_1^0$ LSP should be accessible in direct and indirect dark-matter searches. Indeed, first hints might have already been found in the EGRET data [260]. With ongoing indirect searches, the increasing

Table 6.1 Dark-matter candidates, their identity, and key properties. With the listed production mechanisms, $\Omega_X = \Omega_{\rm dm}$ is possible for each candidate X. The respective production mechanisms lead typically to a cold, warm, or hot dark-matter component, as indicated. Quantities marked with '(?)' seem to be unaccessible in large parts of the parameter space in light of the current understanding of experimental feasibility and/or of cosmological constraints within a standard thermal history

Candidate	Identity	Mass	Interactions	Production	Constraints	Experiments
a	Axion (spin 0) N.-Goldst. boson PQ symm. break.	< 0.01 eV	$(p/f_a)^n$ extremely weak $f_a \gtrsim 6 \times 10^8$ GeV	Misalign. mech.	$\leftarrow$ cold CMB	Direct searches with microwave cavities $\hookrightarrow m_a$, f_a, $g_{a\gamma\gamma}$
$\widetilde{\chi}_1^0$ LSP	Lightest neutralino (spin 1/2) mixture of $\widetilde{B}$, $\widetilde{W}$, $\widetilde{H}_{\rm u}^0$, $\widetilde{H}_{\rm d}^0$	$\mathcal{O}(100$ GeV)	g, g', y_i weak $M_{\rm W} \sim 100$ GeV	Therm. relic $\widetilde{G}$ decay	$\leftarrow$ cold $\leftarrow$ warm/hot BBN	Indirect searches direct searches collider searches $\hookrightarrow m_{\widetilde{\chi}_1^0}$, $\widetilde{\chi}_1^0$ coupl.
$\widetilde{G}$ LSP	Gravitino (spin 3/2) superpartner of the graviton	eV–TeV	$(p/{\rm M_P})^n$ extremely weak ${\rm M_P} = 2.4 \times 10^{18}$ GeV	Therm. prod. NLSP decay	$\leftarrow$ cold $\leftarrow$ warm BBN	$\widetilde{\tau}_1$ prod. at colliders $+\ \widetilde{\tau}_1$ collection $+\ \widetilde{\tau}_1$ decay analysis $\hookrightarrow m_{\widetilde{G}}$, ${\rm M_P}$ (?), $T_{\rm R}$
$\widetilde{a}$ LSP	Axino (spin 1/2) superpartner of the axion	eV–GeV	$(p/f_a)^n$ extremely weak $f_a \gtrsim 6 \times 10^8$ GeV	Therm. prod. NLSP decay	$\leftarrow$ cold/warm $\leftarrow$ warm/hot BBN	$\widetilde{\tau}_1$ prod. at colliders $+\ \widetilde{\tau}_1$ collection $+\ \widetilde{\tau}_1$ decay analysis $\hookrightarrow m_{\widetilde{a}}$ (?), f_a, $T_{\rm R}$ (?)

sensitivity of direct searches, and the advent of the LHC at which $\widetilde{\chi}_1^0$ dark matter could be produced, we will be able to test whether these hints are indeed the first evidence for the existence of SUSY dark matter. While an excess in missing transverse energy could provide a first hint for SUSY at the LHC already within the next three years, the identification of the $\widetilde{\chi}_1^0$ being the LSP will require the reconstruction of the SUSY model realized in nature. If superparticles are within the kinematical reach, precision studies at the ILC will be crucial for this endeavor.

Also an axion discovery is conceivable to occur in the near future. Indeed, a current upgrade of the microwave cavity experiment ADMX aims at a significant experimental exploration of a "natural" part of the $\Omega_a = \Omega_{\rm dm}$ region within the upcoming years. Complementary to that, axion searches with helioscopes such as CAST and those that are performed purely in the laboratory will extend their search ranges. However, a signal in those searches would support the existence of axions as hot/warm dark matter which can only provide a minor fraction of $\Omega_{\rm dm}$. This would leave room for a significant $\Omega_{\rm LSP}$ contribution to $\Omega_{\rm dm}$.

In $\widetilde{G}/\widetilde{a}$ LSP scenarios with conserved R-parity, no dark matter signal should appear in direct or indirect searches. However, since an electrically charged lightest standard-model superpartner such as the $\widetilde{\tau}_1$ is viable in $\widetilde{G}/\widetilde{a}$ LSP scenarios, (quasi-) stable $\widetilde{\tau}_1$'s might occur as muon-like particles instead of an excess in missing transverse energy. Indeed, an excess of (quasi-) stable $\widetilde{\tau}_1$'s could appear as an alternative first hint for SUSY at the LHC in the next three years. Because of the severe limits on the abundance of stable charged particles [2], one would expect that the $\widetilde{\tau}_1$ is the NLSP that decays eventually into the $\widetilde{G}/\widetilde{a}$ LSP or that R-parity is broken. A distinction between those scenarios will require the analysis of $\widetilde{\tau}_1$ decays. For this challenge, the ILC with its tunable beam energy seems crucial [346, 347, 349, 350, 352, 353].

Table 6.1 presents an overview of the dark-matter candidates discussed in this review. The axion and each LSP candidate—the lightest neutralino $\widetilde{\chi}_1^0$, the gravitino $\widetilde{G}$, or the axino $\widetilde{a}$—could provide $\Omega_{\rm dm}$ and could be produced and identified experimentally in the near future.

Acknowledgements I am grateful to A. Brandenburg, L. Covi, A. Freitas, C. Frugiuele, P. Graf, K. Hamaguchi, J. Hamann, M. Kuster, J. Lesgourgues, A. Mirizzi, G. Panotopoulos, T. Plehn, M. Pospelov, J. Pradler, G.G. Raffelt, A. Ringwald, L. Roszkowski, S. Schilling, N. Tajuddin, F. Takahashi, Y.Y.Y. Wong, D. Wyler, and M. Zagermann for valuable discussions and/or collaborations on the topics covered in this review. This research was supported by the DFG cluster of excellence 'Origin and Structure of the Universe' (www.universe-cluster.de).

References

1. E. Komatsu et al. (WMAP) (2008), 0803.0547
2. C. Amsler et al. (Particle Data Group), Phys. Lett. B **667**, 1 (2008)

3. C. Wetterich, Nucl. Phys. B **302**, 668 (1988)
4. B. Ratra, P.J.E. Peebles, Phys. Rev. D **37**, 3406 (1988)
5. R.R. Caldwell, R. Dave, P.J. Steinhardt, Phys. Rev. Lett. **80**, 1582 (1998), astro-ph/9708069
6. A. Ringwald, Y.Y.Y. Wong, J. Cosmol. Astropart. Phys. **0412**, 005 (2004), hep-ph/0408241
7. S. Hannestad, A. Mirizzi, G.G. Raffelt, Y.Y.Y. Wong, J. Cosmol. Astropart. Phys. **0708**, 015 (2007), 0706.4198
8. J. Lesgourgues, S. Pastor, Phys. Rep. **429**, 307 (2006), astro-ph/0603494
9. L. Bergstrom, Rep. Prog. Phys. **63**, 793 (2000), hep-ph/0002126
10. G. Bertone, D. Hooper, J. Silk, Phys. Rep. **405**, 279 (2005), hep-ph/0404175
11. E. Pierpaoli, Phys. Rev. Lett. **92**, 031301 (2004), astro-ph/0310375
12. S. Kasuya, M. Kawasaki, N. Sugiyama, Phys. Rev. D **69**, 023512 (2004), astro-ph/0309434
13. X.L. Chen, M. Kamionkowski, Phys. Rev. D **70**, 043502 (2004), astro-ph/0310473
14. L. Zhang, X. Chen, M. Kamionkowski, Z.g. Si, Z. Zheng, Phys. Rev. D **76**, 061301 (2007), 0704.2444
15. H. Yuksel, M.D. Kistler, Phys. Rev. D **78**, 023502 (2008), 0711.2906
16. M. Oguri, K. Takahashi, H. Ohno, K. Kotake, Astrophys. J. **597**, 645 (2003), astro-ph/0306020
17. K. Takahashi, M. Oguri, K. Ichiki, Mon. Not. R. Astron. Soc. **352**, 311 (2004), astro-ph/0312358
18. K. Ichiki, M. Oguri, K. Takahashi, Phys. Rev. Lett. **93**, 071302 (2004), astro-ph/0403164
19. Y. Gong, X. Chen, Phys. Rev. D **77**, 103511 (2008), 0802.2296
20. S. Palomares-Ruiz, Phys. Lett. B **665**, 50 (2008), 0712.1937
21. R.D. Peccei, H.R. Quinn, Phys. Rev. Lett. **38**, 1440 (1977)
22. R.D. Peccei, H.R. Quinn, Phys. Rev. D **16**, 1791 (1977)
23. P. Sikivie, Nucl. Phys. Proc. Suppl. **87**, 41 (2000), hep-ph/0002154
24. G.G. Raffelt, Lect. Notes Phys. **741**, 51 (2008), hep-ph/0611350
25. S. Weinberg, Phys. Rev. Lett. **40**, 223 (1978)
26. F. Wilczek, Phys. Rev. Lett. **40**, 279 (1978)
27. J. Preskill, M.B. Wise, F. Wilczek, Phys. Lett. B **120**, 127 (1983)
28. L.F. Abbott, P. Sikivie, Phys. Lett. B **120**, 133 (1983)
29. M. Dine, W. Fischler, Phys. Lett. B **120**, 137 (1983)
30. J. Wess, J. Bagger, *Supersymmetry and Supergravity* (Princeton University Press, Princeton, 1992), 259 p.
31. H.P. Nilles, Phys. Rep. **110**, 1 (1984)
32. H.E. Haber, G.L. Kane, Phys. Rep. **117**, 75 (1985)
33. S.P. Martin (1997), hep-ph/9709356
34. M. Drees, R. Godbole, P. Roy, *Theory and Phenomenology of Sparticles: An Account of Four-Dimensional $N = 1$ Supersymmetry in High Energy Physics* (World Scientific, Hackensack, 2004), 555 p.
35. H. Baer, X. Tata, *Weak Scale Supersymmetry: From Superfields to Scattering Events* (Cambridge University Press, Cambridge, 2006), 537 p.
36. H.K. Dreiner (1997), hep-ph/9707435
37. B.C. Allanach et al. (2007), 0710.2034
38. F. Takayama, M. Yamaguchi, Phys. Lett. B **485**, 388 (2000), hep-ph/0005214
39. W. Buchmüller, L. Covi, K. Hamaguchi, A. Ibarra, T. Yanagida, J. High Energy Phys. **03**, 037 (2007), hep-ph/0702184
40. A. Ibarra (2007), 0710.2287
41. D.N. Spergel et al. (WMAP), Astrophys. J. Suppl. **170**, 377 (2007), astro-ph/0603449
42. J. Hamann, S. Hannestad, M.S. Sloth, Y.Y.Y. Wong, Phys. Rev. D **75**, 023522 (2007), astro-ph/0611582
43. R.A. Malaney, G.J. Mathews, Phys. Rep. **229**, 145 (1993)
44. S. Sarkar, Rep. Prog. Phys. **59**, 1493 (1996), hep-ph/9602260
45. D.N. Schramm, M.S. Turner, Rev. Mod. Phys. **70**, 303 (1998), astro-ph/9706069
46. K.A. Olive, G. Steigman, T.P. Walker, Phys. Rep. **333**, 389 (2000), astro-ph/9905320
47. P.D. Serpico et al., J. Cosmol. Astropart. Phys. **0412**, 010 (2004), astro-ph/0408076
48. F. Iocco, G. Mangano, G. Miele, O. Pisanti, P.D. Serpico (2008), 0809.0631
49. G. Mangano, A. Melchiorri, O. Mena, G. Miele, A. Slosar, J. Cosmol. Astropart. Phys. **0703**, 006 (2007), astro-ph/0612150
50. V. Simha, G. Steigman, J. Cosmol. Astropart. Phys. **0806**, 016 (2008), 0803.3465
51. D. Lindley, Astrophys. J. **294**, 1 (1985)
52. J.R. Ellis, D.V. Nanopoulos, S. Sarkar, Nucl. Phys. B **259**, 175 (1985)
53. R.J. Scherrer, M.S. Turner, Phys. Rev. D **33**, 1585 (1986)
54. M.H. Reno, D. Seckel, Phys. Rev. D **37**, 3441 (1988)
55. S. Dimopoulos, R. Esmailzadeh, L.J. Hall, G.D. Starkman, Nucl. Phys. B **311**, 699 (1989)
56. Y.L. Levitan, I.M. Sobol, M.Y. Khlopov, V.M. Chechetkin, Sov. J. Nucl. Phys. **47**, 109 (1988)
57. G. Sigl, K. Jedamzik, D.N. Schramm, V.S. Berezinsky, Phys. Rev. D **52**, 6682 (1995), astro-ph/9503094
58. K. Jedamzik, Phys. Rev. Lett. **84**, 3248 (2000), astro-ph/9909445
59. R.H. Cyburt, J.R. Ellis, B.D. Fields, K.A. Olive, Phys. Rev. D **67**, 103521 (2003), astro-ph/0211258
60. K. Jedamzik, Phys. Rev. D **70**, 063524 (2004), astro-ph/0402344
61. M. Kawasaki, K. Kohri, T. Moroi, Phys. Rev. D **71**, 083502 (2005), astro-ph/0408426
62. K. Jedamzik, Phys. Rev. D **74**, 103509 (2006), hep-ph/0604251
63. M. Kawasaki, K. Kohri, T. Moroi, A. Yotsuyanagi, Phys. Rev. D **78**, 065011 (2008), 0804.3745
64. M. Pospelov, Phys. Rev. Lett. **98**, 231301 (2007), hep-ph/0605215
65. K. Kohri, F. Takayama, Phys. Rev. D **76**, 063507 (2007), hep-ph/0605243
66. M. Kaplinghat, A. Rajaraman, Phys. Rev. D **74**, 103004 (2006), astro-ph/0606209
67. R.H. Cyburt, J.R. Ellis, B.D. Fields, K.A. Olive, V.C. Spanos, J. Cosmol. Astropart. Phys. **0611**, 014 (2006), astro-ph/0608562
68. K. Hamaguchi, T. Hatsuda, M. Kamimura, Y. Kino, T.T. Yanagida, Phys. Lett. B **650**, 268 (2007), hep-ph/0702274
69. C. Bird, K. Koopmans, M. Pospelov (2007), hep-ph/0703096
70. M. Kawasaki, K. Kohri, T. Moroi, Phys. Lett. B **649**, 436 (2007), hep-ph/0703122
71. F. Takayama, Phys. Rev. D **77**, 116003 (2008), 0704.2785
72. T. Jittoh et al., Phys. Rev. D **76**, 125023 (2007), 0704.2914
73. K. Jedamzik, Phys. Rev. D **77**, 063524 (2008), 0707.2070
74. J. Pradler, F.D. Steffen, Phys. Lett. B **666**, 181 (2008), 0710.2213
75. K. Jedamzik, J. Cosmol. Astropart. Phys. **0803**, 008 (2008), 0710.5153
76. M. Kusakabe, T. Kajino, R.N. Boyd, T. Yoshida, G.J. Mathews, Phys. Rev. D **76**, 121302 (2007), 0711.3854
77. M. Kusakabe, T. Kajino, R.N. Boyd, T. Yoshida, G.J. Mathews (2007), 0711.3858
78. M. Pospelov (2007), 0712.0647
79. M. Pospelov, J. Pradler, F.D. Steffen, J. Cosmol. Astropart. Phys. **0811**, 020 (2008), 0807.4287
80. A.D. Linde (2005), hep-th/0503203
81. E.W. Kolb, M.S. Turner, Front. Phys. **69**, 1 (1990)
82. A.D. Linde, Phys. Lett. B **259**, 38 (1991)
83. M. Kawasaki, K. Kohri, N. Sugiyama, Phys. Rev. Lett. **82**, 4168 (1999), astro-ph/9811437
84. M. Kawasaki, K. Kohri, N. Sugiyama, Phys. Rev. D **62**, 023506 (2000), astro-ph/0002127

85. S. Hannestad, Phys. Rev. D **70**, 043506 (2004), astro-ph/0403291
86. K. Ichikawa, M. Kawasaki, F. Takahashi, Phys. Rev. D **72**, 043522 (2005), astro-ph/0505395
87. N. Seto, S. Kawamura, T. Nakamura, Phys. Rev. Lett. **87**, 221103 (2001), astro-ph/0108011
88. K. Nakayama, S. Saito, Y. Suwa, J. Yokoyama, Phys. Rev. D **77**, 124001 (2008), 0802.2452
89. K. Nakayama, S. Saito, Y. Suwa, J. Yokoyama (2008), 0804.1827
90. R.D. Peccei (1998), hep-ph/9807514
91. R.D. Peccei, Lect. Notes Phys. **741**, 3 (2008), hep-ph/0607268
92. J.E. Kim, G. Carosi (2008), 0807.3125
93. G. 't Hooft, Phys. Rev. Lett. **37**, 8 (1976)
94. G. 't Hooft, Phys. Rev. D **14**, 3432 (1976)
95. J.S. Bell, R. Jackiw, Nuovo Cim. A **60**, 47 (1969)
96. S.L. Adler, Phys. Rev. **177**, 2426 (1969)
97. A.A. Belavin, A.M. Polyakov, A.S. Shvarts, Y.S. Tyupkin, Phys. Lett. B **59**, 85 (1975)
98. D.B. Kaplan, A.V. Manohar, Phys. Rev. Lett. **56**, 2004 (1986)
99. W.A. Bardeen, S.H.H. Tye, Phys. Lett. B **74**, 229 (1978)
100. V. Baluni, Phys. Rev. D **19**, 2227 (1979)
101. H. Leutwyler, Phys. Lett. B **378**, 313 (1996), hep-ph/9602366
102. J.E. Kim, Phys. Rev. Lett. **43**, 103 (1979)
103. M.A. Shifman, A.I. Vainshtein, V.I. Zakharov, Nucl. Phys. B **166**, 493 (1980)
104. M. Dine, W. Fischler, M. Srednicki, Phys. Lett. B **104**, 199 (1981)
105. A.R. Zhitnitsky, Sov. J. Nucl. Phys. **31**, 260 (1980)
106. J.E. Kim, Phys. Rep. **150**, 1 (1987)
107. H.Y. Cheng, Phys. Rep. **158**, 1 (1988)
108. P. Fox, A. Pierce, S.D. Thomas (2004), hep-th/0409059
109. M.K. Gaillard, B. Kain, Nucl. Phys. B **734**, 116 (2006), hep-th/0510190
110. P. Svrcek, E. Witten, J. High Energy Phys. **06**, 051 (2006), hep-th/0605206
111. D.B. Kaplan, Nucl. Phys. B **260**, 215 (1985)
112. S. Chang, K. Choi, Phys. Lett. B **316**, 51 (1993), hep-ph/9306216
113. S. Hannestad, A. Mirizzi, G. Raffelt, J. Cosmol. Astropart. Phys. **0507**, 002 (2005), hep-ph/0504059
114. E. Masso, F. Rota, G. Zsembinszki, Phys. Rev. D **66**, 023004 (2002), hep-ph/0203221
115. P. Sikivie, Lect. Notes Phys. **741**, 19 (2008), astro-ph/0610440
116. S. Hannestad, A. Mirizzi, G.G. Raffelt, Y.Y.Y. Wong, J. Cosmol. Astropart. Phys. **0804**, 019 (2008), 0803.1585
117. M. Beltran, J. Garcia-Bellido, J. Lesgourgues, Phys. Rev. D **75**, 103507 (2007), hep-ph/0606107
118. K.J. Bae, J.H. Huh, J.E. Kim (2008), 0806.0497
119. M. Tegmark, A. Aguirre, M. Rees, F. Wilczek, Phys. Rev. D **73**, 023505 (2006), astro-ph/0511774
120. M.P. Hertzberg, M. Tegmark, F. Wilczek, Phys. Rev. D **78**, 083507 (2008), 0807.1726
121. A.D. Linde, D.H. Lyth, Phys. Lett. B **246**, 353 (1990)
122. M.S. Turner, F. Wilczek, Phys. Rev. Lett. **66**, 5 (1991)
123. D.H. Lyth, Phys. Rev. D **45**, 3394 (1992)
124. D.H. Lyth, E.D. Stewart, Phys. Rev. D **46**, 532 (1992)
125. D. Seckel, M.S. Turner, Phys. Rev. D **32**, 3178 (1985)
126. A.D. Linde, Phys. Lett. B **158**, 375 (1985)
127. D.H. Lyth, Phys. Lett. B **236**, 408 (1990)
128. D.H. Lyth, E.D. Stewart, Phys. Lett. B **283**, 189 (1992)
129. M. Kawasaki, K. Nakayama, T. Sekiguchi, T. Suyama, F. Takahashi (2008), 0808.0009
130. D.A. Dicus, E.W. Kolb, V.L. Teplitz, R.V. Wagoner, Phys. Rev. D **18**, 1829 (1978)
131. M.I. Vysotsky, Y.B. Zeldovich, M.Y. Khlopov, V.M. Chechetkin, Pisma Zh. Eksp. Teor. Fiz. **27**, 533 (1978)
132. M.S. Turner, Phys. Rep. **197**, 67 (1990)
133. G.G. Raffelt, Phys. Rep. **198**, 1 (1990)
134. G.G. Raffelt, Annu. Rev. Nucl. Part. Sci. **49**, 163 (1999), hep-ph/9903472
135. G.G. Raffelt, Phys. Rev. D **33**, 897 (1986)
136. T. Altherr, E. Petitgirard, T. del Rio Gaztelurrutia, Astropart. Phys. **2**, 175 (1994), hep-ph/9310304
137. G.G. Raffelt, Phys. Rev. D **37**, 1356 (1988)
138. G.G. Raffelt, *Stars as Laboratories for Fundamental Physics* (University Press, Chicago, 1996), 664 p.
139. H. Schlattl, A. Weiss, G. Raffelt, Astropart. Phys. **10**, 353 (1999), hep-ph/9807476
140. G. Raffelt, A. Weiss, Phys. Rev. D **51**, 1495 (1995), hep-ph/9410205
141. G.G. Raffelt, Phys. Lett. B **166**, 402 (1986)
142. J. Wang, Mod. Phys. Lett. A **7**, 1497 (1992)
143. A.H. Corsico, O.G. Benvenuto, L.G. Althaus, J. Isern, E. Garcia-Berro, New Astron. **6**, 197 (2001), astro-ph/0104103
144. J. Isern, E. Garcia-Berro, Nucl. Phys. Proc. Suppl. **114**, 107 (2003)
145. G. Raffelt, D. Seckel, Phys. Rev. Lett. **60**, 1793 (1988)
146. M.S. Carena, R.D. Peccei, Phys. Rev. D **40**, 652 (1989)
147. J.R. Ellis, K.A. Olive, Phys. Lett. B **193**, 525 (1987)
148. M.S. Turner, Phys. Rev. Lett. **60**, 1797 (1988)
149. R. Mayle et al., Phys. Lett. B **203**, 188 (1988)
150. H.T. Janka, W. Keil, G. Raffelt, D. Seckel, Phys. Rev. Lett. **76**, 2621 (1996), astro-ph/9507023
151. W. Keil et al., Phys. Rev. D **56**, 2419 (1997), astro-ph/9612222
152. A. Burrows, M.S. Turner, R.P. Brinkmann, Phys. Rev. D **39**, 1020 (1989)
153. A. Burrows, M.T. Ressell, M.S. Turner, Phys. Rev. D **42**, 3297 (1990)
154. J. Engel, D. Seckel, A.C. Hayes, Phys. Rev. Lett. **65**, 960 (1990)
155. T. Moroi, H. Murayama, Phys. Lett. B **440**, 69 (1998), hep-ph/9804291
156. R. Battesti et al., Lect. Notes Phys. **741**, 199 (2008), 0705.0615
157. J.E. Moody, F. Wilczek, Phys. Rev. D **30**, 130 (1984)
158. B.R. Heckel et al., Phys. Rev. Lett. **97**, 021603 (2006), hep-ph/0606218
159. D. Grin et al., Phys. Rev. D **75**, 105018 (2007), astro-ph/0611502
160. S.J. Asztalos et al., Phys. Rev. D **69**, 011101 (2004), astro-ph/0310042
161. L.D. Duffy et al., Phys. Rev. D **74**, 012006 (2006), astro-ph/0603108
162. K. Zioutas et al. (CAST), Phys. Rev. Lett. **94**, 121301 (2005), hep-ex/0411033
163. S. Andriamonje et al. (CAST), J. Cosmol. Astropart. Phys. **0704**, 010 (2007), hep-ex/0702006
164. J. Ruz et al., J. Phys. Conf. Ser. **110**, 062023 (2008)
165. M. Minowa et al. (2008), 0809.0596
166. A. Morales et al. (COSME), Astropart. Phys. **16**, 325 (2002), hep-ex/0101037
167. R. Bernabei et al., Phys. Lett. B **515**, 6 (2001)
168. F.T. Avignone et al. (SOLAX), Phys. Rev. Lett. **81**, 5068 (1998), astro-ph/9708008
169. R. Cameron et al., Phys. Rev. D **47**, 3707 (1993)
170. M.A. Bershady, M.T. Ressell, M.S. Turner, Phys. Rev. Lett. **66**, 1398 (1991)
171. M.T. Ressell, Phys. Rev. D **44**, 3001 (1991)
172. B.D. Blout et al., Astrophys. J. **546**, 825 (2001), astro-ph/0006310
173. S. De Panfilis et al., Phys. Rev. Lett. **59**, 839 (1987)
174. W. Wuensch et al., Phys. Rev. D **40**, 3153 (1989)
175. C. Hagmann, P. Sikivie, N.S. Sullivan, D.B. Tanner, Phys. Rev. D **42**, 1297 (1990)
176. R. Bradley et al., Rev. Mod. Phys. **75**, 777 (2003)

177. G. Carosi, K. van Bibber, Lect. Notes. Phys. **741**, 135 (2008), hep-ex/0701025
178. P. Sikivie, Phys. Rev. Lett. **51**, 1415 (1983); **52**, 695 (1984) (erratum)
179. M. Tada et al., Nucl. Phys. Proc. Suppl. **72**, 164 (1999)
180. D.M. Lazarus et al., Phys. Rev. Lett. **69**, 2333 (1992)
181. S. Moriyama et al., Phys. Lett. B **434**, 147 (1998), hep-ex/9805026
182. Y. Inoue et al., Phys. Lett. B **536**, 18 (2002), astro-ph/0204388
183. H. Davoudiasl, P. Huber, Phys. Rev. Lett. **97**, 141302 (2006), hep-ph/0509293
184. D. Grin, T.L. Smith, M. Kamionkowski, Phys. Rev. D **77**, 085020 (2008), 0711.1352
185. J.W. Brockway, E.D. Carlson, G.G. Raffelt, Phys. Lett. B **383**, 439 (1996), astro-ph/9605197
186. J.A. Grifols, E. Masso, R. Toldra, Phys. Rev. Lett. **77**, 2372 (1996), astro-ph/9606028
187. L. Maiani, R. Petronzio, E. Zavattini, Phys. Lett. B **175**, 359 (1986)
188. E. Zavattini et al. (PVLAS), Phys. Rev. Lett. **96**, 110406 (2006), hep-ex/0507107
189. E. Zavattini et al. (PVLAS), Phys. Rev. D **77**, 032006 (2008), 0706.3419
190. A. Brandenburg, L. Covi, K. Hamaguchi, L. Roszkowski, F.D. Steffen, Phys. Lett. B **617**, 99 (2005), hep-ph/0501287
191. A. Brandenburg, M. Maniatis, M.M. Weber (2002), hep-ph/0207278
192. A. Freitas, P.Z. Skands, M. Spira, P.M. Zerwas, J. High Energy Phys. **07**, 025 (2007), hep-ph/0703160
193. A. Brandenburg, M. Maniatis, M.M. Weber, P.M. Zerwas (2008), 0806.3875
194. H. Baer, M.A. Diaz, P. Quintana, X. Tata, J. High Energy Phys. **04**, 016 (2000), hep-ph/0002245
195. G.A. Blair, W. Porod, P.M. Zerwas, Eur. Phys. J. C **27**, 263 (2003), hep-ph/0210058
196. R. Lafaye, T. Plehn, D. Zerwas (2004), hep-ph/0404282
197. P. Bechtle, K. Desch, P. Wienemann, Comput. Phys. Commun. **174**, 47 (2006), hep-ph/0412012
198. E. Cremmer, S. Ferrara, L. Girardello, A. Van Proeyen, Nucl. Phys. B **212**, 413 (1983)
199. M. Dine, A.E. Nelson, Y. Shirman, Phys. Rev. D **51**, 1362 (1995), hep-ph/9408384
200. M. Dine, A.E. Nelson, Y. Nir, Y. Shirman, Phys. Rev. D **53**, 2658 (1996), hep-ph/9507378
201. G.F. Giudice, R. Rattazzi, Phys. Rep. **322**, 419 (1999), hep-ph/9801271
202. L. Randall, R. Sundrum, Nucl. Phys. B **557**, 79 (1999), hep-th/9810155
203. G.F. Giudice, M.A. Luty, H. Murayama, R. Rattazzi, J. High Energy Phys. **12**, 027 (1998), hep-ph/9810442
204. W. Buchmüller, K. Hamaguchi, J. Kersten, Phys. Lett. B **632**, 366 (2006), hep-ph/0506105
205. A. Brignole, L.E. Ibanez, C. Munoz (1997), hep-ph/9707209
206. K.A. Olive (2008), 0806.1208
207. J. Pradler, F.D. Steffen, Phys. Lett. B **648**, 224 (2007), hep-ph/0612291
208. A. Djouadi, J.L. Kneur, G. Moultaka, Comput. Phys. Commun. **176**, 426 (2007), hep-ph/0211331
209. G. Belanger, F. Boudjema, A. Pukhov, A. Semenov, Comput. Phys. Commun. **149**, 103 (2002), hep-ph/0112278
210. G. Belanger, F. Boudjema, A. Pukhov, A. Semenov, Comput. Phys. Commun. **174**, 577 (2006), hep-ph/0405253
211. J.R. Ellis, K.A. Olive, Y. Santoso, Astropart. Phys. **18**, 395 (2003), hep-ph/0112113
212. J.L. Diaz-Cruz, J.R. Ellis, K.A. Olive, Y. Santoso, J. High Energy Phys. **05**, 003 (2007), hep-ph/0701229
213. Y. Santoso (2007), 0709.3952
214. L.E. Ibanez, Phys. Lett. B **137**, 160 (1984)
215. J.R. Ellis, J.S. Hagelin, D.V. Nanopoulos, K.A. Olive, M. Srednicki, Nucl. Phys. B **238**, 453 (1984)
216. J.S. Hagelin, G.L. Kane, S. Raby, Nucl. Phys. B **241**, 638 (1984)
217. W. Buchmüller, L. Covi, J. Kersten, K. Schmidt-Hoberg, J. Cosmol. Astropart. Phys. **0611**, 007 (2006), hep-ph/0609142
218. L. Covi, S. Kraml, J. High Energy Phys. **08**, 015 (2007), hep-ph/0703130
219. J. Ellis, K.A. Olive, Y. Santoso, J. High Energy Phys. **10**, 005 (2008), 0807.3736
220. C. Arina, N. Fornengo, J. High Energy Phys. **11**, 029 (2007), 0709.4477
221. T. Falk, K.A. Olive, M. Srednicki, Phys. Lett. B **339**, 248 (1994), hep-ph/9409270
222. M. Fujii, M. Ibe, T. Yanagida, Phys. Lett. B **579**, 6 (2004), hep-ph/0310142
223. J.L. Feng, S. Su, F. Takayama, Phys. Rev. D **70**, 075019 (2004), hep-ph/0404231
224. T. Kanzaki, M. Kawasaki, K. Kohri, T. Moroi, Phys. Rev. D **75**, 025011 (2007), hep-ph/0609246
225. P. Gondolo et al., J. Cosmol. Astropart. Phys. **0407**, 008 (2004), astro-ph/0406204
226. G. Belanger, F. Boudjema, A. Pukhov, A. Semenov, Comput. Phys. Commun. **176**, 367 (2007), hep-ph/0607059
227. G. Belanger, F. Boudjema, A. Pukhov, A. Semenov, Comput. Phys. Commun. **177**, 894 (2007)
228. A. Djouadi, M. Drees, J.L. Kneur, J. High Energy Phys. **03**, 033 (2006), hep-ph/0602001
229. T. Asaka, S. Nakamura, M. Yamaguchi, Phys. Rev. D **74**, 023520 (2006), hep-ph/0604132
230. M. Endo, F. Takahashi, T.T. Yanagida, Phys. Rev. D **76**, 083509 (2007), 0706.0986
231. M. Bolz, A. Brandenburg, W. Buchmüller, Nucl. Phys. B **606**, 518 (2001), hep-ph/0012052; **790**, 336 (2008) (erratum)
232. J. Pradler, F.D. Steffen, Phys. Rev. D **75**, 023509 (2007), hep-ph/0608344
233. J. Pradler, Electroweak Contributions to Thermal Gravitino Production (2007), 0708.2786
234. V.S. Rychkov, A. Strumia, Phys. Rev. D **75**, 075011 (2007), hep-ph/0701104
235. K. Kohri, T. Moroi, A. Yotsuyanagi, Phys. Rev. D **73**, 123511 (2006), hep-ph/0507245
236. J. Hisano, K. Kohri, M.M. Nojiri, Phys. Lett. B **505**, 169 (2001), hep-ph/0011216
237. W.B. Lin, D.H. Huang, X. Zhang, R.H. Brandenberger, Phys. Rev. Lett. **86**, 954 (2001), astro-ph/0009003
238. M. Fukugita, T. Yanagida, Phys. Lett. B **174**, 45 (1986)
239. S. Davidson, A. Ibarra, Phys. Lett. B **535**, 25 (2002), hep-ph/0202239
240. W. Buchmüller, P. Di Bari, M. Plümacher, Ann. Phys. **315**, 305 (2005), hep-ph/0401240
241. S. Blanchet, P. Di Bari, J. Cosmol. Astropart. Phys. **0703**, 018 (2007), hep-ph/0607330
242. S. Antusch, A.M. Teixeira, J. Cosmol. Astropart. Phys. **0702**, 024 (2007), hep-ph/0611232
243. E. Nardi, Y. Nir, E. Roulet, J. Racker, J. High Energy Phys. **01**, 164 (2006), hep-ph/0601084
244. A. Abada, S. Davidson, F.X. Josse-Michaux, M. Losada, A. Riotto, J. Cosmol. Astropart. Phys. **0604**, 004 (2006), hep-ph/0601083
245. S. Davidson, R. Kitano, J. High Energy Phys. **03**, 020 (2004), hep-ph/0312007
246. T. Hambye, Y. Lin, A. Notari, M. Papucci, A. Strumia, Nucl. Phys. B **695**, 169 (2004), hep-ph/0312203
247. M. Raidal, A. Strumia, K. Turzynski, Phys. Lett. B **609**, 351 (2005), hep-ph/0408015

248. M. Flanz, E.A. Paschos, U. Sarkar, Phys. Lett. B **345**, 248 (1995), hep-ph/9411366
249. L. Covi, E. Roulet, Phys. Lett. B **399**, 113 (1997), hep-ph/9611425
250. A. Pilaftsis, Phys. Rev. D **56**, 5431 (1997), hep-ph/9707235
251. A. Anisimov, A. Broncano, M. Plümacher, Nucl. Phys. B **737**, 176 (2006), hep-ph/0511248
252. F. Hahn-Woernle, M. Plümacher (2008), 0801.3972
253. W. Buchmüller, K. Hamaguchi, M. Ratz, Phys. Lett. B **574**, 156 (2003), hep-ph/0307181
254. E.A. Baltz, M. Battaglia, M.E. Peskin, T. Wizansky, Phys. Rev. D **74**, 103521 (2006), hep-ph/0602187
255. D. Hooper, J. March-Russel, S.M. West, Phys. Lett. B **605**, 228 (2005), hep-ph/0410114
256. G. Bertone (2007), 0710.5603
257. L. Baudis (2007), 0711.3788
258. D. Hooper (2007), 0710.2062
259. W. de Boer (2008), 0810.1472
260. W. de Boer, C. Sander, V. Zhukov, A.V. Gladyshev, D.I. Kazakov, Phys. Lett. B **636**, 13 (2006), hep-ph/0511154
261. G. Angloher et al., Astropart. Phys. **23**, 325 (2005), astro-ph/0408006
262. V. Sanglard et al. (EDELWEISS), Phys. Rev. D **71**, 122002 (2005), astro-ph/0503265
263. D.S. Akerib et al. (CDMS), Phys. Rev. Lett. **96**, 011302 (2006), astro-ph/0509259
264. P. Benetti et al., Astropart. Phys. **28**, 495 (2008), astro-ph/0701286
265. G.J. Alner et al., Astropart. Phys. **28**, 287 (2007), astro-ph/0701858
266. J. Angle et al. (XENON) (2007), 0706.0039
267. Z. Ahmed et al. (CDMS) (2008), 0802.3530
268. R.F. Lang (CRESST) (2008), 0805.4705
269. G. Angloher et al. (CRESST) (2008), 0809.1829
270. R. Bernabei et al. (DAMA), Phys. Lett. B **480**, 23 (2000)
271. R. Bernabei et al. (DAMA), Eur. Phys. J. C **56**, 333 (2008), 0804.2741
272. R. Bernabei et al., Int. J. Mod. Phys. A **21**, 1445 (2006), astro-ph/0511262
273. M. Pospelov, A. Ritz, M.B. Voloshin (2008), 0807.3279
274. C. Savage, G. Gelmini, P. Gondolo, K. Freese (2008), 0808.3607
275. J.L. Feng, J. Kumar, L.E. Strigari (2008), 0806.3746
276. J.L. Feng, J. Kumar, J. Learned, L.E. Strigari (2008), 0808.4151
277. E.A. Baltz, P. Gondolo, Phys. Rev. D **67**, 063503 (2003), astro-ph/0207673
278. E.A. Baltz, P. Gondolo, J. High Energy Phys. **10**, 052 (2004), hep-ph/0407039
279. J.R. Ellis, J.L. Feng, A. Ferstl, K.T. Matchev, K.A. Olive, Eur. Phys. J. C **24**, 311 (2002), astro-ph/0110225
280. M. Battaglia et al., Eur. Phys. J. C **33**, 273 (2004), hep-ph/0306219
281. L. Roszkowski, R. Ruiz de Austri, R. Trotta, J. High Energy Phys. **07**, 075 (2007), 0705.2012
282. M. Drees, C.L. Shan, J. Cosmol. Astropart. Phys. **0706**, 011 (2007), astro-ph/0703651
283. C.L. Shan, M. Drees (2007), 0710.4296
284. A. Duperrin (CDF) (2007), 0710.4265
285. M. Shamim (D0) (2007), 0710.2897
286. M. Tytgat (2007), 0710.1013
287. S. Yamamoto (ATLAS) (2007), 0710.3953
288. N. Ozturk (ATLAS) (2007), 0710.4546
289. G. Weiglein et al. (LHC/LC Study Group), Phys. Rep. **426**, 47 (2006), hep-ph/0410364
290. S.Y. Choi (2008), 0809.1707
291. S.Y. Choi, K. Hagiwara, H.U. Martyn, K. Mawatari, P.M. Zerwas, Eur. Phys. J. C **51**, 753 (2007), hep-ph/0612301
292. A. Ibarra (2008), 0809.2067
293. H. Pagels, J.R. Primack, Phys. Rev. Lett. **48**, 223 (1982)
294. T. Moroi, H. Murayama, M. Yamaguchi, Phys. Lett. B **303**, 289 (1993)
295. M. Bolz, W. Buchmüller, M. Plümacher, Phys. Lett. B **443**, 209 (1998), hep-ph/9809381
296. S. Borgani, A. Masiero, M. Yamaguchi, Phys. Lett. B **386**, 189 (1996), hep-ph/9605222
297. T. Asaka, K. Hamaguchi, K. Suzuki, Phys. Lett. B **490**, 136 (2000), hep-ph/0005136
298. J.R. Ellis, K.A. Olive, Y. Santoso, V.C. Spanos, Phys. Lett. B **588**, 7 (2004), hep-ph/0312262
299. F.D. Steffen, J. Cosmol. Astropart. Phys. **0609**, 001 (2006), hep-ph/0605306
300. E.A. Baltz, H. Murayama, J. High Energy Phys. **05**, 067 (2003), astro-ph/0108172
301. M. Fujii, T. Yanagida, Phys. Lett. B **549**, 273 (2002), hep-ph/0208191
302. M. Fujii, M. Ibe, T. Yanagida, Phys. Rev. D **69**, 015006 (2004), hep-ph/0309064
303. M. Lemoine, G. Moultaka, K. Jedamzik, Phys. Lett. B **645**, 222 (2007), hep-ph/0504021
304. K. Jedamzik, M. Lemoine, G. Moultaka, Phys. Rev. D **73**, 043514 (2006), hep-ph/0506129
305. G. Moultaka (2007), 0710.5121
306. W. Buchmüller, M. Endo, T. Shindou (2008), 0809.4667
307. J.L. Feng, A. Rajaraman, F. Takayama, Phys. Rev. Lett. **91**, 011302 (2003), hep-ph/0302215
308. J. Kang, M.A. Luty, S. Nasri, J. High Energy Phys. **09**, 086 (2008), hep-ph/0611322
309. C.F. Berger, L. Covi, S. Kraml, F. Palorini, J. Cosmol. Astropart. Phys. **0810**, 005 (2008), 0807.0211
310. F.D. Steffen, AIP Conf. Proc. **903**, 595 (2007), hep-ph/0611027
311. M. Ratz, K. Schmidt-Hoberg, M.W. Winkler, J. Cosmol. Astropart. Phys. **0810**, 026 (2008), 0808.0829
312. J. Pradler, F.D. Steffen, Nucl. Phys. B **809**, 318 (2009), 0808.2462
313. F. Mahmoudi, J. High Energy Phys. **12**, 026 (2007), 0710.3791
314. W. Buchmüller, K. Hamaguchi, M. Ibe, T.T. Yanagida, Phys. Lett. B **643**, 124 (2006), hep-ph/0605164
315. D.G. Cerdeno, K.Y. Choi, K. Jedamzik, L. Roszkowski, R. Ruiz de Austri, J. Cosmol. Astropart. Phys. **0606**, 005 (2006), hep-ph/0509275
316. K.Y. Choi, L. Roszkowski, R. Ruiz de Austri, J. High Energy Phys. **04**, 016 (2008), 0710.3349
317. F.D. Steffen, Phys. Lett. B **669**, 74 (2008), 0806.3266
318. J. Pradler, F.D. Steffen, Eur. Phys. J. C **56**, 287 (2008), 0710.4548
319. J.A.R. Cembranos, J.L. Feng, A. Rajaraman, F. Takayama, Phys. Rev. Lett. **95**, 181301 (2005), hep-ph/0507150
320. M. Kaplinghat, Phys. Rev. D **72**, 063510 (2005), astro-ph/0507300
321. K. Jedamzik, M. Lemoine, G. Moultaka, J. Cosmol. Astropart. Phys. **0607**, 010 (2006), astro-ph/0508141
322. W. Hu, J. Silk, Phys. Rev. D **48**, 485 (1993)
323. R. Lamon, R. Durrer, Phys. Rev. D **73**, 023507 (2006), hep-ph/0506229
324. S. Dimopoulos, D. Eichler, R. Esmailzadeh, G.D. Starkman, Phys. Rev. D **41**, 2388 (1990)
325. A. De Rujula, S.L. Glashow, U. Sarid, Nucl. Phys. B **333**, 173 (1990)
326. J. Rafelski, M. Sawicki, M. Gajda, D. Harley, Phys. Rev. A **44**, 4345 (1991)
327. J. Kersten, K. Schmidt-Hoberg, J. Cosmol. Astropart. Phys. **0801**, 011 (2008), 0710.4528
328. M. Kamimura, Y. Kino, E. Hiyama (2008), 0809.4772

329. M. Asplund, D.L. Lambert, P.E. Nissen, F. Primas, V.V. Smith, Astrophys. J. **644**, 229 (2006), astro-ph/0510636
330. G. Bertone, W. Buchmüller, L. Covi, A. Ibarra, J. Cosmol. Astropart. Phys. **0711**, 003 (2007), 0709.2299
331. A. Ibarra, D. Tran, Phys. Rev. Lett. **100**, 061301 (2008), 0709.4593
332. A. Ibarra, D. Tran, J. Cosmol. Astropart. Phys. **0807**, 002 (2008), 0804.4596
333. K. Ishiwata, S. Matsumoto, T. Moroi (2008), 0805.1133
334. L. Covi, M. Grefe, A. Ibarra, D. Tran (2008), 0809.5030
335. J. Hisano, M. Kawasaki, K. Kohri, K. Nakayama (2008), 0810.1892
336. M. Drees, X. Tata, Phys. Lett. B **252**, 695 (1990)
337. A. Nisati, S. Petrarca, G. Salvini, Mod. Phys. Lett. A **12**, 2213 (1997), hep-ph/9707376
338. J.L. Feng, T. Moroi, Phys. Rev. D **58**, 035001 (1998), hep-ph/9712499
339. S. Ambrosanio, B. Mele, S. Petrarca, G. Polesello, A. Rimoldi, J. High Energy Phys. **01**, 014 (2001), hep-ph/0010081
340. J.R. Ellis, A.R. Raklev, O.K. Oye, J. High Energy Phys. **10**, 061 (2006), hep-ph/0607261
341. J. Ellis (2007), 0710.4959
342. S. Bressler (ATLAS) (2007), 0710.2111
343. P. Zalewski (2007), 0710.2647
344. M. Ahlers, J. Kersten, A. Ringwald, J. Cosmol. Astropart. Phys. **0607**, 005 (2006), hep-ph/0604188
345. J.L. Goity, W.J. Kossler, M. Sher, Phys. Rev. D **48**, 5437 (1993), hep-ph/9305244
346. K. Hamaguchi, Y. Kuno, T. Nakaya, M.M. Nojiri, Phys. Rev. D **70**, 115007 (2004), hep-ph/0409248
347. J.L. Feng, B.T. Smith, Phys. Rev. D **71**, 015004 (2005), hep-ph/0409278
348. A. De Roeck et al., Eur. Phys. J. C **49**, 1041 (2007), hep-ph/0508198
349. K. Hamaguchi, M.M. Nojiri, A. de Roeck, J. High Energy Phys. **03**, 046 (2007), hep-ph/0612060
350. O. Cakir, I.T. Cakir, J.R. Ellis, Z. Kirca (2007), hep-ph/0703121
351. W. Buchmüller, K. Hamaguchi, M. Ratz, T. Yanagida, Phys. Lett. B **588**, 90 (2004), hep-ph/0402179
352. H.U. Martyn, Eur. Phys. J. C **48**, 15 (2006), hep-ph/0605257
353. H.U. Martyn (2007), 0709.1030
354. F.D. Steffen (2005), hep-ph/0507003
355. H.P. Nilles, S. Raby, Nucl. Phys. B **198**, 102 (1982)
356. J.E. Kim, H.P. Nilles, Phys. Lett. B **138**, 150 (1984)
357. K. Tamvakis, D. Wyler, Phys. Lett. B **112**, 451 (1982)
358. J.E. Kim, Phys. Lett. B **136**, 378 (1984)
359. J.F. Nieves, Phys. Rev. D **33**, 1762 (1986)
360. K. Rajagopal, M.S. Turner, F. Wilczek, Nucl. Phys. B **358**, 447 (1991)
361. T. Goto, M. Yamaguchi, Phys. Lett. B **276**, 103 (1992)
362. E.J. Chun, J.E. Kim, H.P. Nilles, Phys. Lett. B **287**, 123 (1992), hep-ph/9205229
363. E.J. Chun, A. Lukas, Phys. Lett. B **357**, 43 (1995), hep-ph/9503233
364. G.G. Raffelt, J. Phys. A **40**, 6607 (2007), hep-ph/0611118
365. J.E. Kim, Phys. Rev. Lett. **67**, 3465 (1991)
366. D.H. Lyth, Phys. Rev. D **48**, 4523 (1993), hep-ph/9306293
367. S. Chang, H.B. Kim, Phys. Rev. Lett. **77**, 591 (1996), hep-ph/9604222
368. M. Hashimoto, K.I. Izawa, M. Yamaguchi, T. Yanagida, Phys. Lett. B **437**, 44 (1998), hep-ph/9803263
369. M. Kawasaki, K. Nakayama, M. Senami (2007), 0711.3083
370. A. Brandenburg, F.D. Steffen, J. Cosmol. Astropart. Phys. **0408**, 008 (2004), hep-ph/0405158
371. T. Asaka, T. Yanagida, Phys. Lett. B **494**, 297 (2000), hep-ph/0006211
372. L. Covi, H.B. Kim, J.E. Kim, L. Roszkowski, J. High Energy Phys. **05**, 033 (2001), hep-ph/0101009
373. M.E. Gomez, S. Lola, C. Pallis, J. Rodriguez-Quintero (2008), 0809.1859
374. L. Covi, J.E. Kim, L. Roszkowski, Phys. Rev. Lett. **82**, 4180 (1999), hep-ph/9905212
375. L. Covi, L. Roszkowski, R. Ruiz de Austri, M. Small, J. High Energy Phys. **06**, 003 (2004), hep-ph/0402240